

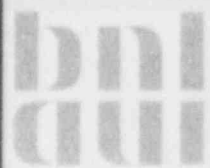
NUREG/CR-2331  
BNL-NUREG-51454  
VOL. 5, NO. 2

# SAFETY RESEARCH PROGRAMS SPONSORED BY OFFICE OF NUCLEAR REGULATORY RESEARCH

QUARTERLY PROGRESS REPORT  
APRIL 1 — JUNE 30, 1985

Date Published — December 1985

DEPARTMENT OF NUCLEAR ENERGY, BROOKHAVEN NATIONAL LABORATORY  
UPTON, NEW YORK 11973



Prepared for the U.S. Nuclear Regulatory Commission  
Office of Nuclear Regulatory Research  
Contract No. DE-AC02-76CH00016

B602240008 851231  
PDR NUREG  
CR-2331 R PDR

# SAFETY RESEARCH PROGRAMS SPONSORED BY OFFICE OF NUCLEAR REGULATORY RESEARCH

QUARTERLY PROGRESS REPORT  
APRIL 1 — JUNE 30, 1985

Herbert J.C. Kouts, Department Chairman  
Walter Y. Kato, Deputy Chairman

Principal Investigators:

R.A. Bari	J.N. O'Brien
J.L. Boccio	W.T. Pratt
R.J. Cerbone	M. Reich
T. Ginsberg	P. Saha
G.A. Greene	J.H. Taylor
J.G. Guppy	D. van Rooyen
R.E. Hall	W. Wulff

W.J. Luckas, Jr.

Compiled by: Allen J. Weiss  
Manuscript Completed October 1985

DEPARTMENT OF NUCLEAR ENERGY  
BROOKHAVEN NATIONAL LABORATORY, ASSOCIATED UNIVERSITIES, INC.  
UPTON, NEW YORK 11973

Prepared for the  
OFFICE OF NUCLEAR REGULATORY RESEARCH  
U.S. NUCLEAR REGULATORY COMMISSION  
CONTRACT NO. DE-AC02-76CH00016  
FINS A-3014,-3015,-3016,-3024,-3208,-3215,-3226,-3227,-3242,  
-3268,-3270,-3272,-3274,-3277,-3281,-3282,-3284

## FOREWORD

The Advanced and Water Reactor Safety Research Programs Quarterly Progress Reports have been combined and are included in this report entitled, "Safety Research Programs Sponsored by the Office of Nuclear Regulatory Research - Quarterly Progress Report." This progress report will describe current activities and technical progress in the programs at Brookhaven National Laboratory sponsored by the Division of Accident Evaluation, Division of Engineering Technology, and Division of Risk Analysis and Operations of the U. S. Nuclear Regulatory Commission, Office of Nuclear Regulatory Research.

The projects reported are the following: High Temperature Reactor Research, SSC/MINET Development, Validation and Application, Thermal-Hydraulic Reactor Safety Experiments, Plant Analyzer, Code Assessment and Application, Code Maintenance (RAMONA-3B), Benchmarking and Verification of LWR Severe Accident Codes; Stress Corrosion Cracking of PWR Steam Generator Tubing, Probability Based Load Combinations for Design of Category I Structures, Soil-Structure Interaction Evaluations, Identification of Age Related Failure Modes; Application of HRA/PRA Results to Resolve Human Reliability and Human Factors Safety Issues, PRA Technology Transfer Program, Protective Action Decisionmaking, and Operational Safety Reliability Research. The previous reports have covered the period October 1, 1976 through March 30, 1985.

TABLE OF CONTENTS

	<u>Page</u>
FOREWORD . . . . .	iii
FIGURES . . . . .	viii
TABLES . . . . .	x
I. DIVISION OF ACCIDENT EVALUATION. . . . .	1
SUMMARY. . . . .	1
1. High Temperature Reactor Research. . . . .	7
1.1 Assessment and Development of Evaluation Methods. . . . .	7
1.2 Effect of Radioactive Decay Chains on Source Terms. . . . .	20
1.3 HTGR Safety Handbook. . . . .	23
1.4 Graphite and Ceramics . . . . .	23
References . . . . .	34
Publications . . . . .	35
2. SSC/MINET Improvement, Validation and Application. . . . .	36
2.1 SSC-S Code. . . . .	36
2.2 Generic Balance of Plant Modeling (MINET) . . . . .	42
2.3 SSC-P Code. . . . .	43
References . . . . .	43
Publications . . . . .	43
3. Thermal-Hydraulic Reactor Safety Experiments . . . . .	45
3.1 Core Debris Thermal-Hydraulic Phenomenology: Ex-Vessel Debris Quenching. . . . .	45
3.2 Core Debris Thermal-Hydraulic Phenomenology: In-Vessel Debris Quenching. . . . .	47
3.3 Core-Concrete Heat Transfer Studies . . . . .	50
References . . . . .	52
4. Plant Analyzer . . . . .	53
4.1 Introduction. . . . .	53
4.2 Assessment of Existing Training Simulators. . . . .	53
4.3 Acquisition of Special-Purpose Peripheral Processor and Ancillary Equipment . . . . .	54
4.4 Model Implementation on AD10 Processor and Developmental Assessment. . . . .	54
4.5 Model Development . . . . .	56
4.6 Remote Access Operations. . . . .	57
4.7 Transatlantic Remote Access . . . . .	59
4.8 Future Plans. . . . .	59
References . . . . .	59



TABLE OF CONTENTS (Cont'd.)

	<u>Page</u>
5. Code Assessment and Application. . . . .	62
5.1 Code Assessment . . . . .	62
References . . . . .	66
6. Code Maintenance (RAMONA-3B) . . . . .	73
6.1 Pressure Suppression Pool (PSP) Model . . . . .	73
6.2 New Cycle of RAMONA-3B/MODO . . . . .	74
6.3 Distribution of RAMONA-3B/MODO/Cycle 10 . . . . .	74
7. Benchmarking and Verification of LWR Severe Accident Codes . . . . .	75
7.1 MELCOR Benchmarking and Verification. . . . .	75
7.2 Source Term Code Package Benchmarking and Verification. . . . .	76
II. DIVISION OF ENGINEERING TECHNOLOGY . . . . .	77
SUMMARY. . . . .	77
8. Stress Corrosion Cracking of PWR Steam Generator Tubing. . . . .	79
8.1 Constant Load . . . . .	79
8.2 U-bends . . . . .	79
8.3 Future Work . . . . .	79
9. Probability-Based Load Combination for Design of Category I Structures . . . . .	80
9.1 Reliability Analysis Method for Shear Wall Structures . . . . .	80
9.2 Probability-Based Load Combinations for Design of Shear Walls . . . . .	80
10. Soil-Structure Interaction Evaluations . . . . .	82
10.1 Lift-Off Effects. . . . .	82
10.2 Water Table Effects . . . . .	82
10.3 Layering Effects. . . . .	82
11. Identification of Age Related Failure Modes. . . . .	84
11.1 Electric Motors . . . . .	84
11.2 Battery Chargers and Inverters. . . . .	85
11.3 Relays and Circuit Breakers . . . . .	85

TABLE OF CONTENTS (Cont'd.)

	<u>Page</u>
III. DIVISION OF RISK ANALYSIS AND OPERATIONS . . . . .	87
SUMMARY. . . . .	87
12. Application of HRA/PRA Results to Resolve Human Reliability and Human Factors Safety Issues. . . . .	89
12.1 Identifying, Collecting, and Storing all HRA/PRA Data . . . . .	89
12.2 Listing of Human Performance Regulatory Issues and Data Needs . . . . .	89
12.3 Comparison of HRA/PRA Data Records and Issues Data Records. . . . .	90
12.4 Grouping of Approaches and Data Types . . . . .	90
13. PRA Technology Transfer Program. . . . .	91
13.1 Objectives. . . . .	91
13.2 Work Performed During Period. . . . .	91
14. Protective Action Decisionmaking . . . . .	93
14.1 Background. . . . .	93
14.2 Project Objectives. . . . .	93
14.3 Technical Approach. . . . .	94
14.4 Project Status. . . . .	94
15. Operational Safety Reliability Research . . . . .	95
15.1 Background. . . . .	95
15.2 Objectives. . . . .	95
15.3 Major Tasks . . . . .	95
15.4 Work Performed During Period. . . . .	96

## FIGURES

	<u>Page</u>
1.1	Elevation of Modular HTGR Reactor Building . . . . . 16
1.2	Schematic of Modular HTGR Reactor Building . . . . . 17
1.3	MINET Representation of Confinement, Designated CFl. . . . . 21
1.4	Atmospheric Radioactivity Release. . . . . 24
1.5	Atmospheric Radioactivity Release. . . . . 25
1.6	Compressive Stress-Strain Curve for Unoxidized Stackpole 2020 Control Sample . . . . . 26
1.7	Compressive Stress-Strain Curve for Oxidized Stackpole 2020 #1 Sample . . . . . 27
1.8	Compressive Stress-Strain Curve for Oxidized Stackpole 2020 #3 Sample . . . . . 28
1.9	Oxidation Rate of TS-1621 Graphite as a Function of $P_{H_2}$ at 850°C in $P_{H_2} = 6 \times 10^{-3}$ atm. . . . . 30
1.10	Oxidation Rate of TS-1621 Graphite as a Function of $P_{H_2}$ at 850°C in $P_{H_2O} = 5 \times 10^{-4}$ atm . . . . . 31
1.11	Oxidation Rate of H-451 Graphite as a Function of $P_{H_2O}$ at 850°C in $P_{H_2} = 5 \times 10^{-3}$ atm. . . . . 32
1.12	Oxidation Rate of H-451 Graphite as a Function of $P_{H_2}$ at 850°C in $P_{H_2O} = 1 \times 10^{-3}$ atm . . . . . 33
2.1	Upper Plenum Velocity Profile 25 Seconds After Scram . . . . . 37
2.2	Upper Plenum Velocity Profile 50 Seconds After Scram . . . . . 38
2.3	Upper Plenum Isotherms 50 Seconds After Scram. . . . . 39
2.4	Upper Plenum Velocity Profile 100 Seconds After Scram. . . . . 40
2.5	Upper Plenum Isotherms 100 Seconds After Scram . . . . . 41
3.1	Steady-State Dryout Heat Flux and Bed Quench . . . . . 46

FIGURES (Cont'd.)

	<u>Page</u>
3.2	Instantaneous Heat Flux Leaving the Debris Bed, H = 850 mm . . . . 48
3.3	Average Heat Flux Per Unit Water Injection Superficial Velocity Per Unit Initial Superheat. . . . . 49
3.4	Liquid-Liquid Film Boiling Run 153: $J_g = 0.00$ cm/s. . . . . 51
4.1	Flow Schematic and Control Blocks for BWR Simulation . . . . . 55
5.1	Comparison Between the Experimental Data and the Code Predictions of Axial Void Fraction for FRIGG Test 313006 . . . . 67
5.2	Comparison Between the Experimental Data and the Code Predictions of Axial Void Fraction for FRIGG Test 313010 . . . . 67
5.3	Comparison Between the Experimental Data and the Code Predictions of Axial Void Fraction for FRIGG Test 313005 . . . . 68
5.4	Comparison Between the Experimental Data and the Code Predictions of Axial Void Fraction for FRIGG Test 313009 . . . . 68
5.5	Comparison Between the Experimental Data and the Code Predictions of Axial Void Fraction for FRIGG Test 313019 . . . . 69
5.6	Comparison Between the Experimental Data and the Code Predictions of Axial Void Fraction for FRIGG Test 313001 . . . . 69
5.7	Comparison Between the Experimental Data and the Code Predictions of Axial Void Fraction for FRIGG Test 313008 . . . . 70
5.8	Comparison Between the Experimental Data and the Code Predictions of Axial Void Fraction for FRIGG Test 313017 . . . . 70
5.9	Comparison Between the Experimental Data and the Code Predictions of Axial Void Fraction for FRIGG Test 313007 . . . . 71
5.10	Comparison Between the Experimental Data and the Code Predictions of Axial Void Fraction for FRIGG Test 313014 . . . . 71
5.11	Comparison Between the Experimental Data and the Code Predictions of Axial Void Fraction for FRIGG Test 313016 . . . . 72
5.12	Comparison Between the Experimental Data and the Code Predictions of Axial Void Fraction for FRIGG Test 313020 . . . . 72

TABLES

	<u>Page</u>
1.1 Density of Helium as Calculated, From Tables, and Per Cent Errors . . . . .	9
1.2 Helium Enthalpy as Calculated, From Tables, and Per Cent Errors. .	10
1.3 Helium Entropy as Calculated, From Tables, and Per Cent Errors . .	11
1.4 Helium Viscosity as Calculated, From Tables, and Per Cent Errors .	12
1.5 Helium Thermal Conductivity as Calculated, From Tables, and Per Cent Errors. . . . .	13
1.6 Helium Property Derivatives as Calculated by Functions, Compared Against Finite Differenced Values. . . . .	14
1.7 Oxidation Rates for 2020, PGX, TS-1621 and H-451 Graphites at 850° with 500 ppm H <sub>2</sub> O/5000 ppm H <sub>2</sub> (Balance He) . . . . .	29
4.1 Tabulated Data Display for Simulation of Indefinite Duration . . .	58
5.1 Operating Conditions for FRIGG Runs. . . . .	64

## I. DIVISION OF ACCIDENT EVALUATION

### SUMMARY

#### High Temperature Reactor Research

The high temperature gas reactor (HTGR) safety research program is structured to provide the generation of information of generic benefit to LWR safety research in those areas of commonality between high priority LWR needs and high priority HTGR needs. HTGR safety research is being applied to generic HTGR concepts in accordance with the development directions of the DOE/Industry program until a specific design is identified for NRC actions. A major task this fiscal year is the acquisition of codes and validated data to assist NRC in performing an independent safety assessment of specific and generic gas-cooled reactor systems.

In the analytical effects, focused to provide the necessary computer codes for HTGR licensing analysis, significant progress was made with both the MINET and ATMOS codes. MINET code helium property functions were verified in a detailed test study, the reactor module design is well along, and a test case simulating the side-by-side modular HTGR design was completed successfully. Substantial progress was made in extending ATMOS to simulate complex multi-cavity configurations, although an undesirable slowdown in numerical integration was encountered using the momentum equation with low form loss factors. By using the MINET code to analyze an equivalent case, it was possible to better focus on this problem, and an alternate formulation was successfully implemented.

In the first phase of our study on the effect of radioactive decay chains on source terms during severe accidents, the effect of fission product decay has been analyzed for an HTGR core. Three groups of isotopes were selected for complete decay treatment: noble gases (Xe, Kr), iodine, and organic iodine. An assumed accident sequence was analyzed using two calculational procedures, one where the decay of the various radioactive nuclides was approximated but precursor decay was neglected, and a second more detailed calculation which included precursor decay. It was determined that treatment of the physical and chemical behavior of precursors, as well as the complete decay treatment of fission product isotopes, can be relatively important for some accident sequences.

As part of the experimental effort, the elastic moduli of oxidized and control samples of 2020 graphite were measured from the slopes of the stress-strain curves which were produced during destructive compressive strength testing. Also, the oxidation rate runs with the larger size H-451 graphite were completed, and a preliminary analysis of the oxidation kinetic data from TS-1621 and H-451 graphite was performed.



## SSC/MINET Improvement, Validation and Application

The SSC/MINET Improvement, Validation and Application Program encompasses a series of computer codes. The prefix SSC denotes the Super System Code, where: (1) SSC-L is for system transients in loop-type liquid metal-cooled reactors (LMRs); (2) SSC-P is for system transients in pool-type LMRs and (3) SSC-S is for long term shutdown transients. In addition to these code development and application efforts, validation of these codes is an ongoing task.

Another component of this program is the generic balance of plant (BOP) modeling effort. It provides for the development and validation of models to represent and link together BOP components that are generic to all types of nuclear power plants. This system transient analysis package is designated MINET to reflect the generality of the models and methods, which are based on a momentum integral network method.

Interfacing of the upper plenum model with the SSC primary loop calculations is progressing smoothly. Currently, reactor outlet flows and temperatures are being input to the upper plenum model, and the average plenum outlet temperature is returned to be used as the SSC hot leg inlet temperature. An example test run is shown and discussed.

Two conduction models, for cylindrical and spherical structures, were developed for implementation in the MINET code. The drift flux model was evaluated and was found to be appropriate for its intended applications. A FORTRAN-77 standard version of MINET was tested successfully, and the important files were backed up on tape.

Upgrading of SSC-P proceeded, with input processor and steady state portions now compatible with Cycle 41 of SSC-L. The effort is now focused on the transient calculations.

## Thermal-Hydraulic Reactor Safety Experiments

Analysis of the data from the ex-vessel, top-flooding bed quench experiments is complete, and a draft of the final report on this task has been prepared.

Analysis of the experimental data for bottom quenching of superheated debris particles (3.18 mm) fixed in place to prevent fluidization was completed. The data indicate that for water injection superficial velocity greater than 4 mm/s, there is a dependence of the peak heat flux from the debris bed upon the depth of the debris bed. This independence is because the wetted area of the debris can increase with increased bed depth, allowing more water to come in contact with superheated debris.

Analysis of liquid-liquid film boiling data of R11 on liquid metal pools revealed that the data consistently exceeded the Berenson film boiling model by approximately 20%. This discrepancy was attributed to an unaccounted for heat loss from the liquid metal axially through the walls of the apparatus.

Correction of the enthalpy balance for the measured conduction heat loss was found to bring the experimental data into excellent agreement with the Berenson model, on the average to within 3%.

### Plant Analyzer

The LWR Plant Analyzer Program is being conducted to develop an engineering plant analyzer capable of performing accurate, real-time and faster than real-time simulations of plant transients and Small-Break Loss of Coolant Accidents (SBLOCAs) in LWR power plants. The first program phase was carried out earlier to establish the feasibility of achieving faster than real-time simulations and faster than mainframe, general-purpose computer (CDC-7600) simulations through the use of modern, interactive, high-speed, special-purpose minicomputers, which are specifically designed for interactive time-critical systems simulations. It has been successfully demonstrated that special-purpose minicomputers can compete with, and outperform, mainframe computers in reactor simulations. The current program phase is being carried out to provide a complete BWR plant simulation capability, including on-line, multicolor graphic display of safety-related parameters.

The plant analyzer program was at first directed primarily toward reactor safety analyses, but it is also useful for on-line plant monitoring and accident diagnosis, for accident mitigation, further for developing operator training programs and for assessing and improving existing and future training simulators. The plant analyzer is now being modified for on-line training in emergency response. Major assets of the simulator under development are its low cost, unsurpassed convenience of operation and high speed of simulation. Major achievements of the program are summarized below.

Existing training simulator capabilities and limitations regarding their representation of the Nuclear Steam Supply System have been assessed previously. Simulators reviewed at the time have been found to be limited to steady-state simulations and to restricted quasi-steady transients within the range of normal operating conditions.

A special-purpose, high-speed peripheral processor had been selected for the plant analyzer, which is specifically designed for efficient systems simulations at real-time or faster computing speeds. The processor is the AD10 from Applied Dynamics International (ADI) of Ann Arbor, Michigan. A PDP-11/34 Minicomputer serves as the host computer to program and control the AD10 peripheral processor. Both the host computer and the peripheral processor have been operating at BNL since March 15, 1982.

A four-equation model for nonequilibrium, nonhomogeneous, two-phase flow in a typical BWR/4 had been implemented on the AD10 processor. It is called HIPA-BWR/4 for High-Speed Interactive Plant Analysis of a BWR/4 power plant. The implementation of HIPA-BWR/4 had been carried out in the high-level language MPS10 of the AD10.

It had been demonstrated during the last quarter of 1982 that the AD10 special-purpose peripheral processor can produce accurate simulations of a BWR design base transient at computing speeds up to 10 times faster than real-time and 110 times faster than the CDC-7600 mainframe computer carrying out the same simulation. Only the BNL Plant Analyzer has achieved this gain in computing speed relative to the CDC-7600 computer.

After the successful completion of the feasibility demonstration, work has continued to expand the simulation capability for simulating the dynamics of the entire nuclear steam supply system as well as the entire balance of plant (steam lines, turbines, condensers and feedwater trains).

Models have been developed and implemented for point neutron kinetics with seven feedback mechanisms and seven automatic scram trip initiations, for thermal conduction in fuel elements, for steam line dynamics capable of simulating acoustical effects from sudden valve actions, for turbines, condensers, feedwater preheaters and feedwater pumps and for emergency cooling systems.

The software systems of both the PDP-11/34 host computer and the AD10 special-purpose peripheral processor have been upgraded to achieve greater computing speed and a larger number of analog input/output channels. Two AD10s are coupled via a direct bus-to-bus interface to compute in parallel.

Models have been developed and implemented for the feedwater controller, the pressure regulator and the recirculation flow controller. Twenty-eight parameters for initiating control systems and valve failures and for selecting set points can be changed on-line from a 32-channel control panel. Sixteen dedicated analog output lines are provided for the simultaneous display of 15 selected parameters in labeled diagrams versus time. All input-output channels are addressed approximately 200 times per second. A silent movie has been produced to show how the plant analyzer is operated and how it responds to on-line analog signals.

During the first reporting period of 1984, we presented the comparison of plant analyzer results with published results from GE for 10 different ATWS events as a part of developmental assessment. The assessment showed that the plant analyzer is capable of simulating ATWS. The plant analyzer has been generalized to simulate any BWR-4 power plant in response to input data changes from the keyboard.

During the second reporting period of 1984, we continued the developmental assessment of the plant analyzer by comparisons against GE, TRAC-BD1, RELAP-5, and RAMONA-3B code results. The results showed that the plant analyzer is capable of realistically simulating a large class of plant transients efficiently at very low cost.

During the third reporting period of 1984, we implemented the capability of simulating flow reversal, continued the implementation of the level tracking model with the drift flux model, and demonstrated successfully the simulation of boron injection and the subsequent cessation of fission power. Several transients were simulated to demonstrate the plant response to manual de-

pressurization and HPCI flow reduction during an ATWS event. These simulations were carried out to assess the efficacy of proposed emergency procedure guidelines. The results indicate that the fission power can be reduced without boron injection and core uncover, by lowering the pressure and by lowering the coolant level in the downcomer and thereby reducing the core flow rate.

The previously distributed draft report documenting the BWR plant analyzer was updated as a final report [Wulff, Cheng, Lekach and Mallen, 1984] It has been printed and distributed.

During the fourth reporting period of 1984, we demonstrated that with the plant analyzer one can simulate, evaluate and document, in less than four days, thirty-seven different transients, induced by both single and multiple failures or events. We achieved the ability to operate the plant analyzer remotely at BNL from an IBM Personal Computer, equipped with 128 Kbyte memory, an RS-232 serial port, a 1200 baud modem, a Plantronics PC+ Colorplus color graphics adapter card and a standard R-G-B color monitor.

During the previous reporting period, we have demonstrated that the BNL Plant Analyzer can now be accessed and operated remotely from anywhere in the United States. There were seven demonstrations given in Washington, D.C., two in California, one in Idaho and one for a utility in New York. Work has started for on-line support of personnel drills in the NRC Emergency Operations Center. The Tektronix 4115B graphics terminal has been received.

During the current reporting period, we have developed the models for dry and wetwell responses to discharge from pipe leaks and from the safety and relief valves. We began to expand thermophysical property tabulations toward low pressures in the vessel, we completed the level tracking simulation in the downcomer and we began to program output processing for long-term simulations. We also prepared for the first transatlantic remote access operation of the plant analyzer.

The interest in the Plant Analyzer Development Program continues to be high, both in domestic and foreign institutions. Eleven presentations with demonstrations were given at BNL to visitors from USNRC, CSN-Spain, Netherlands and the U.S.

#### Code Assessment and Application

Simulation of five FIST Phase 1 tests with TRAC-BD1/MOD1 is at various stages of completion. Preliminary comparison of the TRAC predictions with the experimental data shows good agreement.

Twelve steady-state flow boiling experiments performed in the FRIGG loop have been simulated with the TRAC-BD1/MOD1 code. These tests were simulated earlier with the RAMONA-3B/MODO Cycle 8 code. Comparison of the code predictions with the data shows that both TRAC-BD1/MOD1 and RAMONA-3B (with the

Bankoff-Malnes slip correlation) produce results in good agreement with the measured axial void fractions for low inlet subcoolings ( $<10^{\circ}\text{C}$ ). However, for higher inlet subcoolings ( $>10^{\circ}\text{C}$ ), both codes need improvement in the subcooled boiling region.

#### Code Maintenance (RAMONA-3B)

A simple model for calculating the pressure suppression pool bulk water temperature and level has been implemented in RAMONA-3B. Also, a new cycle of RAMONA-3B containing a number of code improvements and corrections has been created. This new cycle, i.e., RAMONA-3B/MODO/Cycle 10, is being distributed to several U.S. organizations.

#### Benchmarking and Verification of LWR Severe Accident Codes

In these projects, BNL staff will benchmark and verify specific LWR severe accident codes. The first project will evaluate the potential for the MELCOR computer code to be used as a source term code. MELCOR is currently being developed for NRC by Sandia National Laboratories (SNL) to be used in probabilistic risk assessment (PRA) studies. In addition, the project will also benchmark MELCOR against more mechanistic codes. In the second project, BNL will obtain the NRC source term code package (STCP) which was developed at Battelle Columbus Laboratory (BCL). The STCP will be reviewed specifically to ensure that models and options are adequate and have been correctly implemented.



## 1. High Temperature Reactor Research (J. G. Guppy)

The high temperature gas reactor (HTGR) safety research program is structured to provide the generation of information of generic benefit to LWR safety research in those areas of commonality between high priority LWR needs and high priority HTGR needs. HTGR safety research is being applied to generic HTGR concepts in accordance with the development directions of the DOE/Industry program until a specific design is identified for NRC actions. A major task this fiscal year is the acquisition of codes and validated data to assist NRC in performing an independent safety assessment of specific and generic gas-cooled reactor systems.

### 1.1 Assessment and Development of Evaluation Methods (P. G. Kroeger, G. J. Van Tuyle, R. Ashley)

#### 1.1.1 MINET Representation of a Side-by-Side Modular Concept (G. J. Van Tuyle)

The vertical-in-line modular HTGR representation previously developed, using the MINET code, was altered to represent a side-by-side configuration. This required adding a couple of modules (pipes) to the input deck, altering the module connections somewhat, and adjusting the elevations so the steam generator was positioned below the core. An LOPW ATWS with circulator trip transient was run to ten minutes to observe the system response, with the natural circulation flow effectively inhibited by the low position of the steam generator. We observed a flow reversal after the circulator coasted down, and a return of the flow rate (towards zero) by the end of the ten minute period. A slowly oscillating and quite low primary loop flow rate appeared to be developing, a not-unexpected response. As a great deal of estimation was involved in specifying the system details, further analysis of the system should be deferred until some of the uncertainties can be addressed, i.e., when design details are better known.

#### 1.1.2 MINET Reactor Module (G. J. Van Tuyle)

The generic MINET reactor module is currently under development. This generic module will be quite similar to other MINET modules, especially the pipes and the heat exchangers, with the principal difference being the calculation of the heating term. This heating term is composed of the reactor power, the decay heat, and losses and gains due to the structure and moderators. Core power is to be either a user-input function of time, or calculated from the reactivity, using a six-group point kinetics equation. Reactivity contributions from control rods, xenon, fuel temperature, moderator temperature, coolant temperature, and foreign matter in the coolant (e.g. water or air for an HTGR) will be factored into the total. While each of the various calculations is relatively straightforward, the calculations do have to be carefully packaged in order to assure proper flexibility for the user, so that the various options can be controlled through input data.



1A, as taken from (Bammert, 1969) and (Tallackson, 1975), has been tested over a pressure range of 1 to 1000 bar and a temperature range of 273 to 1773K. These property correlations are as follows:

$$h = 5196T + .0313 \left( T^{-4/3} - \frac{4715}{T^2} \right) P - 14170.0$$

$$c_p = 5196 - 0.01043 \left( T^{-4/3} - \frac{28300}{T^2} \right) P/T$$

$$S = 5196 \ln T - 2078 \ln P + .00783 \left( T^{-4/3} - \frac{12580}{T^2} \right) P/T + 24240$$

$$\rho = \frac{P}{\left\{ 2078 T + \left( .02348 T^{-4/3} - \frac{49.2486}{T^2} \right) P \right\}}$$

$$k = \left( .002682 + 3.011886 \times 10^{-11} \cdot P \right) T^{.71 - 1.42 \times 10^{-9} \cdot P}$$

$$\mu = 3.674 \times 10^{-7} T^{0.7}$$

---

Units:	T in K	S in J/kgK
	P in Pa	$\rho$ in kg/m <sup>3</sup>
	h in J/kg	k in w/(mK)
	$c_p$ in J/(kg·K)	$\mu$ in Ns/m <sup>2</sup>

The MINET helium functions were tested by generating properties over a wide range of temperatures and pressures, and comparing these values to published tables. The results are shown in Tables 1.1 - 1.6.

Results for the density function are given in Table 1.1. As helium is nearly an ideal gas, the agreement between the MINET functions and the tables is not surprising. (It should be noted that the tabular values in (Perry, 1984) for 20 bars and 773 K, 1073 K, and 1273 K are highly suspect, and we consider the MINET values to be much more reliable, given the good agreement with (Reynolds, 1979) and (Banerjee, 1978)).

The MINET enthalpy calculations were compared against tabular values from the same three references, again with excellent results, as can be seen in Table 1.2. (Because enthalpy has an arbitrary zero point, values from some of the references had to be adjusted to align at the 1 bar, 273 K point.)

Table 1.1 Density of Helium as Calculated, from Tables, and Per Cent Errors

		DENSITY (KG/M <sup>3</sup> )						
P (BAR)	T (K)	MINET	REY.	PERRY	GER.	%ERR-R	%ERR-P	%ERR-G
1	273	0.17618	0.17859	0.17615	0.1761	-1.349	0.017	0.045
1	473	0.10171	0.10313	0.10172	0.1017	-1.377	0.010	0.010
1	773	0.06224	0.06311	0.06225	0.0623	-1.378	-0.016	-0.096
1	1073	0.04484	0.04546	0.04486	0.0449	-1.363	-0.044	-0.133
1	1273	0.03780	0.03851	0.03781	0.0378	-1.331	-0.026	0.000
1	1473	0.03266	0.03311		0.0327	-1.359		-0.122
5	273	0.87009	0.87961	0.87873	0.8788	-0.059	0.041	0.033
5	473	0.50798	0.50818	0.50813	0.5080	-0.039	-0.030	-0.004
5	773	0.31104	0.31112	0.31104	0.3111	-0.026	0.000	-0.019
5	1073	0.22413	0.22420	0.22417	0.2242	-0.031	-0.018	-0.031
5	1273	0.18894	0.18900	0.18900	0.1890	-0.032	-0.032	-0.032
5	1473	0.16330	0.16335		0.1633	-0.031		0.000
10	273	1.7536	1.7543	1.7531	1.7530	-0.040	0.029	0.034
10	473	1.0145	1.0152	1.0142	1.0142	-0.069	0.030	-0.010
10	773	0.6216	0.6217	0.62150	0.6217	-0.016	0.016	-0.016
10	1073	0.4480	0.4481	0.44803	0.4481	-0.022	-0.007	-0.022
10	1273	0.3777	0.3778	0.37779	0.3778	-0.026	-0.024	-0.026
10	1473	0.3265	0.3266		0.3266	-0.031		-0.031
20	273	3.4892	3.4898	3.4880	3.4877	-0.017	0.034	0.043
20	473	2.0233	2.0239	2.0235	2.0237	-0.030	-0.010	-0.020
20	773	1.2413	1.2416	1.1000	1.2415	-0.024	12.8	-0.016
20	1073	0.8952	0.8954	0.7500	0.8953	-0.022	19.4	-0.011
20	1273	0.7548	0.7551	0.5424	0.7550	-0.040	39.2	-0.026
20	1473	0.6525	0.6528		0.6526	-0.045		-0.015
50	273	8.5897		8.5910	8.5842		-0.015	0.064
50	473	5.0157		5.0175	5.0183		-0.036	-0.052
50	773	3.0889		3.0703	3.1397		0.605	-0.025
50	1073	2.2312		2.2316	2.2315		-0.044	-0.013
50	1273	1.8825		1.8830	1.8827		-0.027	-0.011
50	1473	1.6281			1.6282			-0.005
100	273	16.759	16.765	16.750	16.7364	-0.036	0.054	0.137
100	473	9.8929	9.8992	9.9009	9.9027	-0.054	-0.081	-0.099
100	773	6.1309	6.1317	6.1312	6.1331	-0.013	-0.005	-0.036
100	1073	4.4401	4.4420	4.4405	4.4403	-0.043	-0.009	0.005
100	1273	3.7500	3.7514	3.7500	3.7498	-0.037	0.000	0.005
100	1473	3.2454	3.2466		3.2450	-0.037		0.012
500	273	69.807	70.600			-0.987		
500	473	44.536	44.908			-0.828		
500	773	28.900	29.010			-0.379		
500	1073	21.344	21.400			-0.261		
500	1273	18.166	18.209			-0.236		
500	1473	15.807	15.846			-0.246		
1000	273	115.85	119.67			-3.192		
1000	473	79.224	81.190			-2.279		
1000	773	53.940	54.667			-1.329		
1000	1073	40.736	41.128			-0.953		
1000	1273	34.928	35.268			-0.822		
1000	1473	30.628	30.867			-0.780		

REY = W.C. REYNOLDS, THERMODYNAMIC PROPERTIES (IN S.I.), DEPARTMENT OF MECH. ENG., STANFORD U., 1979.

PERRY = PERRY'S CHEMICAL ENGINEERING HANDBOOK, 6TH EDITION, NEW YORK, 1984.

GER = A. BANERJEA ET AL., THERMODYNAMISCHE STOFFWERTE VON HELIUM IM BEREICH 20 BIS 1500C UND 1 BIS 100 BAR, RHEINISCH-WESTFÄLISCHEN TECHNISCHEN ÜBERWACHUNGS-VEREIN E.V. UND DER INTERATOM GMBH, 1978.

Table 1.2 Helium Enthalpy as Calculated, from Tables, and Per Cent Errors

		ENTHALPY (KJ/KG)						
P (BAR)	T (K)	MINET	REY.	PERRY	GER.	%ERR-R	%ERR-P	%ERR-G
1	273	1404.6	1402.8	1404.6	1404.6	0.128	0.0	0.0
1	473	2443.9	2441.3	2443.3	2443.6	0.025	0.024	0.012
1	773	4002.7	3999.2	4001.3	4002.6	0.097	0.035	0.003
1	1073	5561.4	5557.1	5559.3	5560.6	0.077	0.038	0.014
1	1273	6600.6	6595.7	6597.3	6599.6	0.074	0.050	0.015
1	1473	7639.8	7634.3		7638.6	0.072		0.015
5	273	1405.8	1403.9	1405.9	1406.0	0.135	-0.007	-0.014
5	473	2445.2	2442.6	2444.3	2444.6	0.106	0.049	0.057
5	773	4003.9	4000.4	4002.3	4003.6	0.087	0.040	0.007
5	1073	5562.6	5558.3	5560.3	5561.6	-0.103	0.041	0.018
5	1273	6601.7	6596.9	6598.3	6600.6	0.073	-0.052	0.017
5	1473	7640.9	7635.5		7639.6	0.071		0.017
10	273	1407.2	1405.6	1407.5	1407.8	0.114	-0.021	-0.043
10	473	2446.9	2444.2	2446.3	2446.6	0.110	0.024	0.012
10	773	4005.5	4002.2	4004.3	4004.6	0.007	0.030	0.022
10	1073	5564.1	5559.9	5561.3	5562.6	0.076	0.050	0.027
10	1273	6603.1	6598.4	6600.3	6601.6	0.071	0.042	0.023
10	1473	7642.2	7636.9		7640.6	0.069		0.021
20	273	1410.0	1408.7	1410.8	1411.6	0.092	-0.050	-0.106
20	473	2450.3	2447.5	2449.3	2449.6	0.114	0.041	0.029
20	773	4008.7	4004.6	4007.3	4007.6	0.102	0.035	0.027
20	1073	5567.0	5562.9	5564.3	5565.6	0.073	0.049	0.025
20	1273	6605.9	6601.3	6603.3	6604.6	0.070	0.039	0.020
20	1473	7644.9	7639.9		7643.6	0.065		0.017
50	273	1418.6		1420.6	1422.3		-0.141	-0.260
50	473	2460.3		2459.3	2459.6		0.040	0.028
50	773	4018.2		4016.3	4016.6		0.047	0.040
50	1073	5575.8		5573.3	5573.6		0.045	0.039
50	1273	6614.3		6611.3	6612.6		0.045	0.026
50	1473	7653.0			7651.6			0.018
100	273	1432.8	1434.2	1442.0	1440.3	-0.099	-0.693	-0.534
100	473	2477.1	2473.5	2475.3	2475.6	0.186	0.072	0.061
100	773	4034.0	4029.7	4031.3	4031.6	0.107	0.066	0.060
100	1073	5590.4	5586.9	5588.3	5587.6	0.081	0.038	0.050
100	1273	6628.3	6625.0	6626.3	6626.6	0.050	0.030	0.043
100	1473	7666.4	7663.0		7664.6	0.044		0.003
500	273	1546.6	1559.7			-0.840		
500	473	2611.4	2599.3			0.466		
500	773	4160.5	4151.2			0.358		
500	1073	5707.6	5703.5			0.072		
500	1073	5707.6	5703.5			0.072		
500	1473	7773.7	7774.5			-0.010		
1000	273	1688.8	1710.8			-1.284		
1000	473	2779.3	2750.3			1.054		
1000	773	4318.7	4295.6			0.538		
1000	1073	5854.1	5841.8			0.211		
1000	1273	6880.0	6874.0			0.087		
1000	1473	7907.8	7906.3			0.019		

REY = W.C. REYNOLDS, THERMODYNAMIC PROPERTIES IN S.I., DEPARTMENT OF MECH. ENG., STANFORD U., 1978.

PERRY = PERRY'S CHEMICAL ENGINEERING HANDBOOK, 6TH EDITION, NEW YORK, 1984.

GER = A. BANERJEA ET AL., THERMODYNAMISCHE STOFFWERTE VON HELIUM IM BEREICH 20 BIS 1500C UND 1 BIS 100 BAR, RHEINISCH-WESTFÄLISCHEN TECHNISCHEN ÜBERWACHUNGS-VEREIN E.V. UND DER INTERATOM GMBH, 1978.

Table 1.3 Helium Entropy as Calculated, from Tables, and Per Cent Errors

		ENTROPY (KJ/KG-K)						
P (BAR)	T (K)	MINET	REY.	PERRY	GER.	%ERR-R	%ERR-P	%ERR-G
1	273	2.9463	2.9164	2.9478	2.9463	1.025	-0.025	0.000
1	473	3.2319	3.2229	3.2319	3.2532	0.280	0.000	-0.654
1	773	3.4871	3.4784	3.4869	3.4868	0.250	0.006	0.009
1	1073	3.6575	3.6493	3.6572	3.6571	0.225	0.008	0.011
1	1273	3.7463	3.7337	3.7459	3.7459	0.337	0.011	0.011
1	1473	3.8221	3.8179		3.8217	0.110		0.010
5	273	2.6118	2.5779	2.6123	2.6121	1.315	+0.019	-0.011
5	473	2.8975	2.8914	2.8976	2.8974	0.211	-0.003	0.003
5	773	3.1527	3.1470	3.1526	3.1525	0.181	0.003	-0.003
5	1073	3.3231	3.3178	3.3229	3.3228	0.160	0.005	0.009
5	1273	3.4191	3.4020	3.4116	3.4116	0.291	0.009	0.009
5	1473	3.4877	3.4863		3.4874	0.040		0.008
10	273	2.4678	2.4409	2.4684	2.4532	0.938	-0.024	0.350
10	473	2.7535	2.7474	2.7537	2.7535	0.222	-0.007	0.000
10	773	3.0087	3.0030	3.0087	3.0085	0.190	0.000	0.007
10	1073	3.1791	3.1739	3.1789	3.1788	0.164	0.006	0.010
10	1273	3.2679	3.2581	3.2677	3.2676	0.301	0.006	0.009
10	1473	3.3437	3.3423		3.3434	0.042		0.009
20	273	2.3237	2.2969	2.3245	2.3244	1.167	-0.034	-0.030
20	473	2.6096	2.6035	2.6095	2.6096	0.234	-0.008	0.000
20	773	2.8648	2.8648	2.8648	2.8646	0.000	0.000	0.007
20	1073	3.0351	3.0300	3.0350	3.0349	0.168	0.003	-0.003
20	1273	3.1239	3.1142	3.1237	3.1237	0.311	0.006	0.006
20	1473	3.1997	3.1984		3.1995	0.416		0.006
50	273	2.1331		2.1345	2.1347		-0.066	-0.075
50	473	2.4196		2.4195	2.4196		0.004	0.000
50	773	2.6746		2.6744	2.6745		0.004	0.002
50	1073	2.8449		2.8446	2.8447		0.010	0.007
50	1273	2.9336		2.9333	2.9334		0.010	0.007
50	1473	3.0094			3.0092			0.007
100	273	1.9888	1.9629	1.9900	1.9919	1.319	-0.100	-0.156
100	473	2.2761	2.2352	2.2760	2.2762	1.830	0.004	-0.004
100	773	2.5410	2.5254	2.5308	2.5308	0.252	0.008	0.008
100	1073	2.7012	2.6962	2.7009	2.7009	0.185	0.011	0.011
100	1273	2.7899	2.7803	2.7896	2.7896	0.345	0.011	0.011
100	1473	2.8656	2.8544		2.8653	0.042		0.010
500	273	1.6528	1.6316			1.259		
500	473	1.9465	1.9395			0.356		
500	773	2.2003	2.1943			0.273		
500	1073	2.3694	2.3646			0.203		
500	1273	2.4576	2.4485			0.372		
500	1473	2.5330	2.5305			0.020		
1000	273	1.5066	1.4922			0.965		
1000	473	1.8088	1.8008			0.454		
1000	773	2.0606	2.0542			0.312		
1000	1073	2.2299	2.2238			-0.045		
1000	1273	2.3163	2.3075			0.381		
1000	1473	2.3912	2.3912			0.000		

REY. = W. C. REYNOLDS, THERMODYNAMIC PROPERTIES IN S. I., DEPARTMENT OF MECH. ENG., STANFORD U., 1979.

PERRY = PERRY'S CHEMICAL ENGINEERING HANDBOOK, 6TH EDITION, NEW YORK, 1984.

GER = A. BANERJEA ET AL., THERMODYNAMISCHE STOFFWERTE VON HELIUM IM BEREICH 20 BIS 1500C UND 1 BIS 100 BAR, RHEINISCH-WESTFÄLISCHEN TECHNISCHEN ÜBERWACHUNGS-VEREIN E. V. UND DER INTERATOM GMBH, 1978.

Table 1.4 Helium Viscosity as Calculated, from Tables, and Per Cent Errors

VISCOSITY (10E-5 NS/M2)

P (BAR)	T (K)	MINET	VAR.	GER.	%ERR-V	%ERR-G
1	273	1.8640	1.860	1.865	0.215	-0.054
1	373	2.3192	2.292	2.320	1.186	-0.034
1	473	2.7387	2.688	2.739	1.886	-0.011
1	773	3.8625	3.745	3.863	3.138	-0.013
1	1073	4.8591		4.860		-0.019
1	1273	5.4767	5.264	5.477	4.040	-0.005
1	1773	6.9061		6.907		-0.013
1.0133	273	1.8640		1.865		-0.054
1.0133	373	2.3192		2.320		-0.034
1.0133	473	2.7387		2.739		-0.011
1.0133	773	3.8625		3.863		-0.013
1.0133	1073	4.8591		4.860		-0.019
1.0133	1273	5.4767		5.477		-0.005
1.0133	1773	6.9061		6.907		-0.013
10	273	1.8640		1.865		-0.054
10	373	2.3192		2.320		-0.034
10	473	2.7387		2.739		-0.011
10	773	3.8625		3.863		-0.013
10	1073	4.8591		4.860		-0.019
10	1273	5.4767		5.477		-0.005
10	1773	6.9061		6.907		-0.013
50	273	1.8639	1.862	1.865	0.100	-0.059
50	373	2.3191		2.320		-0.036
50	473	2.7387		2.739		-0.011
50	773	3.8625		3.863		-0.013
50	1073	4.8592		4.860		-0.016
50	1273	5.4767		5.477		-0.005
50	1773	6.9061		6.907		-0.013
100	273	1.8636	1.864	1.865	-0.021	-0.075
100	373	2.3191	2.299	2.320	0.670	-0.039
100	473	2.7387	2.693	2.739	1.697	0.011
100	773	3.8625		3.863		-0.013
100	1073	4.8592		4.860		-0.016
100	1273	5.4767		5.477		-0.005
100	1773	6.9061		6.907		-0.013
200	273	1.8640	1.873			-0.480
200	373	2.3191	2.312		0.307	
200	473	2.7387	2.700		1.433	
200	773	3.8626	3.750		3.003	
200	1073	4.8592				
200	1273	5.4768	5.265		4.023	
200	1773	6.9061				
500	273	1.8640	1.975		-5.620	
500	373	2.3191	2.372		-2.230	
500	473	2.7389	2.743		-0.149	
500	773	3.8625	3.770		2.453	
500	1073	4.8597				
500	1273	5.4768	5.280		3.537	
500	1773	6.9061				

VAR = VARGAFTIK, N.B. (1975) TABLES ON THE THERMOPHYSICAL PROPERTIES OF LIQUIDS AND GASES, 2ND ED., HEMISPHERE PUBLISHING CORPORATION, WASHINGTON.

GER = A. BANERJEA ET AL., THERMODYNAMISCHE STOFFWERTE VON HELIUM IM BEREICH 20 BIS 1500C UND 1 BIS 100 BAR, DECEMBER, 1978, RHEINISCH-WESTFÄLISCHEN TECHNISCHEN ÜBERWACHUNGS-VEREIN E. V. UND CER (INTERNATOM O/8H).

Table 1.5 Helium Thermal Conductivity as Calculated,  
from Tables, and Per Cent Errors

THERMAL CONDUCTIVITY (10E-1 W/MK)					
P (BAR)	T (K)	MINET	VAR.	GER.	%ERR-V
1	273	1.4397	1.429	1.440	0.700
1	373	1.7968	1.742	1.797	3.146
1	473	2.1268	2.088	2.217	1.858
1	773	3.0140	2.970	3.014	1.481
1	1073	3.8040	3.722	3.804	2.203
1	1273	4.2947	4.232	4.295	1.482
1	1773	5.4334		5.434	
1.0133	273	1.4397	1.429	1.440	0.700
1.0133	373	1.7968	1.742	1.797	3.146
1.0133	473	2.1268	2.088	2.217	1.858
1.0133	773	3.0140	2.970	3.014	1.481
1.0133	1073	3.8040	3.722	3.804	2.203
1.0133	1273	4.2947	4.232	4.295	1.482
1.0133	1773	5.4236		5.434	
10	273	1.4439		1.444	
10	373	1.8012		1.807	
10	473	2.1314		2.137	
10	773	3.0187		3.019	
10	1073	3.8083		3.809	
10	1273	4.2986		4.299	
10	1773	5.4360		5.436	
50	273	1.4606	1.452	1.461	0.592
50	373	1.8190	1.743	1.820	4.360
50	473	2.1495	2.108	2.150	1.969
50	773	3.0359	2.980	3.036	1.876
50	1073	3.8229	3.732	3.823	2.435
50	1273	4.3109	4.235	4.311	1.755
50	1773	5.4413		5.442	
100	273	1.4780	1.476	1.479	0.136
100	373	1.8368	1.783	1.837	3.017
100	473	2.1670	2.123	2.167	2.073
100	773	3.0499	2.990	3.050	2.003
100	1073	3.8315	3.742	3.832	2.392
100	1273	4.3154	4.243	4.316	1.697
100	1773	5.4342		5.434	
200	273	1.5029	1.539		-2.346
200	373	1.8592	1.777		4.626
200	473	2.1860	2.159		1.251
200	773	3.0553	3.010		1.505
200	1073	3.8205	3.680		3.818
200	1273	4.2925	4.255		0.881
200	1773	5.7399			

VAR = VARGAFTIK, N.B. (1975) TABLES ON THE THERMOPHYSICAL PROPERTIES OF LIQUIDS AND GASES, 2ND ED., HEMISPHERE PUBLISHING CORPORATION, WASHINGTON.

GER = A. BANERJEA ET AL., THERMODYNAMISCHE STOFFWERTE VON HELIUM IN BEREICH 20 BIS 1500C UND 1 BIS 1000 BAR DECEMBER, 1978, RHEINISCH-WESTFALLEN TECHNISCHEN UBERWACHUNGS-VEREIN E.V. UND DER INTERATOM GMBH.

\*\*NOTE (THE GERMAN PAPER BY COINCIDENCE USED THE SAME HELIUM FUNCTIONS AS MINET, THUS ERROR CALCULATIONS AGAINST IT WERE RATHER POINTLESS.)



Table 1.6 Helium Property Derivatives as Calculated by Functions,  
Compared Against Finite Differenced Values

P(MPA)	T(K)	CP(KJ/KGK)	(DR/DH)	(DR/DP)	
.1	273.0	5196.9	-.12412E-06	.17613E-05	(FUNCTION)
		5196.9	-.12412E-06	.17613E-05	(FIN. DIFF.)
.1	373.0	5196.2	-.66516E-07	.12894E-05	(FUNCTION)
		5196.2	-.66512E-07	.12894E-05	(FIN. DIFF.)
.1	773.0	5195.9	-.15495E-07	.62241E-06	(FUNCTION)
		5195.9	-.15494E-07	.62241E-06	(FIN. DIFF.)
.1	1273.0	5195.9	-.57143E-08	.37798E-06	(FUNCTION)
		5195.9	-.57141E-08	.37798E-06	(FIN. DIFF.)
.1	1573.0	5196.0	-.37426E-08	.30591E-06	(FUNCTION)
		5196.0	-.37425E-08	.30591E-06	(FIN. DIFF.)
.5	273.0	5200.3	-.61760E-06	.17554E-05	(FUNCTION)
		5200.3	-.61766E-06	.17554E-05	(FIN. DIFF.)
.5	373.0	5196.9	-.33154E-06	.12864E-05	
		5196.9	-.33145E-06	.12864E-05	
.5	773.0	5195.6	-.77386E-07	.62184E-06	
		5195.6	-.77369E-07	.62184E-06	
.5	1273.0	5195.7	-.28554E-07	.37780E-06	
		5195.7	-.28551E-07	.37780E-06	
.5	1573.0	5195.8	-.18705E-07	.30579E-06	
		5195.8	-.18703E-07	.30579E-06	
2.5	273.0	5217.5	-.30147E-05	.17262E-05	(FUNCTION)
		5217.5	-.30162E-05	.17263E-05	(FIN. DIFF.)
2.5	373.0	5200.5	-.16320E-05	.12717E-05	
		5200.5	-.16300E-05	.12717E-05	
2.5	773.0	5193.9	-.38468E-06	.61900E-06	
		5193.9	-.38426E-06	.61900E-06	
2.5	1273.0	5194.5	-.14235E-06	.37691E-06	
		5194.5	-.14226E-06	.37691E-06	
2.5	1573.0	5194.8	-.93313E-07	.30524E-06	
		5194.8	-.93267E-07	.30524E-06	
10.0	273.0	5282.2	-.11042E-04	.16237E-05	(FUNCTION)
		5282.2	-.11065E-04	.16238E-05	(FIN. DIFF.)
10.0	373.0	5214.0	-.61627E-05	.12188E-05	
		5214.0	-.61325E-05	.12187E-05	
10.0	773.0	5187.7	-.15057E-05	.60856E-06	
		5187.7	-.14992E-05	.60854E-06	
10.0	1273.0	5189.9	-.56306E-06	.37357E-06	
		5189.9	-.56165E-06	.37357E-06	
10.0	1573.0	5191.1	-.37012E-06	.30320E-06	
		5191.1	-.36940E-06	.30320E-06	
100.0	273.0	6057.8	-.46041E-04	.89239E-06	(FUNCTION)
		6057.5	-.46976E-04	.89505E-06	(FIN. DIFF.)
100.0	373.0	5376.3	-.34020E-04	.79408E-06	
		5376.2	-.32356E-04	.78860E-06	
100.0	773.0	5112.9	-.11825E-04	.50477E-06	
		5112.8	-.11319E-04	.50317E-06	
100.0	1273.0	5134.7	-.49514E-05	.33750E-06	
		5134.7	-.48276E-05	.33715E-06	
100.0	1573.0	5146.6	-.33560E-05	.28052E-06	
		5146.6	-.32909E-05	.28035E-06	

Entropy values were also compared to those from these same three references, again with excellent results, as shown in Table 1.3 (again the zeroes were aligned, when necessary). Entropy is currently used only in the MINET turbine module calculations, so it is not an essential property at the moment.

Viscosity and thermal conductivity data are not as broadly available, so the comparisons provided in Tables 1.4 and 1.5 are not as extensive as the three previous properties. Further, the MINET functions are German in origin, and these same property functions were probably used to generate the German tables. Thus, the tabular values from (Vargaftik, 1975) provide the only truly independent verification. Fortunately, the MINET functions compare well to the Vargaftik tables, given that viscosity and thermal conductivity values are really accurate to only 5% or so.

Three property derivative functions are used in the MINET code: 1) specific heat, 2) the derivative of density with respect to enthalpy, and 3) the derivative of density with respect to pressure. As these properties are dependent on the five properties already verified, it was only necessary to perform a consistency check. This was done by evaluating each of the three derivative functions over a wide range of temperatures and pressures, and by estimating the derivatives via finite differencing of the basic property functions. The results of this study are shown in Table 1.6. As can be seen, the derivative functions are in excellent agreement with the finite difference estimates.

One other property function (temperature as a function of enthalpy and pressure) is also used in MINET. This is simply an inverse of the enthalpy as a function of temperature and pressure function, and verification was performed by calculating enthalpy from temperature and the temperature from enthalpy and comparing over a wide range of pressures and temperatures.

As a result of this testing process, we can say with a high degree of confidence that the MINET helium properties are accurate over a wide pressure range and a fairly wide temperature range. We did not study the accuracy of the ideal gas law models, but believe the tables included could be useful in the performance of such a study.

#### 1.1.4 Reactor Building Transients with a Modified ATMOS Code (P. G. Kroeger)

Efforts to extend the ATMOS code to confinement or containment type reactor buildings were initiated. In its previous version, the ATMOS code analyzed containment building atmosphere transients subsequent to the initial blowdown for large HTGRs. Its main emphasis was to evaluate the containment building (CB) gas temperatures, pressures and gas composition to assess the CB failure potential from over-pressurization or from gas burning.

To apply the code to reactor building (RB) transients in modular reactors, several extensions of the ATMOS code are required. A typical RB for a modular HTGR is shown in Figure 1.1. In Figure 1.2, a schematic representation of the most essential parts of the RB is given. The major point of importance here is, that the RB for a modular reactor consists of several

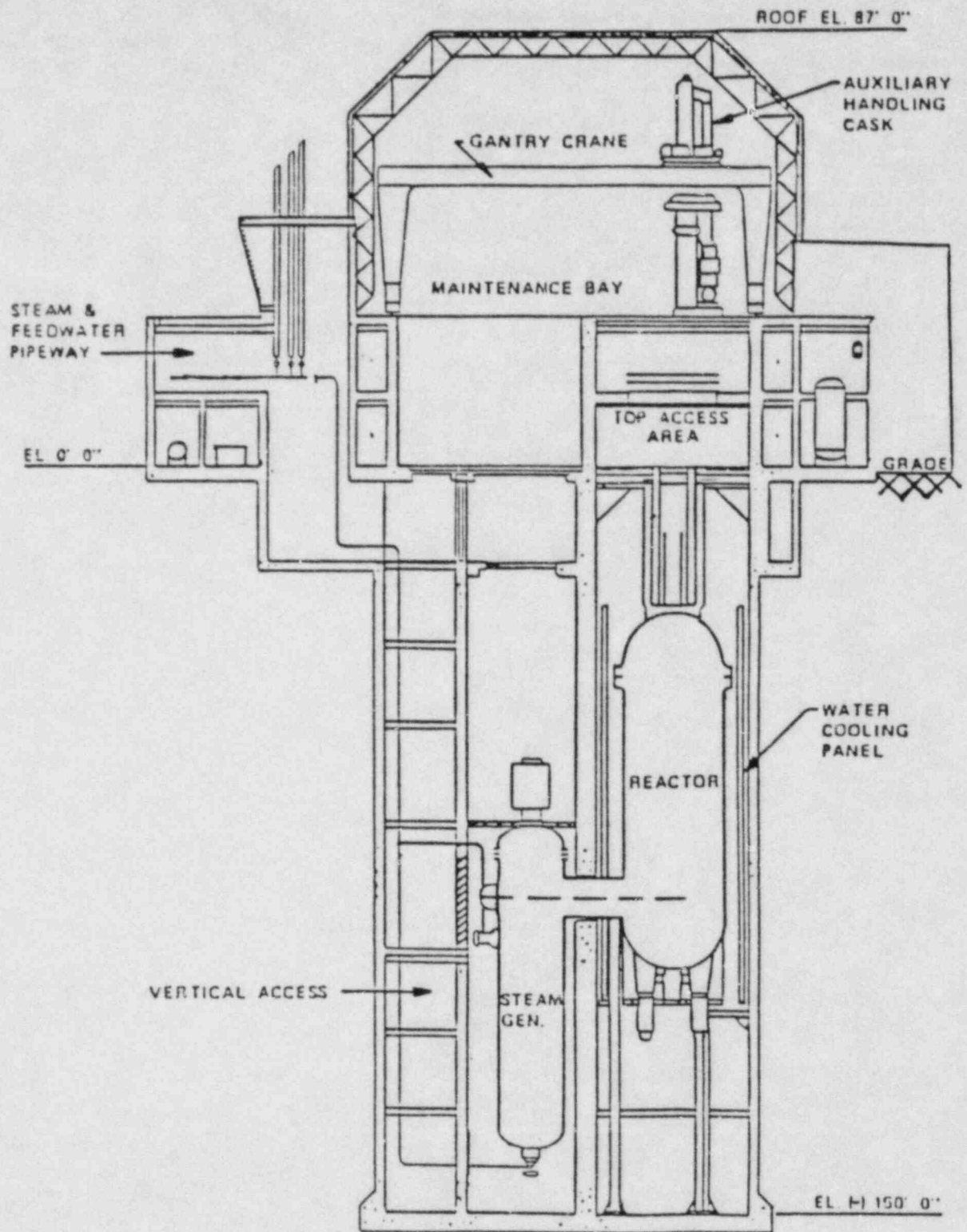


Figure 1.1 Elevation of Modular HTGR Reactor Building

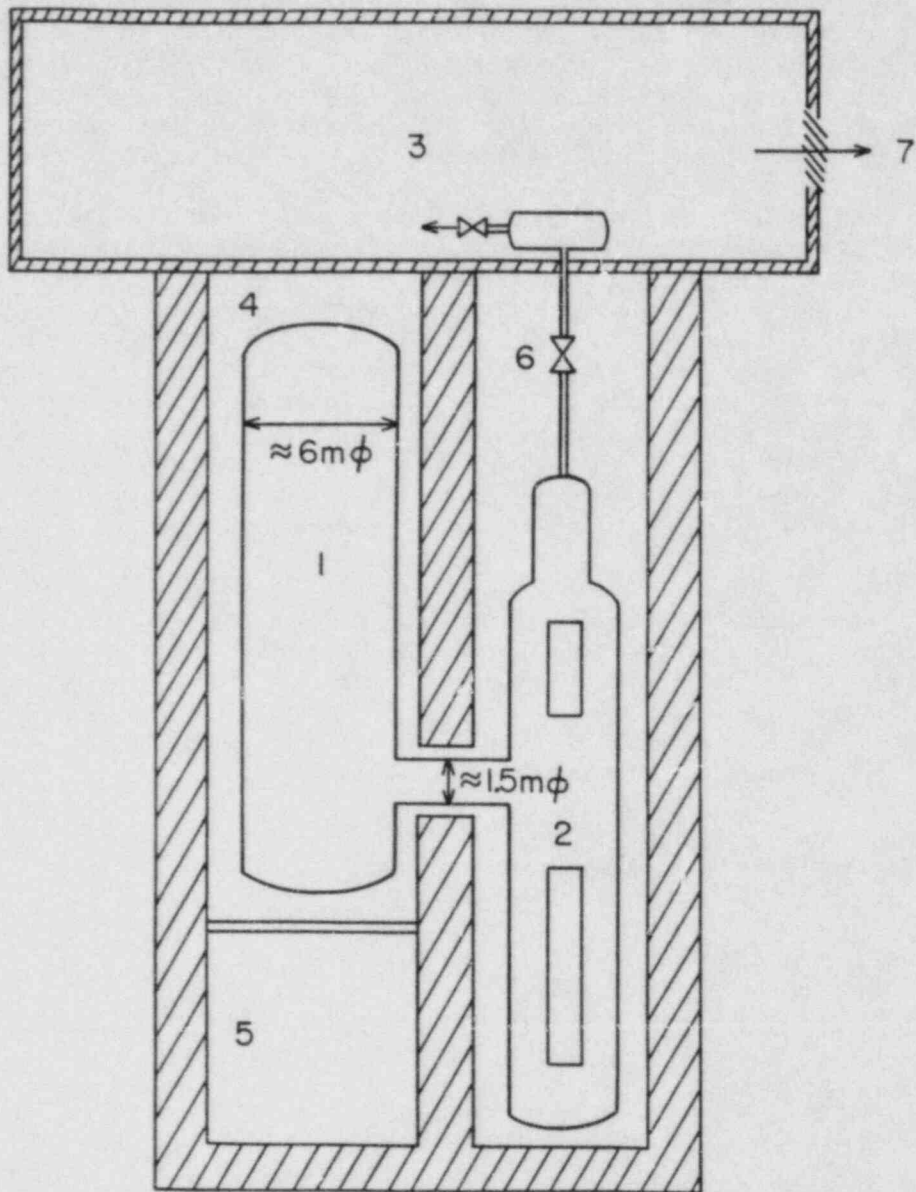


Figure 1.2 Schematic of Modular HTGR Reactor Building



"cavities" with no pressure boundary between them, but with limited mixing between the gas atmospheres of the various cavities. Also, for modular reactors, the vendor intends to suggest a confinement type RB, vented to the atmosphere. Figure 1.2 shows a safety valve discharge from the steam generator into the upper part of the RB (cavity 3). This is not necessarily the location of the safety valve discharge point, and different flow sequences and gas mixing would result if the discharge point were in one of the other cavities.

The main objective of the safety analyses of reactor building atmosphere transients is to evaluate the release of fission products from the RB during such transients. In pressurized (containment type) RBs, the main concern is for potential building failure due to over pressure, requiring an assessment of the gas temperatures, pressures, and flammability conditions in the various cavities. For vented (confinement type) RBs, there is an initial gas release from the RB to the atmosphere at the time of depressurization (generally long before fuel failures have occurred), plus potential slow releases later, during long core heatup transients. Again, to assess the gas release rates from the vented RB, the gas temperature histories in the various parts of the RB and the flammability conditions are the variables of major interest.

In contrast to CB transients in large HTGRs, cavities 4 and 2 (Figure 1.2) can be heated here directly from the reactor vessel, and, depending on the status of the Reactor Cavity Cooling System (RCCS), this can significantly affect the transient. As heat transfer to the surrounding solid structures was found to be the most important factor in previous work, it is intended to permit specification of an arbitrary number of solid structures in each cavity, similar to the approach taken in CNTB7 (Landoni, 1979).

The geometric arrangement of the RB as given in Figures 1.1 and 1.2 is certainly not the only configuration to be investigated in the safety evaluation of DOE/Industry concepts. The code modifications will, therefore, permit the user to specify the number of cavities and the desired flow connections between them. Similarly, heat exchange between cavities across solid capacitances (e.g. reactor vessel) will be a user specified option. Other features to be included were listed in Section 3.4 of our draft report on the assessment of modeling needs (Kroeger and Van Tuyle, 1985).

At this time, a general model for flow between heated and cooled cavities has been formulated, programmed and tested as a stand-alone set of routines, using the configuration of Figure 1.2. The inter-cavity flows over most of the long RB transients (except during the relatively short blowdown period) are predominantly due to gas expansion and contraction in the various cavities, with essentially uniform pressure in all cavities. For such cases, a limiting flow model can be obtained strictly from the ideal gas law, yielding the limiting flow required to keep the pressure uniform in space, but not necessarily in time. This model had been applied very successfully in the current ATMOS code. Considering its application to a user prescribed number of cavities with arbitrary flow connections, it was found that this model cannot provide unique solutions in case of closed loops in the system, as exists for instance between cavities 3, 4 and 6 of Figure 1.2. (See also Figure 1.3, Section 1.1.5). An alternate model using quasi-stationary momentum equations

was, therefore, provided. While both models have given identical results in testing thus far, the limiting flow model executes one to two orders of magnitude faster than a momentum equation model, which, due to the very low flow rates and low pressure drops, tends to make the system of ODEs and AEs very stiff. (A MINET application to this problem is represented in Section 1.1.5.) As closed loops are generally not essential in RB transients, we are currently proceeding to permit user options for the inter-cavity flows as follows:

- a. Limiting flow model, with some user specified flow relationship for any flow connection causing a closed loop. This model will execute rapidly and will be suitable for most applications.
- b. Inter-cavity flows computed from quasi-stationary momentum equations. This model works slower, but can fully evaluate closed loops.

At this time, the previous ATMOS model for heat conduction into solids has been revised into an implicit modular routine so that it can now be applied to any number of solid structures.

Before beginning with the final inclusion of the above items into the code, an alternate solution method was investigated. The current code, with 3 cavities and a maximum of 6 gas species per cavity, thus has 18 gas concentrations state variables for which mass conservation ODEs must be solved. It is, in principle, possible to substitute one single ODE for the total gas in the system and obtain the gas distribution over the cavities from algebraic equations. The advantage of this procedure would be the significantly lower number of ODEs to be integrated. However, in this second approach, the "updated" gas volume fractions in each cavity are not available at the beginning of a time step and must either be "lagged" (i.e., use last time step values), or be obtained by iteration. Furthermore, the flow rates between cavities, needed for solution of the gas energy equations, must be obtained from numerically computed derivatives in this method. Before initiating a major revision of the current code, it was felt to be desirable to investigate this option. The current code was modified to execute in this revised form with 17 less ODEs. It was found that time savings of only about 10 to 15% were obtainable from the revised method. However, since truncation errors were higher (even though tolerable), and since the coding became more cumbersome, it was judged to be preferable to retain the current method, since current code run times for 10 day transients range from 3 to 20 s (i.e., quickly enough so a 10% reduction is unimportant).

#### 1.1.5 Confinement Analysis Using MINET (G. J. Van Tuyle, P. G. Kroeger)

In a recent effort to extend the capabilities of the ATMOS code, which is used to perform containment/confinement building atmosphere transient analysis, some difficulties were encountered in representing multiply connected chambers (i.e., portions of the building connecting with two or more other portions forming closed loops). With such multiply connected regions, momentum equations have to be employed to determine the various flow rates. When the momentum equations were added to ATMOS, unacceptably small time steps became necessary, unless the form loss factors (between regions) were set



artificially high (e.g., 20). At the low pressure drops and flow rates prevailing, this has no significant effect on the resulting flow rates, and only changes cavity pressures in the fourth or fifth significant figure. Nevertheless, it is preferable to avoid such an artifice. As ATMOS employs a sophisticated DGEAR integration package that has been widely tested and applied, we were somewhat puzzled by the difficulties that were encountered.

In an effort to better understand the ATMOS difficulties, we set up and ran an equivalent representation using the MINET code. The system corresponded to a side-by-side modular HTGR confinement, as shown schematically in Figure 1.2. In representing this layout using MINET, we used 6 volume modules for the various chambers, along with 10 short pipes, and 4 boundary modules, as shown in Figure 1.3. Of the boundary modules, only the vent to atmosphere is important, as the ones labelled "trace" are extremely small and used only for initialization (to obtain non-zero flows). The MINET simulation of this system proceeded smoothly, and the time step size problem that was evident in the ATMOS analysis was absent from the MINET run, even for low form loss factors (e.g., 2). It should be noted that the total effort to set up, test, and run the MINET code for this case was about one man-day, and that the simulation of 100 seconds of transient time required less than 1 second of CPU time on a CDC 7600 mainframe.

These results show that the MINET numerics can handle such low pressure drop transients better than the well known CONAK package, at least for this test application. While the above MINET run times are significantly slower than those of the version of ATMOS with the limiting expansion/contraction flow model, which runs at 20 s machine time for a 10 day transient, this test assures us of a valuable backup option should we encounter future difficulties in ATMOS with multiply-connected cells.

#### 1.2 Effect of Radioactive Decay Chains on Source Terms (P. Kohut, A. L. Aronson)

The purpose of this effort is to evaluate the effect of fission product transmutation and decay on fission product transport during severe accident conditions. In the first phase of this study, the effect of fission product decay has been analyzed for an HTGR core. The hypothetical accident sequence involved the failure of the liner cooling system leading to total core degradation. The build-up and assumed deflagration of combustible gases eventually lead to the failure of the containment building, releasing a significant amount of radiation fission products. The details of the various models included to describe a) the release of fission products from the fuel, their subsequent transport through the graphite, upper plenum and containment building, and b) the decomposition of structural materials, are discussed in (Reilly et al., 1984). The present study is an analysis relative to those of (Reilly et al., 1984), where the complete treatment of the various decay schemes has been simplified using a decay factor based on more detailed calculations.

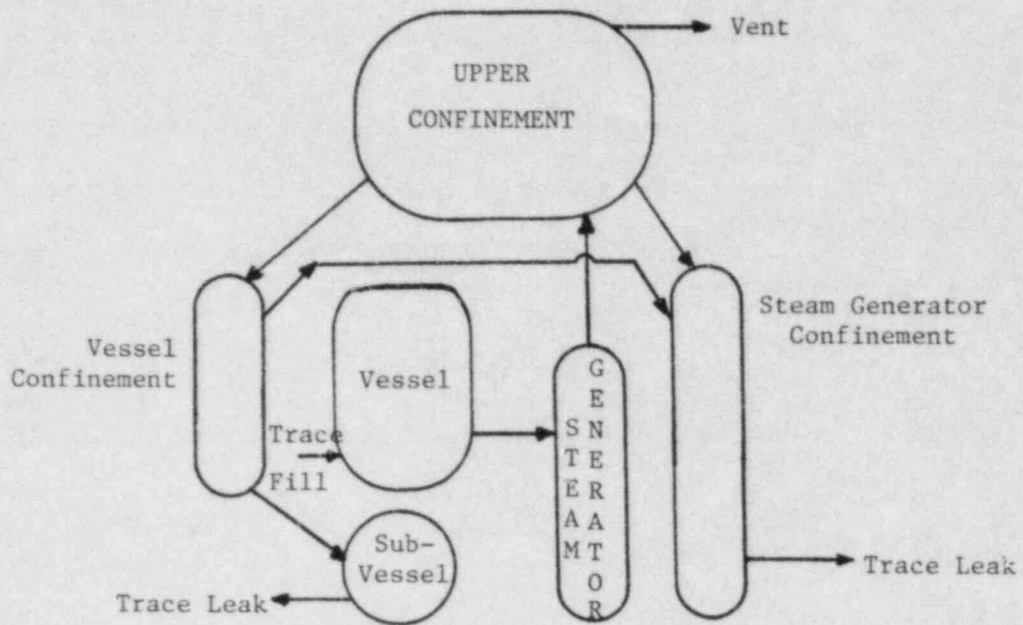


Figure 1.3 MINET Representation of Confinement,  
Designated CFI

Three groups of isotopes have been selected for complete decay treatment:

- noble gases (Xe, Kr)
- iodine
- organic iodine

The fraction of iodine converted to organic form has been set in accordance with (Reilly et al., 1984).

The initial fission product inventory has been determined using the isotope generation and depletion code, ORIGEN (Bell, 1973). A two year HTGR fuel cycle has been assumed, with 20% enriched fuel, at a core power level of 2240 MWt. The resulting initial inventory of hundreds of radioactive actinide fission products and structural material isotopes has been lumped into several groups for calculational purposes. The BNL in-house code, FPATMOS has been used to calculate the distribution and transport of the various radioactive isotopes, through the fuel, graphite, plenum and containment. The decay equations for all selected isotopes are solved separately in each volume, accounting for the differences in the transport and distribution of the precursors. The accident sequence has been analyzed by two sets of calculations.

In (Reilly et al., 1984) the inventory of radioactive nuclides is decreased by a decay factor, which represents the fraction of radioactive nuclides remaining after 10 hr. of decay.

The decay factor was derived from more detailed calculations with ORIGEN. This approximation accounts for the decay of each isotope rather well, with a few exceptions (~10-20% error after 300 hr.). However, the increase in inventory due to precursor decay is totally neglected.

In the second calculation, these approximations have been replaced with complete decay treatment for the three groups of selected isotopes.

In the analyzed accident all forced cooling is lost, the primary system depressurizes, the liner cooling system does not function, and the core heats up. Subsequently, the concrete starts decomposing, generating non-condensable gases. Due to the build-up and deflagration of combustible gases, the containment building fails at 140 hr into the accident. The major consequences are (Reilly et al., 1984):

- a) Noble gases (Xe, Kr) and organic iodine are essentially released to the environment,
- b) Iodine is primarily deposited on the containment building floor,
- c) The Te group is also deposited on the containment building floor, in the form of settled aerosols, and
- d) Only a small fraction of the remaining fission products will escape to the environment.

The main results of the present study relative to (Reilly et al., 1984) are shown in Figures 1.4 and 1.5. The total atmospheric radioactivity releases due to all fission products have been substantially reduced, by ~40%. This is mainly due to the ~55% reduction in the activity of the released noble gases (Xe, Kr). However, the iodine and organic iodine group behaves somewhat differently. Here, primarily due to the precursor Te ( $^{132}\text{Te} + ^{132}\text{I}$ ), the amount of iodine and organic iodine present in each volume can actually increase. Since all organic iodine is suspended in the containment building atmosphere, and iodine settles out at a particular rate, the atmospheric release will contain all organic iodine and only a fraction of the iodine isotopes. Even though the total atmospheric release due to all fission products is decreased by ~40%, the iodine release is reduced by only ~10% due to the build-up of  $^{132}\text{I}$  from the decaying precursor  $^{132}\text{Te}$ . This effect is even more significant in the case of organic iodine, where the atmospheric activity release actually increases by a factor of ~2.5.

In summary, the physical and chemical behavior of precursors, as well as the complete decay treatment of fission product isotopes, are relatively important effects which, depending on accident sequences, cannot be neglected.

### 1.3 HTGR Safety Handbook (K. J. Araj et al.)

A draft of all handbook sections assigned to Brookhaven National Laboratory was completed and submitted to the NRC for comments and review.

### 1.4 Graphite and Ceramics (J. H. Heiser, III, D. Wales, C. Finfrock, B. S. Lee)

As part of the experimental effort, the elastic moduli of oxidized and control samples of 2020 graphite were measured from the slopes of the stress-strain curves which were produced during destructive compressive strength testing. Also, the oxidation rate runs with the larger size H-451 graphite were completed, and a preliminary analysis of the oxidation kinetic data from TS-1621 and H-451 graphite was performed.

#### 1.4.1 Modulus of Elasticity of 2020 Graphite

The elastic module for HIL 2020 graphite samples #1 and #3 and one unoxidized control sample were measured from the slope of stress-strain curves (Figures 1.6 - 1.8) produced during destructive compressive strength testing. The elastic modulus was obtained from the linear portion of the curves where compression is elastic. This occurs near the origin of the stress-strain curves. Young's modulus for the control sample was 7.5 GPa, for sample #1 (5.9% B.O.) it was 6.9 GPa, and for sample #3 (7.8% B.O.) it was 5.0 GPa. These values are in agreement with values from GA. Young's modulus was also measured for sample #3 and the control via strain gages glued to the sample surfaces. Sample #3 yielded a value of 3.6 GPa and the control yielded 7.1 GPa. Agreement between curve values and strain gage values was good for the unoxidized control but poor for sample #3. This may be due to the high surface oxidation on specimen #3.



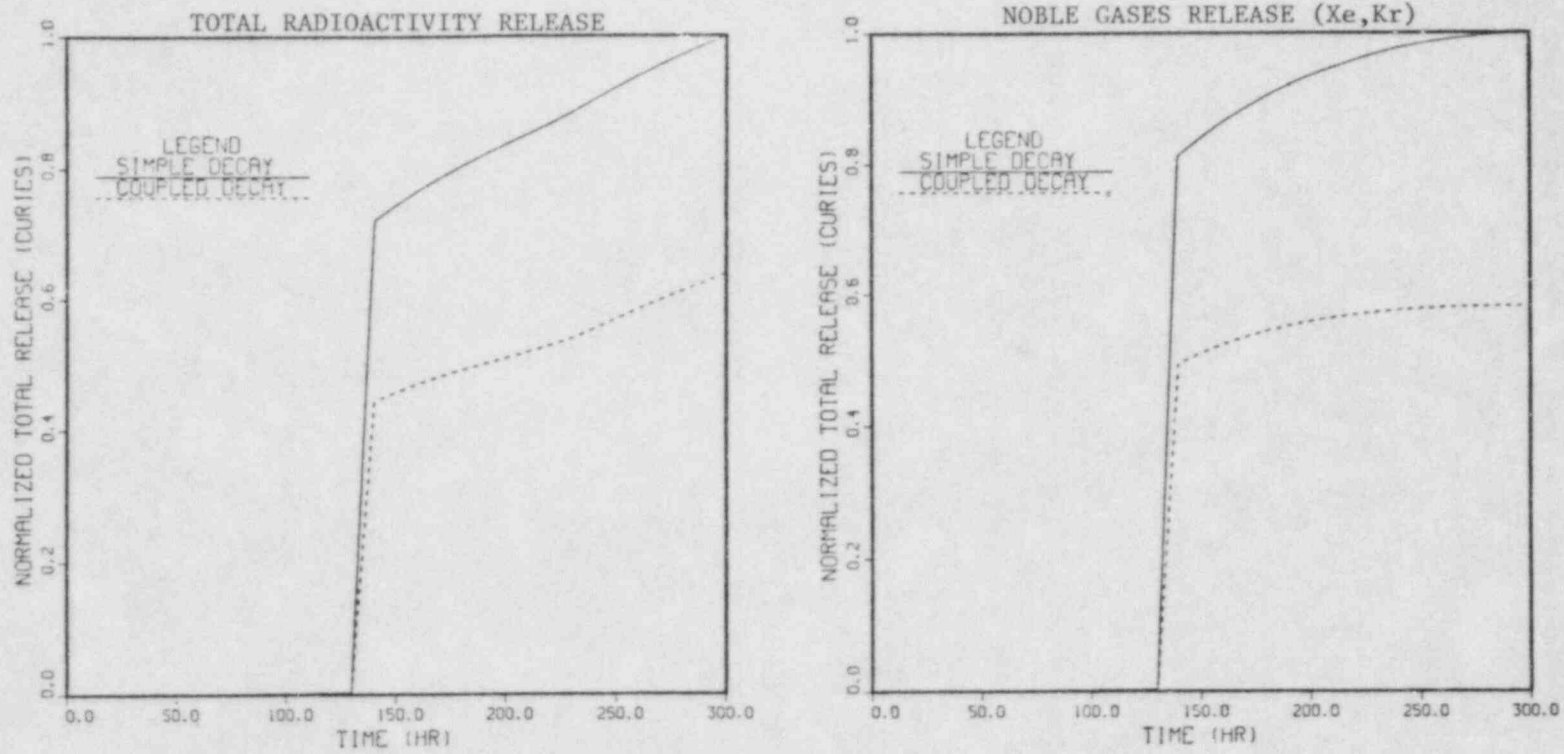


Figure 1.4 Atmospheric Radioactivity Release



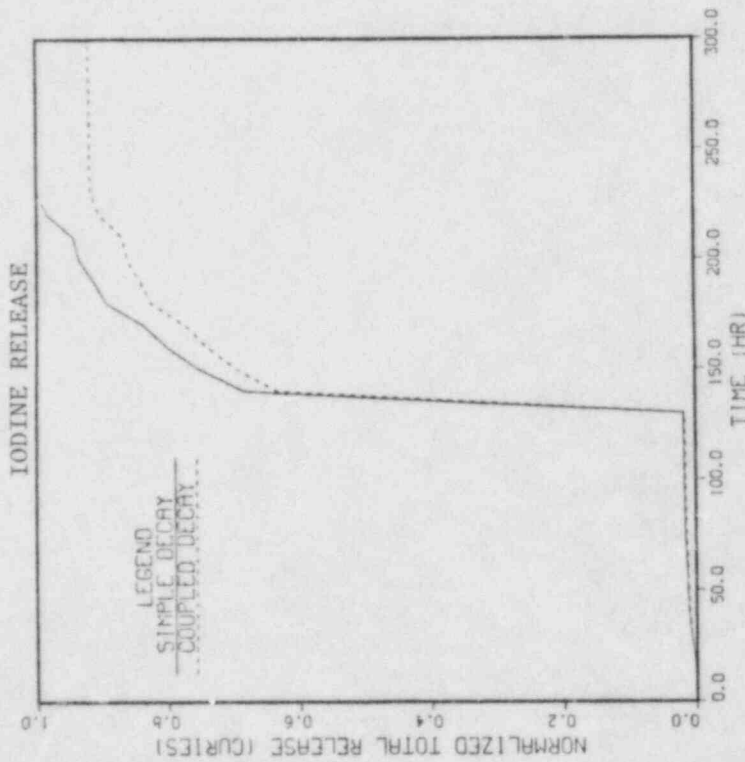
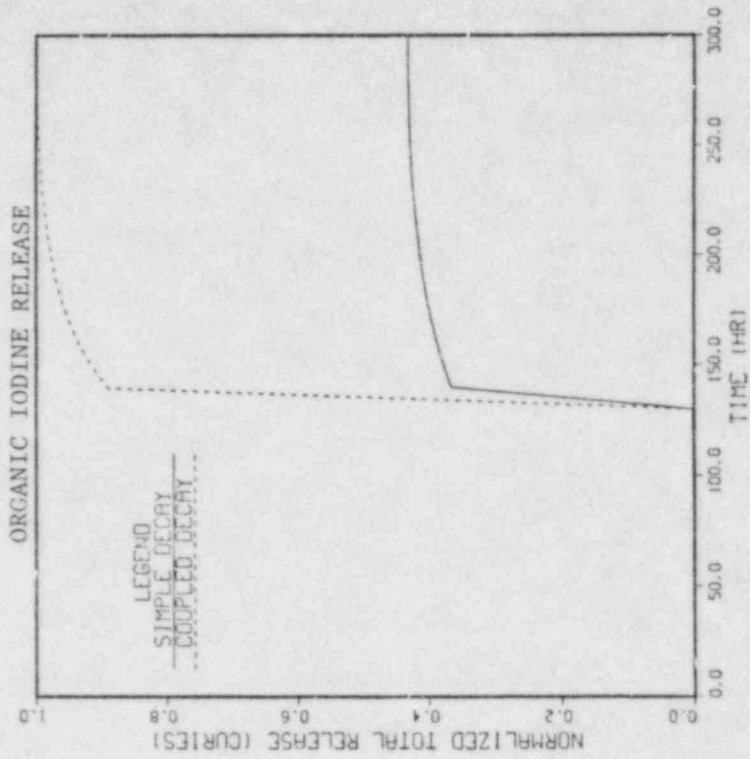


Figure 1.5 Atmospheric Radioactivity Release

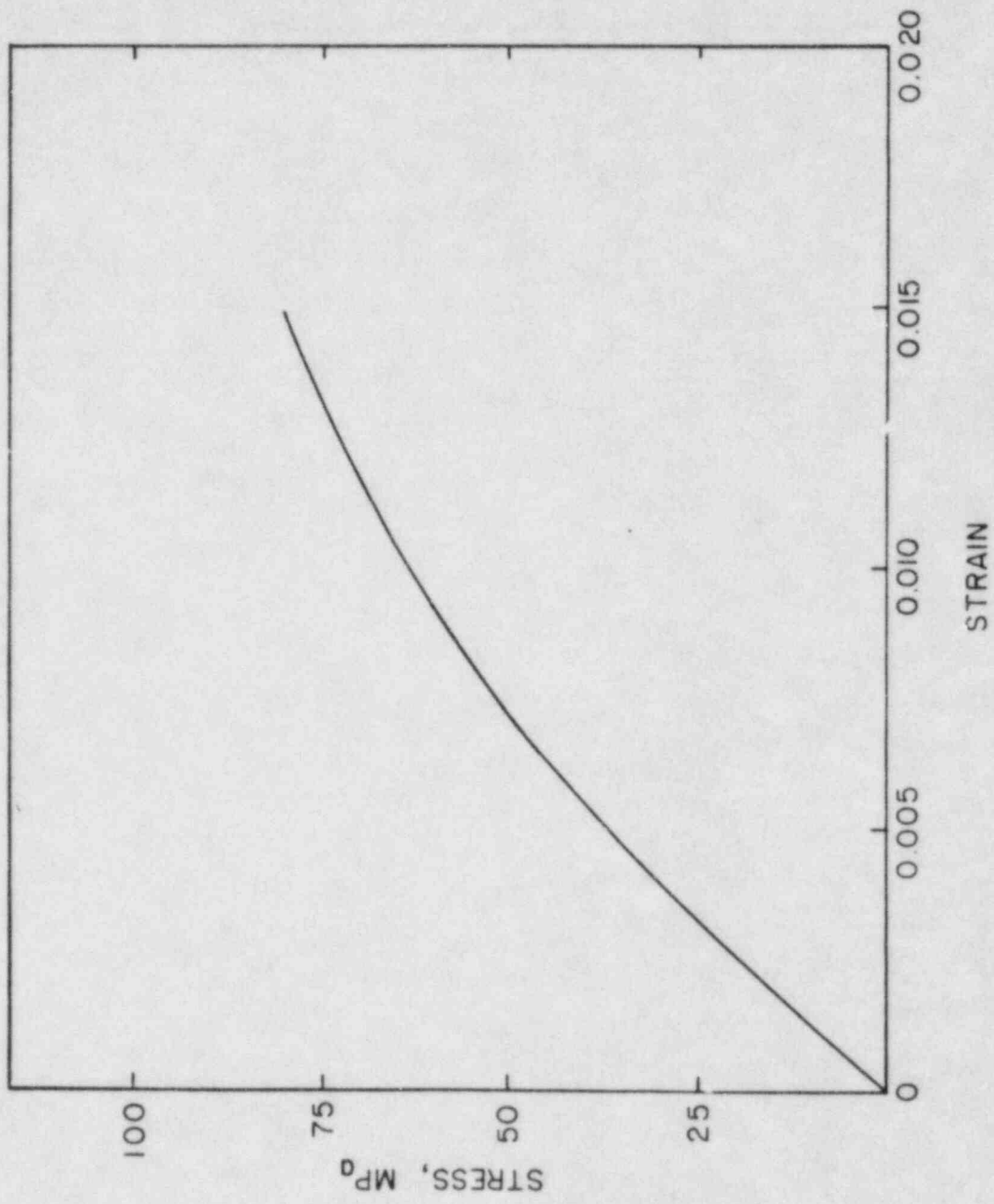


Figure 1.6 Compressive Stress-Strain Curve for Unoxidized Stackpole 2020 Control Sample

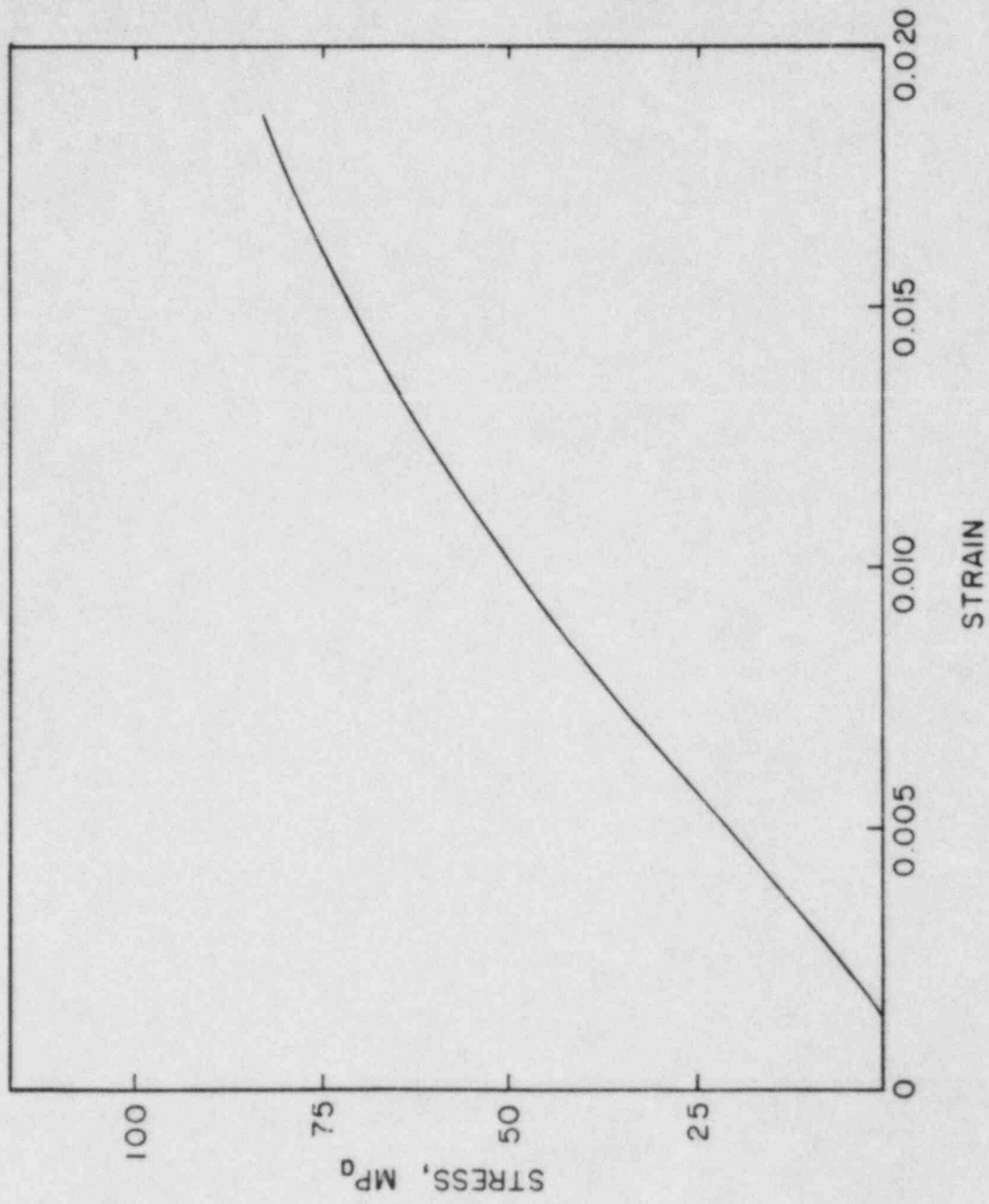


Figure 1.7 Compressive Stress-Strain Curve for Oxidized Stackpole 2020 #1 Sample

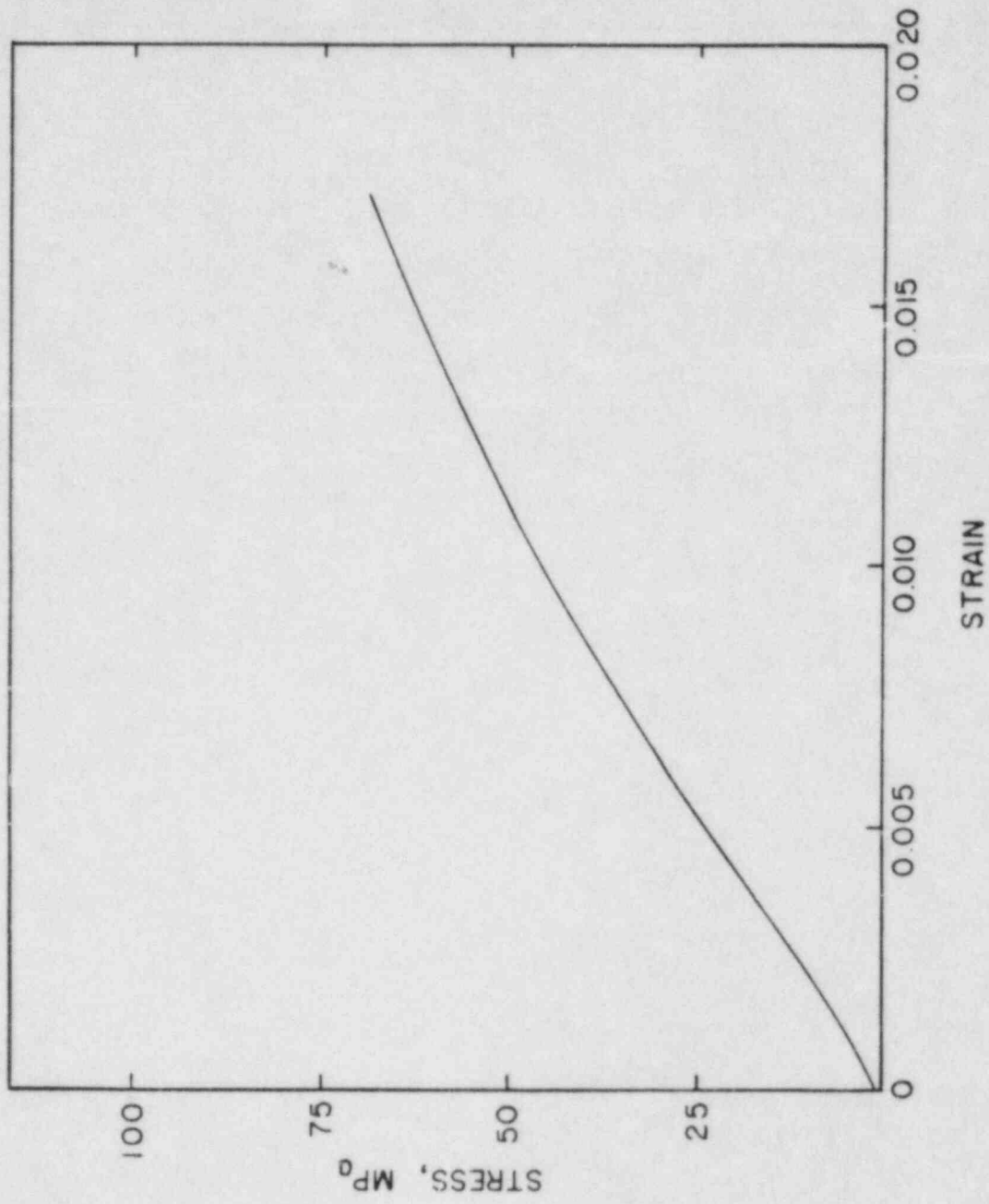


Figure 1.8 Compressive Stress-Strain Curve for Oxidized Stackpole 2020 #3 Sample

#### 1.4.2 Oxidation Kinetics Measurements

The oxidation rate runs with larger size (5.97 cm x 5.72 cm x 15.24 cm) H-451 graphite have been completed, and preliminary analyses of the oxidation kinetic data from TS-1621 and H-451 graphites have been conducted.

In the previous progress report (Guppy et al., 1985), it was shown that 2020 graphite followed a Gadsby-Hinshelwood type relationship at 850°C for the gas composition studied. It was also reported that PGX graphite also followed the same relationship when  $H_2/H_2O \approx 1.7$  to 10 at 850°C. The details of the analysis were discussed in that report.

The plot of  $1/R$  vs.  $1/P_{H_2O}$  for TS-1621 graphite, Figure 1.9, shows that the oxidation behavior can be expressed by a Gadsby-Hinshelwood type equation. The same conclusion can be drawn from the plot of  $1/R$  vs.  $\sqrt{P_{H_2}}$ , Figure 1.10. The total weight loss for the TS-1621 graphite sample was 1.06%.

The preliminary analysis of the plot of  $1/R$  vs.  $1/P_{H_2O}$  shows that the  $F$  value, product of burnoff factor ( $F^b$ ) and catalysis factor ( $F^c$ ), is  $\sim 0.9$  when the  $F$  for 2020 graphite is set as 1, which indicates that TS-1621 graphite is about 0.9 times reactive compared to 2020 graphite. This result is consistent with the measured oxidation rates shown in Table 1.7 (see after 440 hours).

Table 1.7

Oxidation Rates for 2020, PGX, TS-1621 and H-451 Graphites at 850° with 500 ppm  $H_2O$ /5000 ppm  $H_2$  (Balance He)

Graphite	Oxidation Rate (ppm (CO+CO <sub>2</sub> )/hr)		
	Initial Rate	After 50 hrs	After 440 hrs
202	278	239	262
PGX	673	1273	3746
TS-1621	451	340	242
H-451	198	199	40

The plots of  $1/R$  vs.  $1/P_{H_2O}$  and  $1/R$  vs.  $\sqrt{P_{H_2}}$  for H-451 graphite show that the oxidation rate can also be expressed by a Gadsby-Hinshelwood type relationship as shown in Figures 1.11 and Figures 1.12, respectively.

The preliminary analysis of the plot of  $1/R$  vs.  $1/H_2O$  and  $1/R$  vs.  $\sqrt{P_{H_2}}$  resulted in the  $F$  values of 0.08 and 0.19, respectively, which indicate that the reactivity of H-451 graphite is between  $\sim 8$  and  $\sim 19\%$  of that of the 2020 graphite. This result is consistent with the measured oxidation rates shown in Table 1.7 (see after 440 hours).



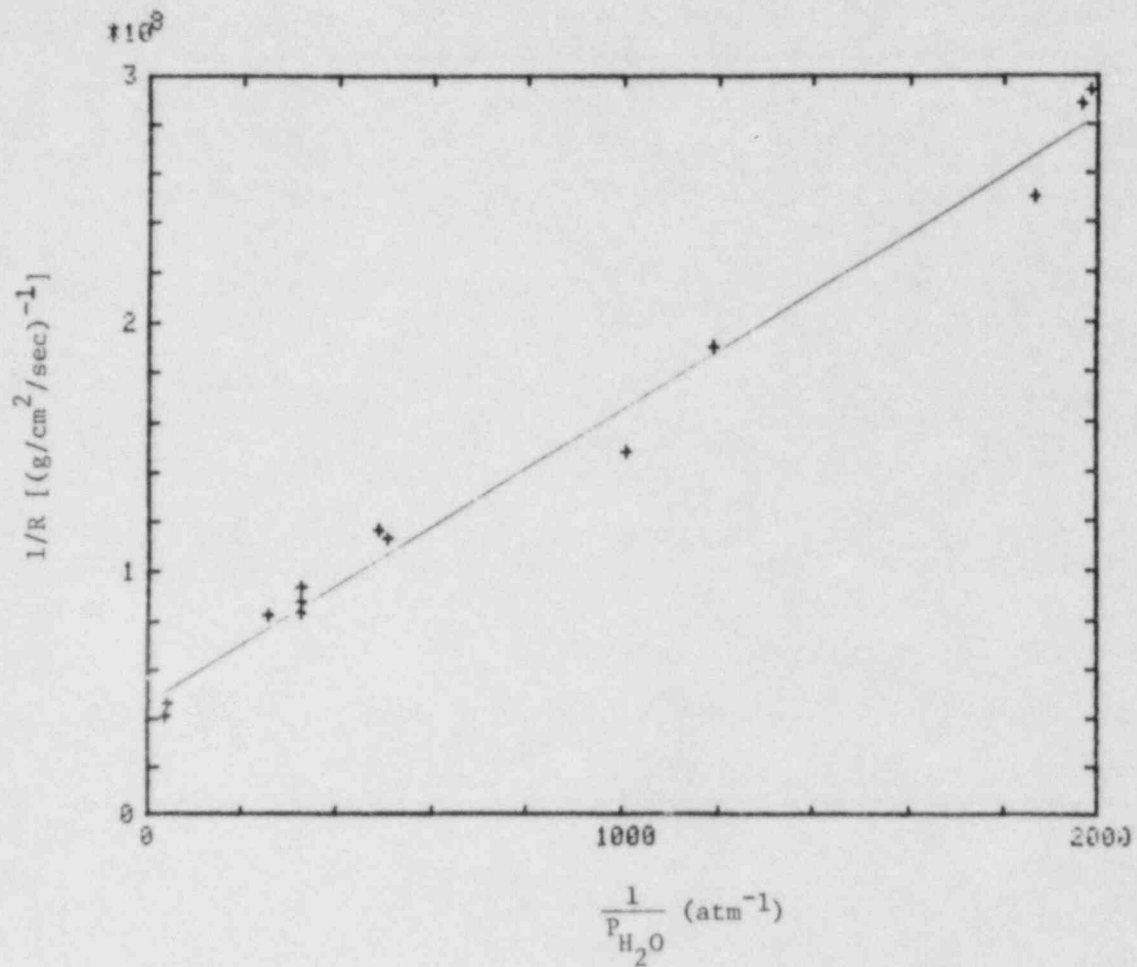


Figure 1.9 Oxidation Rate of TS-1621 Graphite as a Function of  $P_{H_2}$  at 850°C in  $P_{H_2O} \approx 6 \times 10^{-3}$  atm

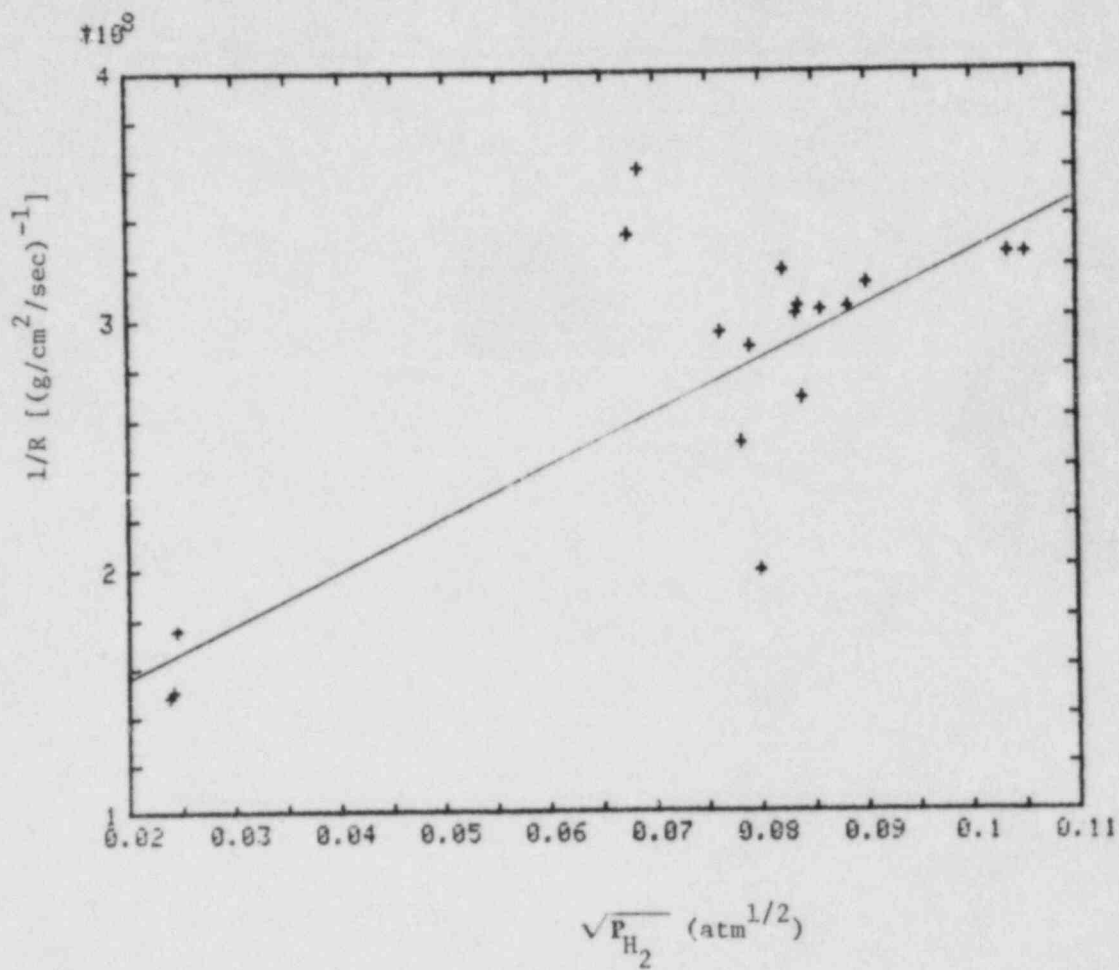


Figure 1.10 Oxidation Rate of TS-1621 Graphite as a Function of  $P_{H_2}$  at  $850^\circ C$  in  $P_{H_2O} \approx 5 \times 10^{-4} atm$

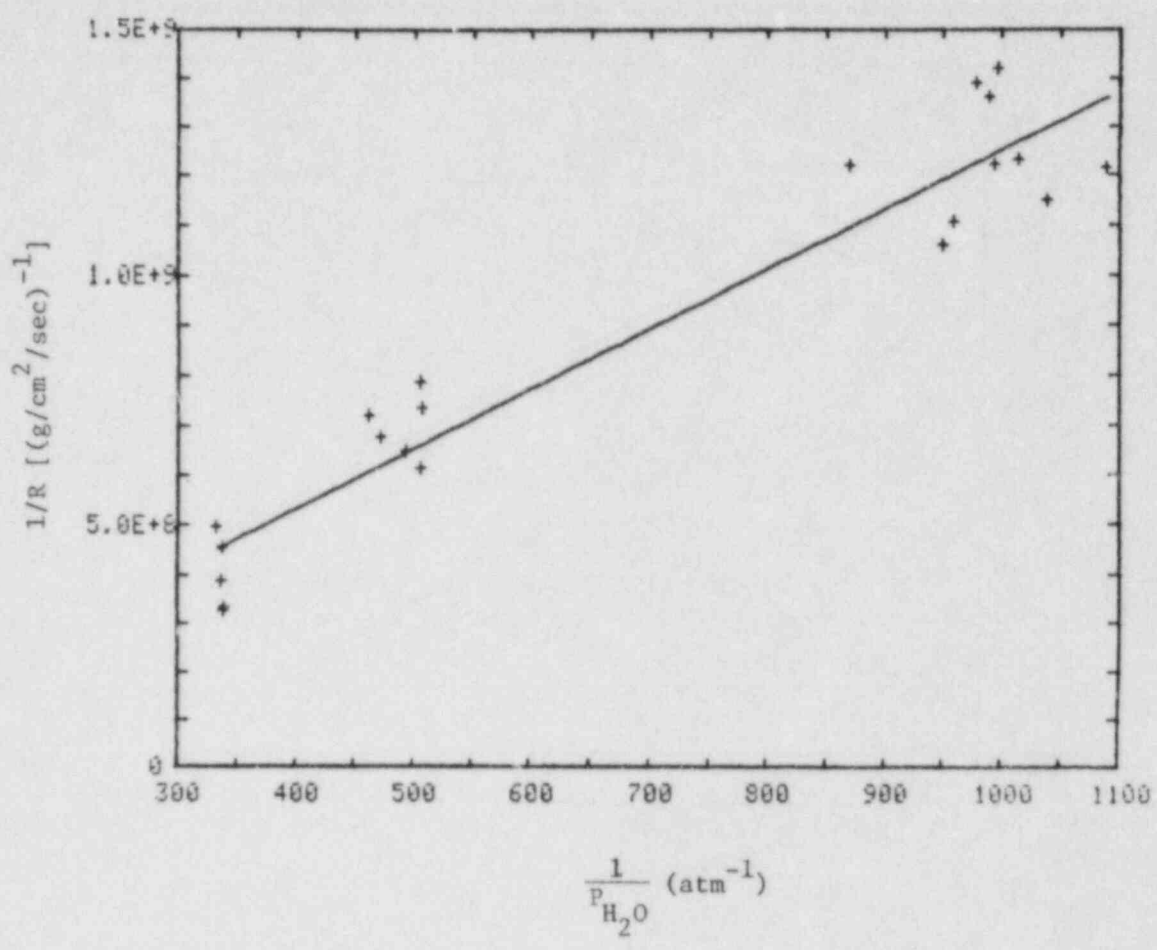


Figure 1.11 Oxidation Rate of H-451 Graphite as a Function of  $P_{H_2O}$  at 850°C in  $P_{H_2} \approx 5 \times 10^{-3}$  atm

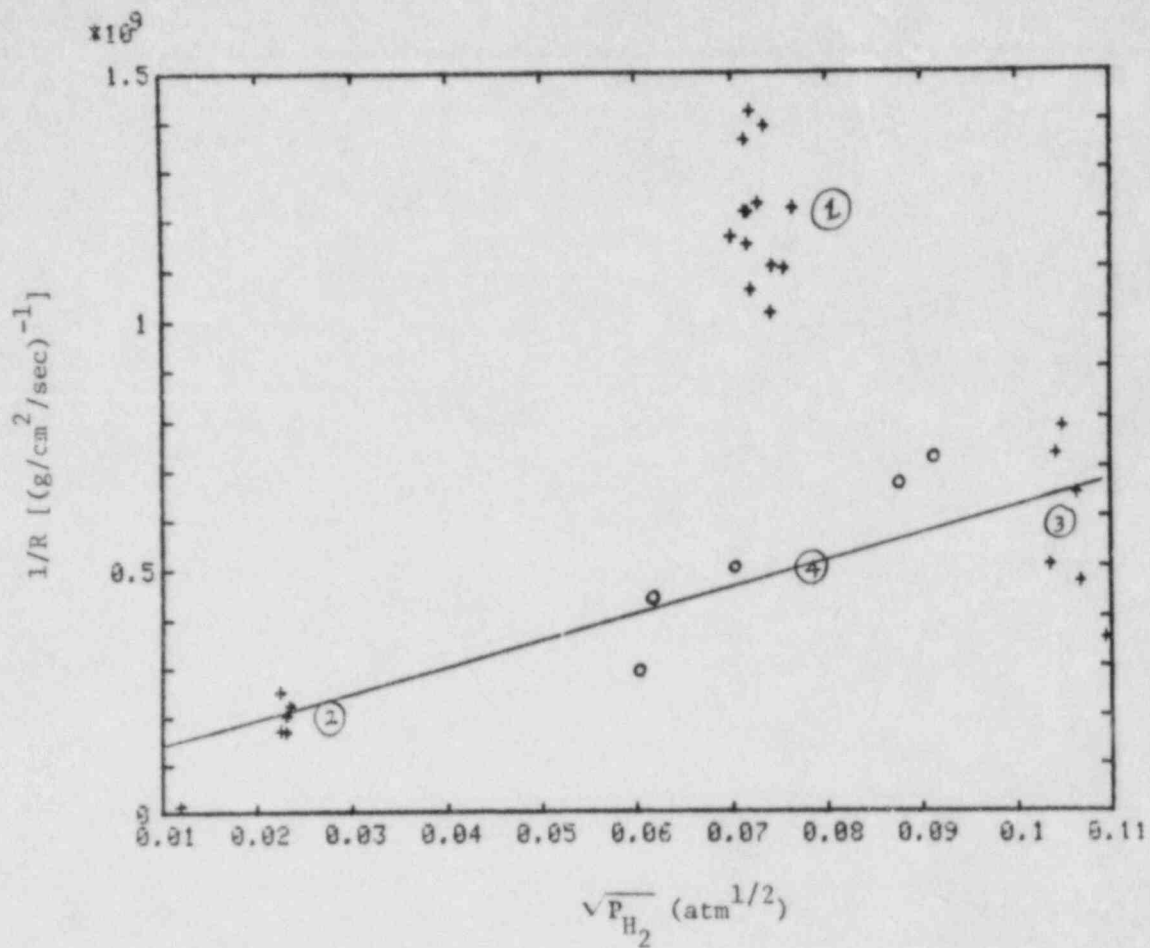


Figure 1.12 Oxidation Rate of H-451 Graphite as a Function of  $P_{\text{H}_2}$  at  $850^\circ\text{C}$  in  $P_{\text{H}_2\text{O}} \approx 1 \times 10^{-5}$  atm

For the H-451 graphite runs, after about 10 runs, it was difficult to keep the  $P_{H_2O}$  at  $\sim 5 \times 10^{-4}$  atm (it was higher than this level without any injection of  $H_2O$ ). It was speculated that, due to the very low  $H_2O$  consumption by the sample (very low oxidation rates), water was condensing on the inner surface of the tubes (at room temperature), close to the outlet of the gas from the reaction chamber, and was accumulating. This problem was circumvented by running most of the experiments at  $H_2O$  levels higher than  $1 \times 10^{-3}$  atm.

Figure 1.12 shows the four groups of data points in the order in which they were collected. For instance, group 1 data are from the early stage of the experiment (1400 ~ 1800 hours of duration) and group 4 data are from the last stage (2700 ~ 3000 hours). The period between group 1 and group 2,  $P_{H_2O}$  of  $\sim 2 \times 10^{-3}$  atm and  $\sim 3 \times 10^{-3}$  atm were used and as shown in Figure 1.12, the oxidation rates were high for these  $H_2O$  levels. Thus, it is believed that the major amount of oxidation occurred in the period between group 1 and group 2. The total relative weight loss for the H-451 sample was 0.63%.

Assuming that the catalytic effect of the impurities for H-451 is negligible, which is acceptable because of the very low impurities level of this graphite, it can be said that 0.63% burnoff caused an oxidation rate that was about two times higher than if there was no burnoff:

#### REFERENCES

- BAMMERT, K., (1969), "The Thermodynamic Properties of Helium as a Working Medium for Nuclear Power Plant Gas Turbines," Keintechnik #2, Feb. 1969.
- BANERJEA, A. et al., (1978), "Thermodynamische Stoffwerte von Helium im Bereich von 20 Bis 1500°C und 1 Bis 100 Bar," Kernforschungsanlage Juelich GmbH, Juel-1562.
- BELL, M. J., (1973), "ORIGEN - The ORNL Isotope Generation and Depletion Code," Oak Ridge National Laboratory Report ORNL-4628.
- GUPPY, J. G. et al., (1985), "High Temperature Reactor Research," Safety Research Programs Sponsored by Office of Nuclear Regulatory Research Quarterly Progress Report, Jan. 1 - Mar. 31, 1984, Brookhaven National Laboratory Report to be published.
- KROEGER, P. G. and VAN TUYLE, G. J., (1985), "Assessment of Modelling Needs for Safety Analysis of Current HTGR Concepts," Brookhaven National Laboratory Draft Report, February 1985.
- LANDONI, (1979), "The CNTB Program for the Analysis of Partially Mixed Containment Atmospheres during Depressurization Events," GA Technologies Inc., Report GA-A-13753.
- PERRY, (1934), Chemical Engineering Handbook, 6th Edition, New York.



REILLY, H. J. et al., (1984), "Preliminary Evaluation of HTGR Severe Accident Source Terms," (Appendix H - Analysis of Accidental Fission Product Releases to Atmosphere), Idaho National Engineering Laboratory, EGG-REP-6565, April 1984.

REYNOLDS, W. C., (1979), Thermodynamic Properties in SI, Department of Mechanical Engineering, Stanford University, Stanford, CA.

TALLACKSON, J. R., (1975), "The Thermal Transport Properties of Helium... for the Cache Program," Oak Ridge National Laboratory Report, ORNL/TM-4931.

VARGAFTIK, N. B., (1975), Tables on the Thermophysical Properties of Liquids and Gases, 2nd ed., Hemisphere Publishing Corporation, Washington.

#### PUBLICATIONS

CHAN, B. C. and KENNETT, R. J., "HTGR Containment Building Thermal Analysis," Brookhaven National Laboratory report to be published.

KROEGER, P. G. and CHAN, B. C., "Containment Building Atmosphere Response During Unrestricted Core-Heatup Accidents in High Temperature Gas-Cooled Reactors," Third International Meeting on Reactor Thermal Hydraulics, Newport, RI, October 15-18, 1985.

LEE, B. S. and HEISER, J. H., "Oxidation Kinetics Study on HTGR Graphites, 2020 and PGX," Extended Abstracts, 17th Biennial Conference on Carbon, University of Kentucky, Lexington, Kentucky, June 1985.

## 2. SSC/MINET Improvement, Validation and Application (J. G. Guppy)

The SSC/MINET Improvement, Validation and Application Program deals with advanced thermohydraulic codes to simulate transients in liquid metal-cooled reactors (LMRs). During this reporting period, work continued on three codes in the Super System Code (SSC) series. These codes are: (1) SSC-L for simulating short-term transients in loop-type LMRs; (2) SSC-P which is analogous to SSC-L except that it is applicable to pool-type designs and (3) SSC-S for long-term (shutdown) transients occurring in either loop- or pool-type LMRs. In addition to these code development and application efforts, validation of these codes is an ongoing task. Reference is made to the previous quarterly progress report (Guppy, 1985) for a summary of accomplishments prior to the start of the current period.

Additionally, this program deals with a generic balance of plant (BOP) modeling effort, which encompasses the development of safety analysis tools for system simulation of nuclear power plants. It provides for the development and validation of models to represent and link together BOP components (e.g., steam generator components, feedwater heaters, turbine/generator, condensers) that are generic to all types of nuclear power plants. This system transient analysis package is designated MINET to reflect the generality of the models and methods, which are based on a momentum integral network method. The code is fast-running and capable of operating as a self-standing code or to be easily interfaced to other system codes.

### 2.1 SSC-S Code (B. C. Chan)

#### 2.1.1 Upper Plenum Model Coupling (B. C. Chan, R. J. Kennett)

The two-dimensional upper plenum thermal-hydraulic model has been interfaced with the SSC code. This module can be used in the steady-state and the transient calculations. Several test cases of the upper plenum model have been performed. These cases are testing the flexibility of the model, as it applies to various plena with differing dimensions, internal structures, grid number and grid spacing. All of these can be controlled from the external input data. A seven channel core model simulation, representing an LMR transient, has been chosen for debugging and testing purposes. Work is continuing.

#### 2.1.2 Testing of SSC - Upper Plenum Interface (B. C. Chan, R. J. Kennett)

As the interfacing of the 2-D upper plenum model with the SSC code proceeds, calculations are routinely performed to test the interfaces. Selected results from one of these tests are shown in Figures 2.1 through 2.5.

The upper plenum domain was modeled in cylindrical coordinates as a two-dimensional axi-symmetric field, using an 11 x 13 grid (radial x axial) of variably-spaced cells. Upper plenum structure is represented as a cylinder located above the core outlet, and the sodium has to pass above (full flow conditions) or below (low flow conditions) the cylinder in order to exit the region directly above the core.

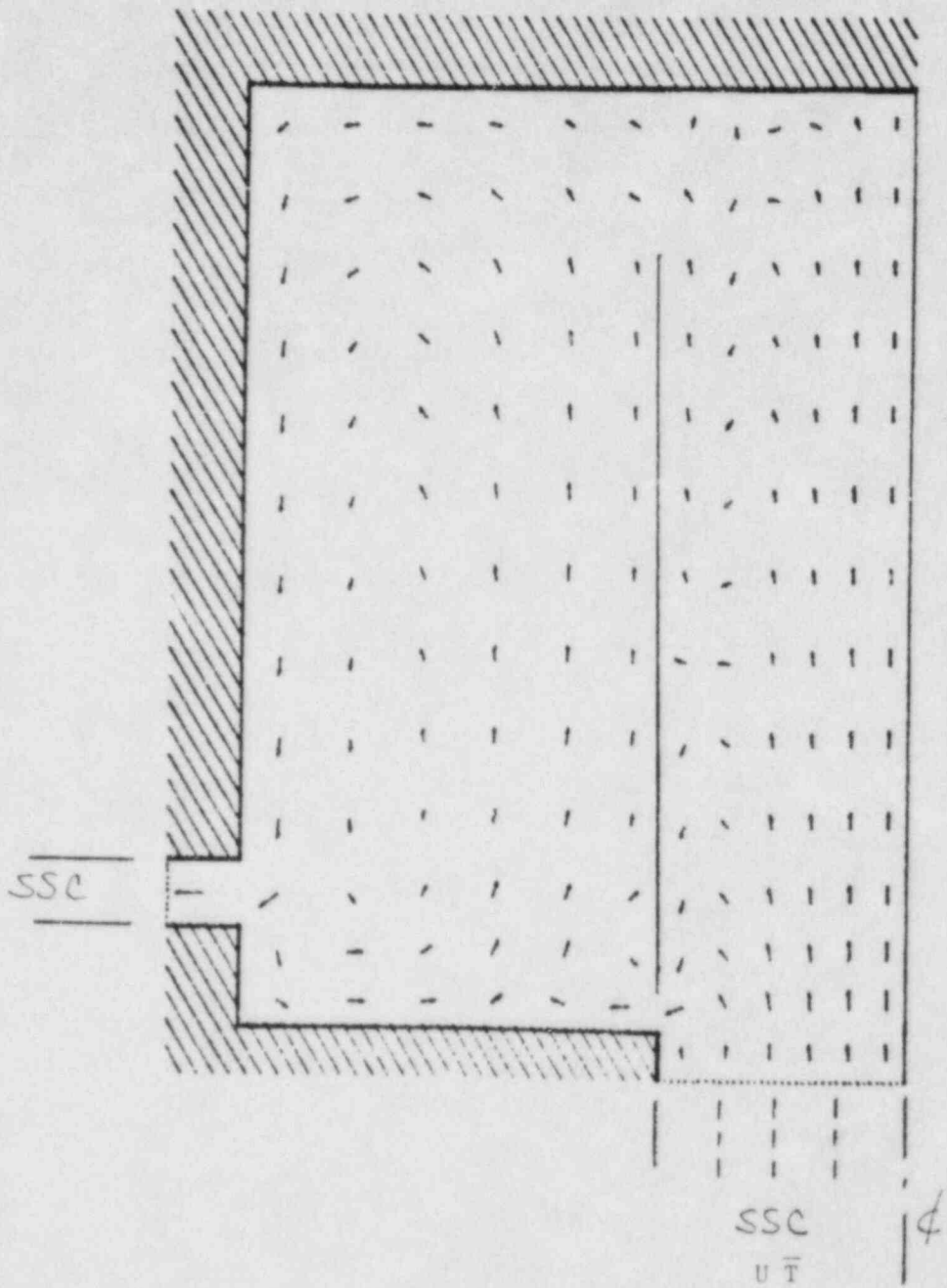


Figure 2.1 Upper Plenum Velocity Profile 25 Seconds After Scram

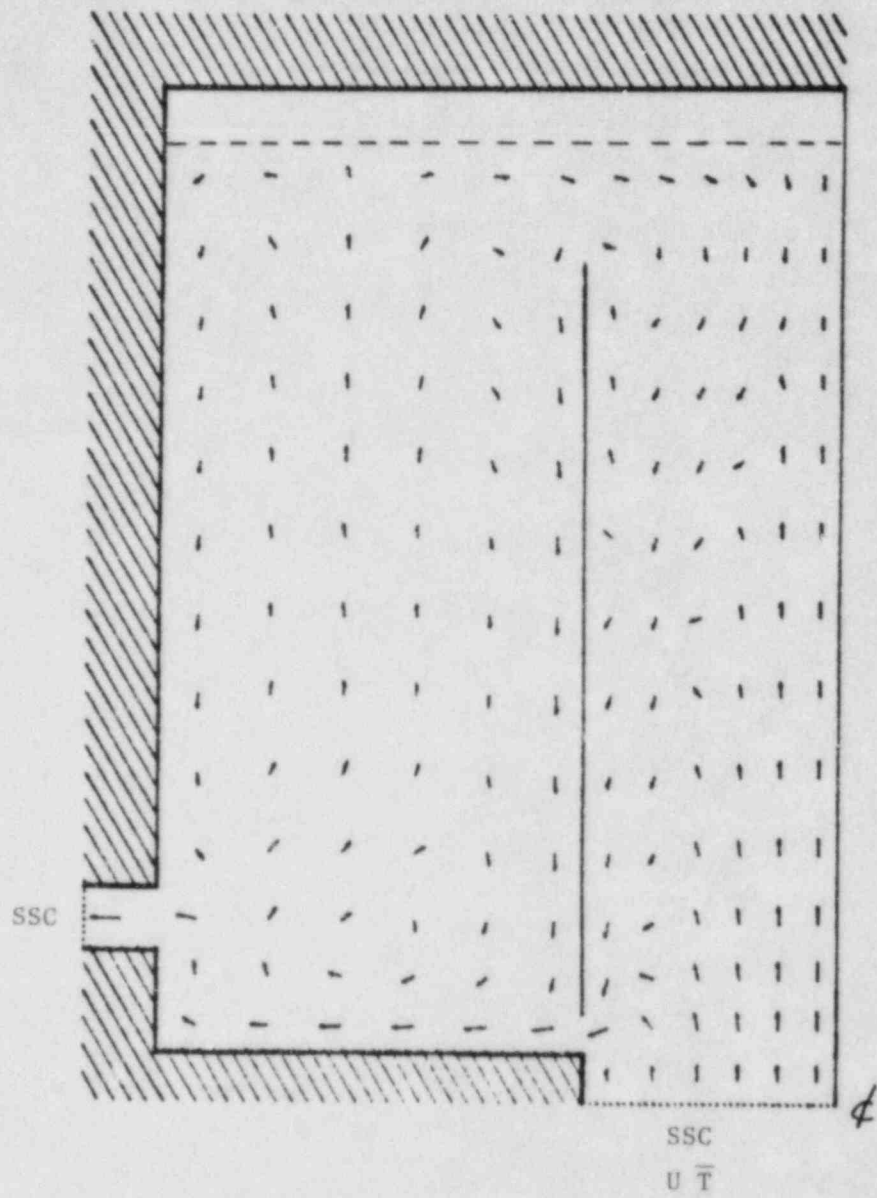


Figure 2.2 Upper Plenum velocity Profile 50 Seconds After Scram

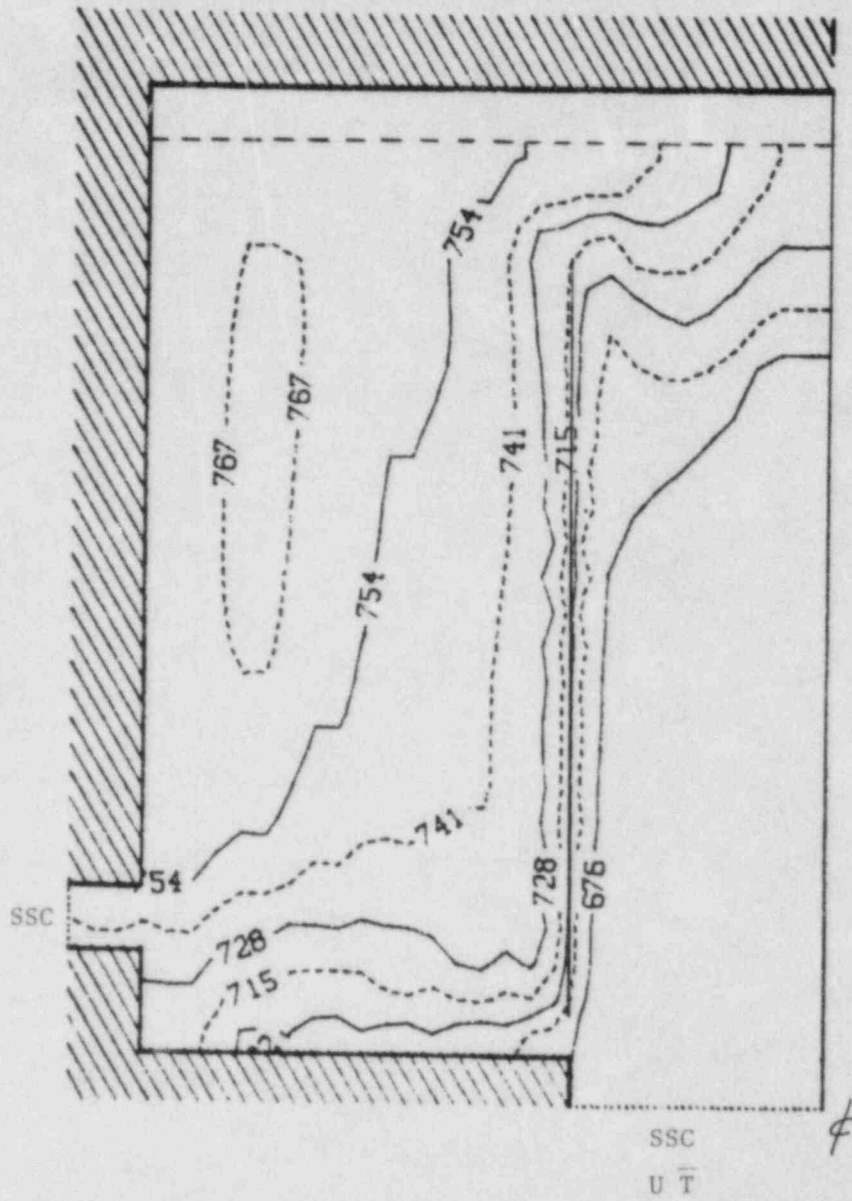


Figure 2.3 Upper Plenum Isotherms 50 Seconds After Scram



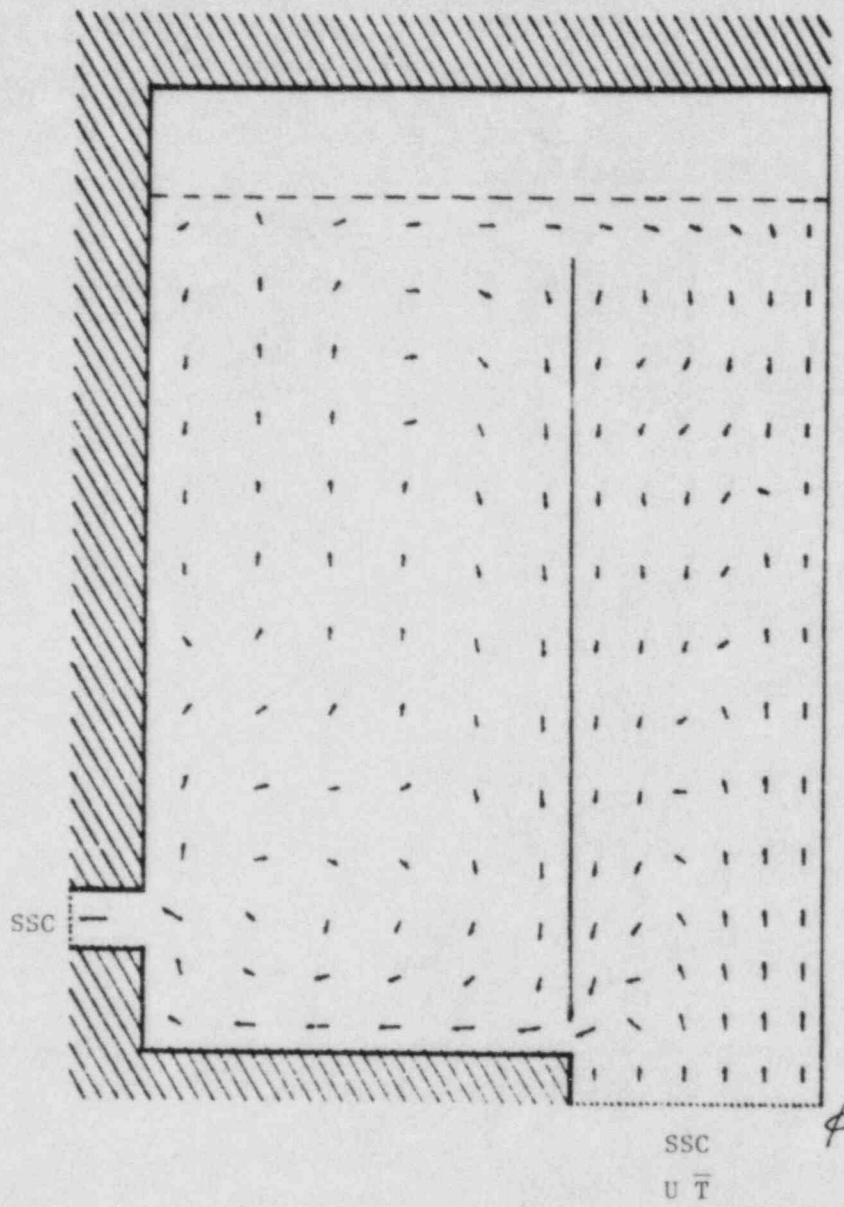


Figure 2.4 Upper Plenum Velocity Profile 100 Seconds After Scram

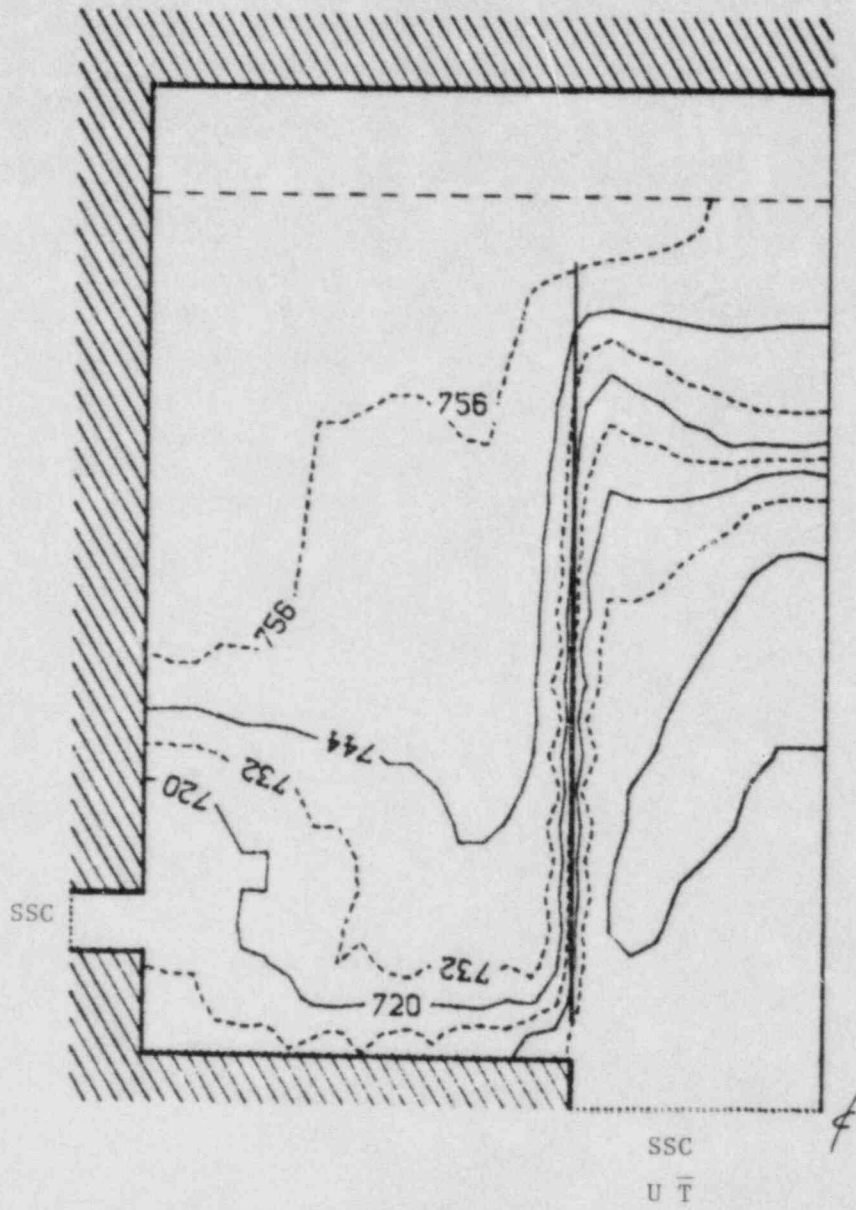


Figure 2.5 Upper Plenum Isotherms 100 Seconds After Scram

The test transient was a reactor scram from full power, followed by a pump trip and coastdown to natural circulation. Fluid velocities entering the upper plenum were determined from the SSC core channel flow rates, and an average of the channel outlet temperatures was used for upper plenum inlet temperatures. The temperature of the sodium exiting the upper plenum and entering the hot leg inlet is passed back to the SSC calculations. (Presently, the pressure calculations in the upper plenum model and in the remainder of the SSC calculations are decoupled, and this is where our current efforts are focused.)

The flow patterns 25 seconds after scram are shown in Fig. 2.1. This flow pattern resembles that at steady state, in that most of the sodium penetrates up through the structure before passing outward from the region directly above the core.

As the transient proceeds, the average sodium temperature decreases and the density increases, causing the sodium level (below cover gas) to fall. This can be observed in Fig. 2.2, which shows the flow field 50 seconds after scram. Note that at the reduced flow rates, the sodium is exiting below the structure cylinder, and that the flow above the cylinder is inward toward the region directly above the core. From the isotherms at 50 seconds, shown in Fig. 2.3, one can observe that the cooler sodium is passing directly from the core outlet to the plenum exit, leaving a region of hotter sodium trapped above the exit.

The flow pattern and isotherms at 100 seconds after the scram are shown in Figs. 2.4 and 2.5, respectively. At this stage in the transient, the pattern of sodium passing directly to the plenum exit is firmly established, and stratification of the sodium is apparent both above the core and above the plenum exit.

This test case illustrates the need for such detailed modeling of the upper plenum. From Figures 2.2 - 2.5, it is obvious that the sodium entering the hot leg inlet is much closer to the core outlet temperature than the plenum average temperature. Of course, at higher flow rates, a somewhat different response could be expected.

## 2.2 Generic Balance of Plant Modeling (MINET) (G. J. Van Tuyle)

### 2.2.1 Balance of Plant Models (G. J. Van Tuyle, J. E. Meyer, MIT)

Computational modules for the steady state and transient analysis of heat conduction in cylinders and spheres have been completed and tested. The cylindrical module will be useful in simulating heat losses in piping, and the spherical package is applicable for analyzing losses in large tanks and other structures.

The drift flux model currently available in the developmental version of MINET (1A) was reviewed in some detail. It was determined to be acceptable, and appropriate for its intended applications. An error was found in the treatment of the mixture enthalpy term, and this error will be corrected when

time and priorities permit. Alternative correlations for the drift flux parameters  $C_0$  and  $V_{gj}$  were also suggested, although it is not clear that this alternate package would be any better or worse than the package we adapted from the TRAC code.

### 2.2.2 MINET Code Improvements (G. J. Van Tuyle, T. C. Nepsco)

The steady-state and transient code modules are now operational in the CDC environment, using the FTN5 compiler under SCOPE 2.1.5 on the 7600. A transient based on the MINET X2 Sample Problem was run to normal termination.

All files necessary to construct the FORTRAN 77 Version from MINET Version 1.10 have been backed up on tape.

### 2.2.3 MINET Standard Input Decks (G. J. Van Tuyle)

A new deck for side-by-side modular HTGR systems was developed and tested, and designated deck HT2. Testing included a successful null (steady-state) transient and a ten minute LOFW ATWS with circulator trip, which gave results that appeared to be reasonable and consistent.

## 2.3 SSC-P Code (W. C. Horak)

### 2.3.1 Code Upgrade (W. C. Horak, R. J. Kennett, I. K. Madni)

Work on this effort was intensified during this reporting period. The Phenix input deck was made compatible with Cycle 41 of the SSC base program library. Those independent subroutines, which are only needed for SSC-P related calculations, were made compatible with and inserted into Cycle 41. Due to recent changes in the steady-state solution algorithm, the logic for the overall SSC-P steady-state procedure had to be extensively revised. These changes were developed and successfully implemented. The computations are now complete through the input processor and the steady-state initialization segments of SSC-P.

## REFERENCES

GUPPY, J. G., et al., (1984), "SSC Development, Validation and Application," Safety Research Programs Sponsored by Office of Nuclear Regulatory Research Quarterly Progress Report, Jan. 1 - March 31, 1985, Brookhaven National Laboratory Report to be published.

## PUBLICATIONS

HORAK, W. C., GUPPY, J. G. and WOOD, P. M., "The Effect of Pipe Insulation Losses on a Loss-of-Heat Sink Accident for an LMR," Proceedings of the 2nd Specialists' Meeting on Decay Heat Removal and Natural Convection in LMFBRs, Brookhaven National Laboratory, BNL-NUREG-36636.



VAN TUYLE, G. J. et al., "RAMONA-3B/MINET Composite Representation of BWR Thermal-Hydraulic Systems," Proceedings of the Third International Meeting on Reactor Thermal Hydraulics, Newport, RI, October 1985.

VAN TUYLE, G. J., "A Momentum Integral Network Method for Thermal-Hydraulic Systems Analysis," Article to be published in Nuclear Engineering & Design, 1985.



### 3. Thermal-Hydraulic Reactor Safety Experiments

#### 3.1 Core Debris Thermal-Hydraulic Phenomenology: Ex-Vessel Debris Quenching (T. Ginsberg, J. Klein, J. Klages, and C.E. Schwarz)

This task is directed towards development and experimental evaluation of analytical models for prediction of the rate of steam generation during quenching of core debris under postulated LWR core meltdown accident conditions. This program is designed to support development of LWR containment analysis computer codes.

##### 3.1.1 Comparison of Bed Heat Flux During Quenching with Steady-State Bed Heat Removal Data and Model

Analysis of the data from the ex-vessel, top-flooding bed quench experiments is complete, and the draft of the final report on this task has been prepared.

Data from the experiments are compared with mathematical models of the debris bed quench process and with data from other sources. Figure 3.1 compares the experimental data from the quench experiments with available steady-state debris dryout heat flux data and with the Lipinski debris bed dryout heat flux model (Lipinski, 1984). Also shown is a data point from the quench experiments of Cho et al. (1982). These results indicate overlap of the transient bed quench and steady-state dryout heat flux data, suggesting that the mechanism of heat removal in the transient and steady-state regimes is similar. In fact, the agreement, at least to first order, is taken to imply that the mechanism which limits the bed heat removal rate during the quench process is that of countercurrent two-phase flux within the top region of the bed where the steam and liquid fluxes are the greatest.

It is also observed that the steady-state Lipinski model agrees reasonably well with bed quench data. This model, however, does not account for two mechanisms which differentiate the bed quench process from steady-state decay heat removal, i.e., fillup of voids and superheating of the steam and steam cooling of the debris during the quench process. Both of these mechanisms act to reduce the bed heat removal rate. Thus, the agreement between the quench data and the steady-state model may be somewhat fortuitous.

A model of the bed quench process has been developed which incorporates the above two effects. The model uses the framework of the Lipinski model for the debris bed hydrodynamics together with energy equations for the solid particles and the steam. It was found necessary to adjust the bed permeability parameters in order to obtain good agreement with the bed heat flux data. The parameters  $n_1$  and  $n_2$  are exponents in the bed permeability relationship, given by

$$\kappa_g = \alpha^{n_1}$$

$$\eta_g = \alpha^{n_2}$$

$$\kappa_l = (1-\alpha)^{n_1}$$

$$\eta_l = (1-\alpha)^{n_2}$$

where  $\kappa$  and  $\eta$  are the relative bed permeability and turbulent bed permeability, respectively, and the subscripts g and l refer to the vapor and liquid phases. The quantity  $\alpha$  is the volume fraction of vapor in the free space of the bed. Lipinski proposes  $(n_1, n_2) = (3, 5)$ . Use of these parameters in the bed quench model, which incorporates the effects of void fillup and steam superheating, led to underestimation of the data by as much as 40%. Agreement to within approximately 15% was achieved by adjusting the parameters to  $(n_1, n_2) = (3, 3)$  for beds whose particle diameters are greater than 3 mm and  $(n_1, n_2) = (2, 3)$  for smaller particles.

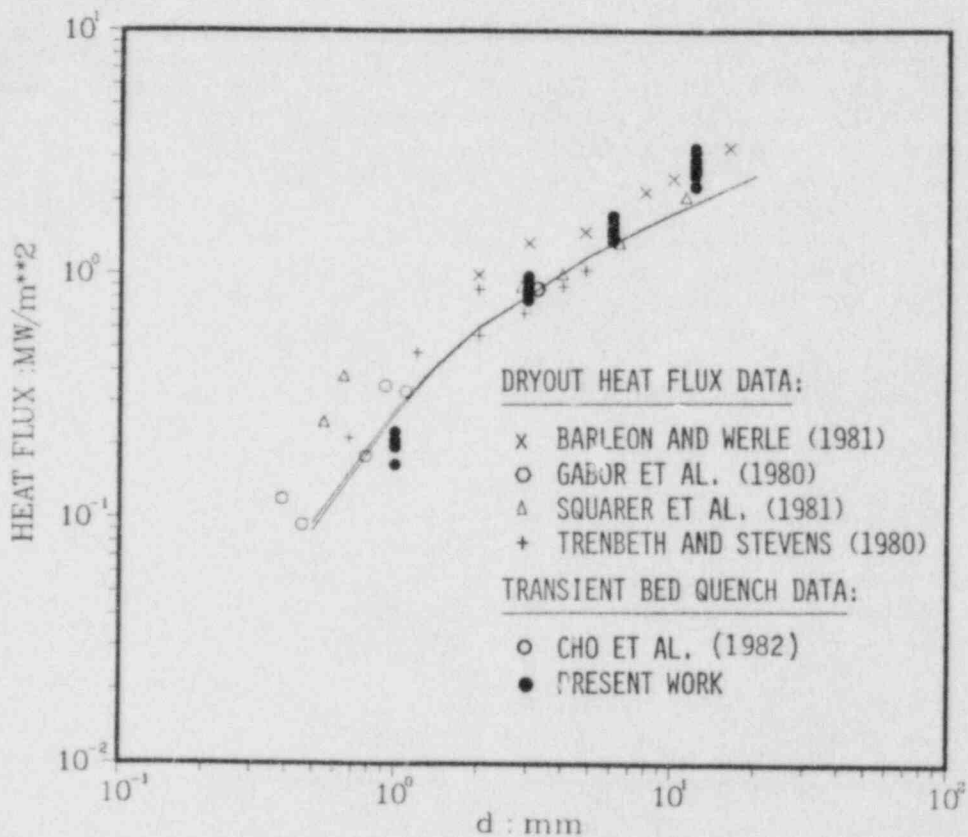


Figure 3.1 Steady-State Dryout Heat Flux and Bed Quench Heat Flux Data Compared with Steady-State Lipinski Model:  $P = 0.1$  MPa, Porosity = 0.4,  $(n_1, n_2) = (3, 5)$ , Bed Height = 0.3, 0.4 m

### 3.2 Core Debris Thermal-Hydraulic Phenomenology: In-Vessel Debris Quenching (N. K. Tutu, T. Ginsberg, J. Klein, J. Klages, and C.E. Schwarz)

The purpose of this task is to develop an understanding of the transient quenching of in-vessel debris beds (formed in the reactor core region) when the coolant is injected from below. The experimental results would, in addition, generate a data base for verifying the transient thermal-hydraulic models for the quenching process. The present experimental and model development effort is directed towards the case where the coolant is being injected at a constant rate.

#### 3.2.1 Experimental Program

A debris bed consisting of 3.18-mm stainless steel spheres is formed in a stainless steel test vessel of 108-mm inside diameter, and is held between two fixed screens to prevent fluidization during the quenching process. After the debris bed is heated to a predetermined initial temperature, water at saturation temperature is injected from below at a constant flowrate to begin the quenching process. Analysis of the acquired data during a new series of debris bed quench experiments was completed. Here, we present a few results.

Figure 3.2 shows the observed instantaneous heat flux at the top of the debris bed for the cases where the nominal initial debris bed superheat,  $\Delta T_{\infty}^S$  was 424K. These results (for a bed height of 0.85 m) are qualitatively similar to those obtained for a bed height, H of 0.422 m. However, for water injection superficial velocities greater than 4 mm/s, the peak heat fluxes are much larger than those observed for H = 0.422 m. This is because at relatively large water injection rates, water reaches the top of the debris bed before significant bottom portions of the bed have completely quenched. Thus if the debris bed height is increased, more of the debris can come into contact with the liquid, and hence increase the instantaneous heat flux.

Figure 3.3 shows the measured time averaged heat flux leaving the top of the debris bed per unit water injection superficial velocity ( $J_L^0$ ), per unit initial particle superheat for various experimental conditions. The solid line in the figure is the prediction from the 1-D quasi-steady model (Tutu et al., 1984). Considering the scatter in the data, the agreement is reasonable. These results are similar to those observed for a bed height of 0.422 m.

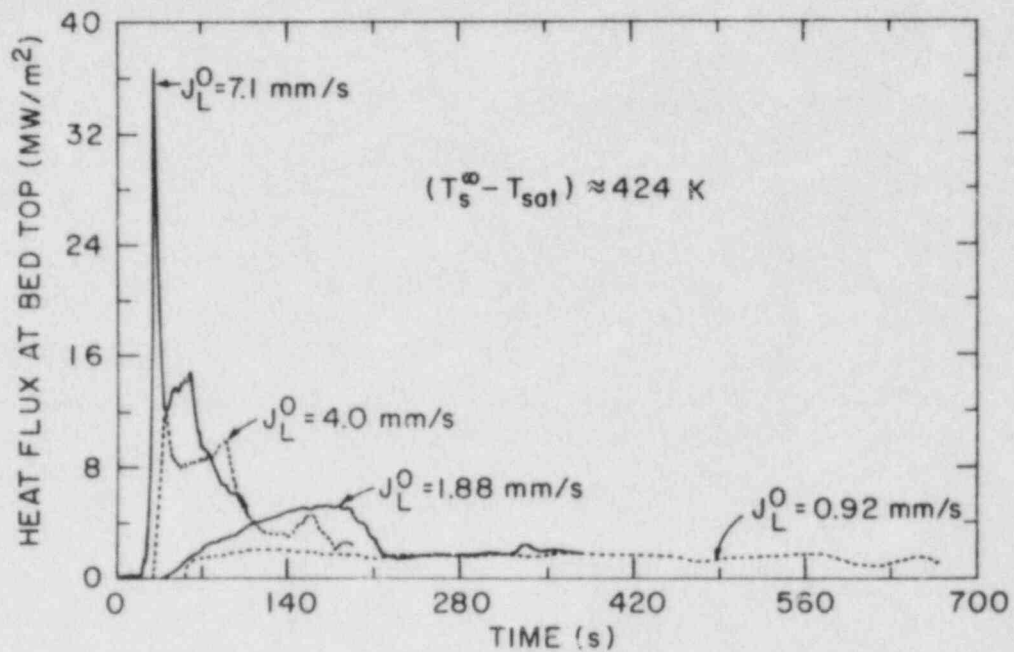


Figure 3.2 Instantaneous Heat Flux Leaving the Debris Bed,  $H = 850$  mm

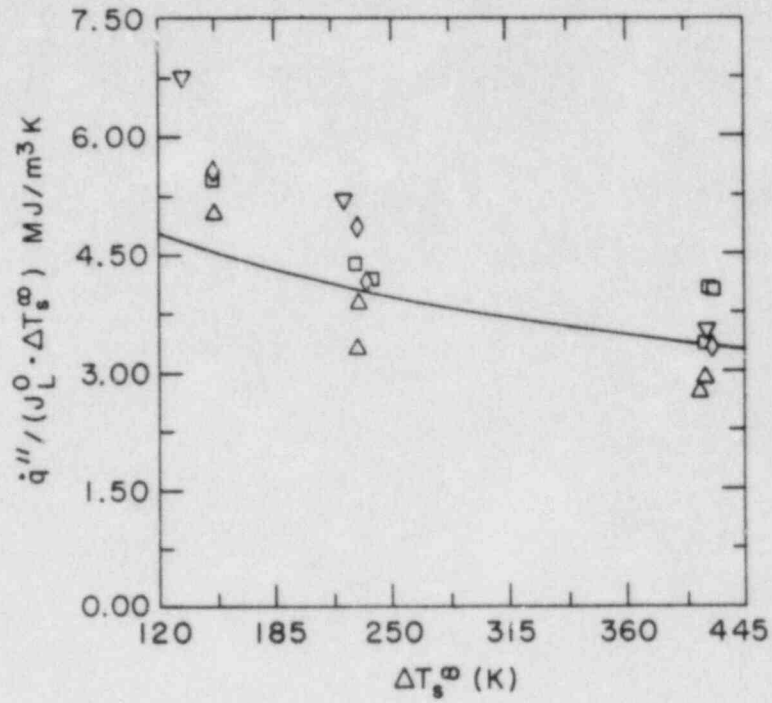


Figure 3.3 Average Heat Flux Per Unit Water Injection Superficial Velocity Per Unit Initial Superheat

$\square$ :  $J_L^0 \approx 1$  mm/s ,       $\diamond$ :  $J_L^0 \approx 2$  mm/s ,  
 $\Delta$ :  $J_L^0 \approx 4.2$  mm/s ,       $\nabla$ :  $J_L^0 \approx 7.2$  mm/s ,  
 ———: Quasi-Steady 1-D Model Prediction



### 3.3 Core-Concrete Heat Transfer Studies (G. A. Greene)

The purpose of this task is to study the mechanisms of liquid-liquid boiling heat transfer and its effect on the ex-vessel attack of molten core debris on concrete. This effort is in support of the CORCON and VANESA development programs at Sandia National Laboratories.

#### 3.3.1 Experimental Development

Previous analysis of experimental liquid-liquid film boiling data with R11 and liquid metal melts has indicated that the data for the cases with zero non-condensable gas flux exceeded the Berenson film boiling model prediction by approximately 20% on the average. Examination of some of the thermocouple data suggests that one possible source of error in the experimental heat balance could be neglect of axial heat conduction in the walls of the test apparatus vertically above the plane of the melt surface.

In order to account for this possible effect, modifications to the test apparatus were effected. A series of eight exposed-junction microthermocouples were spot welded into the wall of the test apparatus in a vertical array in order to map the transient thermal response of the wall both above and below the location of the liquid metal surface. Two of the thermocouples were above this plane and the other six were below.

#### 3.3.2 Experimental Test Series

After completion of the modifications to the experimental apparatus, a series of eight experiments were performed with saturated R11 in film boiling over melts of Wood's metal, lead, and bismuth. The temperature of the molten pool was monitored as in previous experiments as well as the transient response of the walls of the apparatus. In the analysis of the experimental data, the measured spatial temperature distribution of the wall was curve-fitted and the axial conduction heat losses from the vessel were evaluated from the derivative of the temperature field at the location of the liquid metal interface. This heat loss was subtracted from the lumped parameter energy balance at each time step.

#### 3.3.3 Comparison of Experimental Results to the Berenson Model

The experimental data for liquid-liquid film boiling were analyzed and compared to the Berenson film model. The results of this data analysis are shown for experiment 153 in Figure 3.4. It was found that correcting the pool heat balance for axial heat losses through the walls brought the experimental data into excellent agreement with the Berenson film boiling model. For the case of experiment 153, the deviation between the experimental data and the Berenson model was found to be 3% on the average, within the experimental uncertainty.

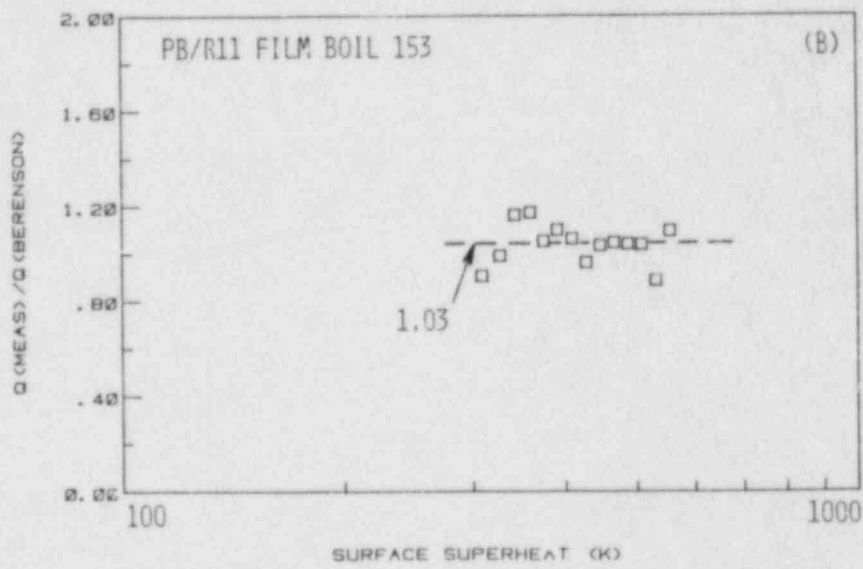
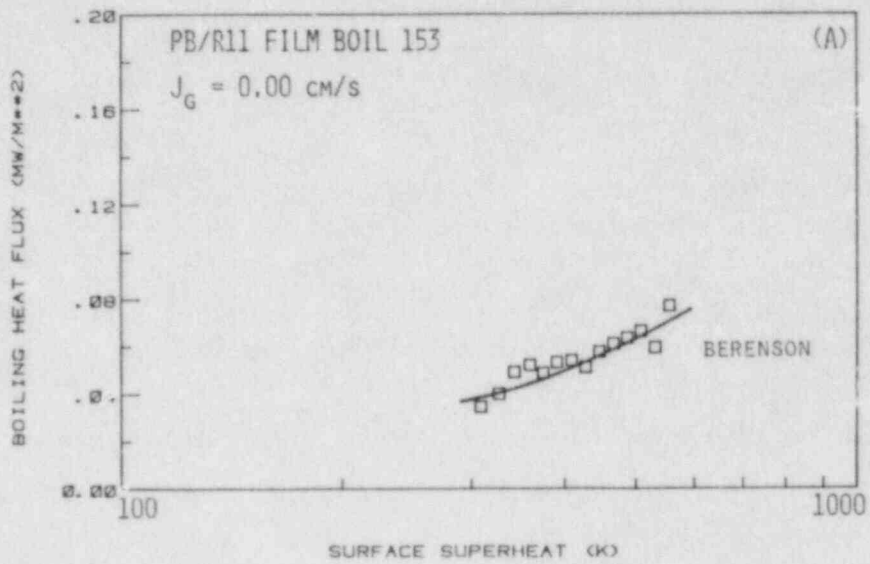


Figure 3.4 Liquid-Liquid Film Boiling Run 153:  $J_g = 0.00$  cm/s

#### REFERENCES

- BARLEON, L. and WERLE, H. "Dependence of Dryout Heat Flux on Particle Diameter for Volume and Bottom-Heated Debris Beds," KFK 3138 (November 1981).
- CHO, D.H., et al., "Debris Bed Quenching Experiments," Proceedings of International Meeting on Thermal Nuclear Reactor Safety, Chicago, IL, NUREG/CR-0027, Vol. 2, p. 987 (August 1982).
- GABOR, J.D., EPSTEIN, M., JONES, S.W. and CASSULO, J.C., "Status Report on Limiting Heat Fluxes in Debris Beds," ANL/RAS 80-21 (September 1980).
- SQUARER, D., PIECZYNSKI, T., and HOCHREITER, L.E., "Effects of Debris Bed Pressure, Particle Size and Distribution on Degraded Core Coolability," ASME Winter Annual Meeting, Washington, DC (November 1981).
- TRENBETH, R.E. and STEVENS, G.F., "An Experimental Study of Boiling Heat Transfer and Dryout in Heated Particulate Beds," AEEW-R1342 (July 1980).
- TUTU, N.K., et al., "Debris Bed Quenching Under Bottom Flood Conditions (In-Vessel Degraded Core-Cooling Phenomenology)," NUREG/CR-3850, BNL-NUREG-51788 (1984).

#### 4. Plant Analyzer (W. Wulff)

##### 4.1 Introduction

This program is being conducted to develop an engineering plant analyzer, capable of performing accurate, real-time and faster than real-time simulations of plant transients and Small-Break Loss of Coolant Accidents (SBLOCAs) in LWR power plants. The engineering plant analyzer is being developed by utilizing a modern, interactive, high-speed, special-purpose peripheral processor, which is designed for time-critical systems simulations. The engineering plant analyzer currently supports safety analyses and NRC staff training, but it can also serve as the basis of technology development for nuclear power plant monitoring, for on-line accident diagnosis and mitigation, and for upgrading operator training programs and existing training simulators.

Originally, there were three activities related to the LWR Plant Analyzer Development Program; namely, (1) the assessment of the capabilities and limitations of existing simulators for nuclear power plants, (2) the selection and acquisition of a special-purpose, high-speed peripheral processor suitable for real-time and faster than real-time simulation of power plant transients, and (3) the development of mathematical models and the software for this peripheral processor.

Below is a brief summary of previous results and a detailed summary of achievements during the current reporting period.

##### 4.2 Assessment of Existing Training Simulators (W. Wulff and H. S. Cheng)

The assessment of the current simulator capabilities consisted of evaluating qualitatively the thermohydraulic modeling assumptions in the training simulator and comparing quantitatively the predictions from the simulator with results from the detailed systems code RETRAN.

The results of the assessment have been published earlier in three reports (Wulff, 1980; Wulff, 1981a; Cheng and Wulff, 1981). It had been found that the reviewed training simulators were limited to the simulation of steady-state conditions and quasi-steady transients within the parameter range of normal operations. Most PWR simulators delivered before 1980 cannot simulate two-phase flow conditions in the primary reactor coolant loops, nor the motion of the two-phase mixture level beyond the narrow controls range in the steam generator secondary side. Most BWR simulators delivered before 1980 cannot simulate two-phase flow conditions in the recirculation loops or in the downcomer and lower plenum, nor can they simulate coolant level motions in the steam dome, the lower regions of the downcomer (below the separators), or in the riser and core regions. These limitations arise from the lack of thermohydraulic models for phase separation and mixture level tracking (Wulff, 1980; 1981a).

The comparison between PWR simulator and corresponding RETRAN results, carried out for a reactor scram from full power, showed significant discrepancies for primary and secondary system pressures and for mean coolant

temperatures of the primary side. The discrepancies were found even after the elimination of differences in fission power, feedwater flow and rate of vapor discharge from the steam dome. Good agreement was obtained between simulator and RETRAN calculations for only the early part (narrow control range) of the water level motion in the steam generator. The differences between simulator and RETRAN calculations have been explained in terms of modeling differences (Cheng and Wulff, 1981).

#### 4.3 Acquisition of Special-Purpose Peripheral Processor and Ancillary Equipment (A.N. Mallen, R.J. Cerbone and S.V. Lekach)

The AD10 had been selected earlier as the special-purpose peripheral processor for high-speed, interactive systems simulation through integrating large systems of nonlinear ordinary differential equations. A brief description of the processor has been published in a previous Quarterly Progress Report (Wulff, 1981b). A PDP-11/34 DEC computer serves as the host computer. An IBM Personal Computer is used for graphics displays and for remote access via commercial telephone lines.

Two AD10 units, coupled directly to each other by a bus-to-bus interface and equipped with a total of one megaword of memory, have been installed with the PDP-11/34 host computer, two 67 megabyte disc drives, a tape drive and a line printer. On-line access is facilitated by a model 4012 Tektronix oscilloscope terminal and a 28-channel signal generator. The system is accessed remotely via up to four ADPS CRT terminals and two DEC Writer terminals, one also equipped with a line printer. An IBM Personal Computer is also used to access the PDP-11/34 host computer remotely via commercial telephone lines and to generate labeled, multicolored graphs from AD10 results. A Tektronix 4115B multicolor graphics terminal has been purchased for direct on-line display of simulated parameters generated by the AD10 at real-time or faster computing speeds.

#### 4.4 Model Implementation on AD10 Processor and Developmental Assessment

A four-equation model for nonhomogeneous, nonequilibrium two-phase flow had been formulated and supplemented by constitutive relations from an existing BWR reference code, then scaled and adapted to the AD10 processor to simulate the Peach Bottom-2 BWR power plant (Wulff, 1982a). The resulting High-Speed Interactive Plant Analyzer code (HIPA-PB2) has been programmed in the high-level language MPS10 (Modular Programming System) of the AD10. After implementing the thermohydraulics of HIPA-PB2 on the AD10, we compared the computed results and the computing speed of the AD10 with those of the CDC-7600 mainframe computer, to demonstrate the feasibility of achieving engineering accuracy at high simulation speeds with the low-cost AD10 mini-computer (Wulff, 1982b).

It has been demonstrated (Wulff, 1982b) that (i) the high-level, state equation-oriented systems simulation language MPS10 compressed 9,950 active FORTRAN statements into 1,555 calling statements to MPS10 modules, (ii) the hydraulics simulation occupies one-fourth of available program memory, (iii) the difference between AD10 and CDC-7600 results is only approximately +5% of total parameter variations during the simulation of a severe licensing base



transient, (iv) the AD10 is 110 times faster than the CDC-7600 for the same transient, and (v) the AD10 simulates the BWR hydraulics transients up to 10 times faster than real-time process speed. It has been demonstrated that even after the inclusion of models for neutron kinetics, conduction, balance of plant dynamics and controls, the AD10 still achieves 9 times real-time simulation speed for all transients reported earlier (Wulff, 1983c). The program includes now more than 4,500 calling statements to MPS10 modules (subroutines).

The expanded version is called HIPA-BWR/4 and simulates all BWR/4 reactor plants. The simulation includes neutron kinetics (point kinetics), thermal conduction in fuel elements, reactor hydraulics, acoustical effects in the steam lines and the safety and relief valve logic (Wulff, 1982c; 1983a and Wulff et al., 1984), and further, the balance of plant components, such as the turbines, condensers, feedwater trains and suppression pool, as well as the control and plant protection systems as shown in Figure 4.1 below (Wulff, 1984). It also includes the boron tracking simulation (Wulff, 1983d; 1984a).

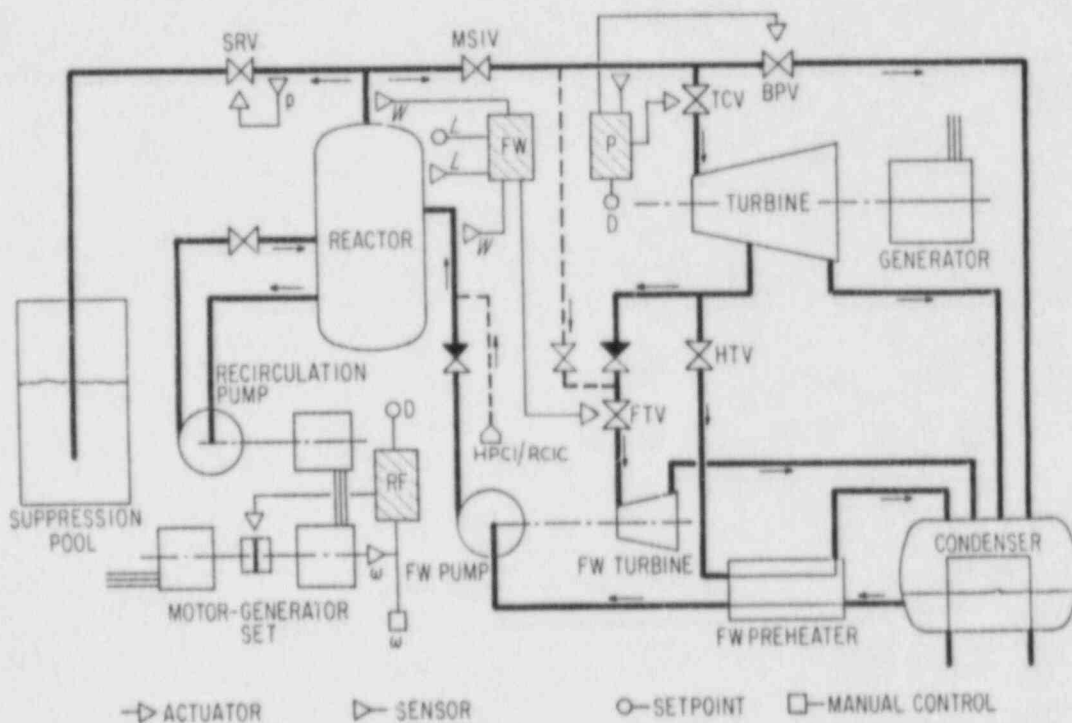


Figure 4.1 Flow Schematic and Control Blocks for BWR Simulation;  
 FW - Feedwater Controller, P - Pressure Controller,  
 RF - Recirculation Flow Controller

Extensive developmental assessment has been carried out for HIPA-BWR/4. Thirty-seven transients have been documented (Wulff, 1984a; 1984b and Wulff et al., 1984) comprising the comparisons of plant analyzer results with calculations from GE, TRAC-BD1, RELAP5 and RAMONA-3B. The comparisons have shown that the plant analyzer can simulate a large number of severe abnormal transients and that it produces the same results as TRAC, RELAP5 and RAMONA-3B, but at a considerably lower cost and in a much shorter time: 37 transients have been simulated, checked for consistency and documented with hard-copy graphs, using the plant analyzer, in less than four days by two staff members.

The graphics capabilities had been significantly enhanced during the second reporting period of 1984 to allow the on-line display of two parameter variations versus time on the four-color monitor of the IBM PC. The parameters are displayed in separate colors on labeled diagrams. Also, a Local Area Network had been assembled to display on-line simulation results from the plant analyzer in a remote conference room (Wulff, 1984a). The graphics capabilities had been expanded to permit the storage of 15 selected parameters in IBM PC memory, while a simulation is being performed at the simulation speed nine times greater than real-time process speed.

Finally, we developed the software for remote access of the plant analyzer via commercial telephone lines, using the IBM personal computer. The necessary accessories and a condensed user guide for remote access were reported earlier (Wulff, 1984d). We demonstrated in the previous reporting period that the plant analyzer is fully operational from the keyboard of the IBM. Two parameters are displayed as functions of time during the calculation and while 100 additional parameters are stored on disc in the host computer for later replay. All operator actions and malfunctions can be entered on-line without interrupting the simulation. The plant response to input changes is instantly displayed.

Specific accomplishments of the current reporting period are described below in Sections 4.5 and 4.6.

#### 4.5 Model Development (H.S. Cheng and W. Wulff)

The level tracking model for the downcomer is now completed. The time limit for an individual simulation run was used earlier for scaling the signal delay times associated with the engineered safety system. The model of this system has been made independent of an operational reference time and can now simulate indefinitely long transients. A valve leakage model has been implemented to predict the escape of radioactive steam from the vessel through the Main Steam Isolation Valves and into the turbine and condenser buildings. Work has been started to expand thermophysical properties for the vessel hydraulics to the low pressure region.

The main focus of model development during the current reporting period was on the containment models. The containment is modeled in three parts: the drywell, the wetwell and the systems for emergency core injection, residual heat rejection and containment cooling.

Four state variables determine the drywell conditions, namely the masses  $M_{V1}$  and  $M_{G1}$  of the vapor and the vapor-nitrogen mixture, respectively, the internal energy  $(Mu)_{G1}$  of the mixture and the liner wall temperature  $T_{W1}$ . Seven state variables describe the conditions in the wetwell, namely in the wetwell atmosphere, the suppression pool liquid and the suppression pool torous with its internal structures. The seven state variables are the masses  $M_{L2}$ ,  $M_{V2}$  and  $M_{G2}$ , respectively, of liquid, of vapor above the pool and of the nitrogen-vapor mixture above the pool, further, the internal energies of the pool liquid  $(Mu)_{L2}$  and the gaseous atmosphere above the pool  $(Mu)_{G2}$  and, finally, the pool wall temperatures  $T_{W21}$  and  $T_{W22}$  of the pool structures above and below, respectively, of the pool liquid level elevation. All the state variables are predicted by integrating global mass and energy balances.

The use of two gas mass balances each for the dry- and wetwells provides the means for computing relative humidity under all conditions of disequilibrium between liquid and vapor of water.

Rates of mass flows from, between and into the containment compartments are computed from quasi-steady mechanical energy balances with frictional losses for turbulent and laminar flow regimes.

Rates of condensation and evaporation at the pool liquid surface are computed on the basis of the similarity between heat and mass transfer (Kreith, 1973). Bulk condensation in the containment atmosphere is predicted from a relaxation model and with the difference between vapor and saturation pressures as the driving potential. The combination of heat and mass transfer is modeled to occur at the liner walls.

The Residual Heat Rejection coolers are modeled as tube and shell heat exchangers in countercurrent flow. The drywell air cooler is modeled as a cross-flow heat exchanger. The heat exchanger models imply quasi-steady heat transfer and thermal inertia will be accounted for by first-order delay approximations.

#### 4.6 Remote Access Operations (E. Cazzoli, H.S. Cheng, and A.N. Mallen)

The remote access capability has been further developed for simulating reactor transient over indefinitely long periods of time. This capability is needed for long-term simulations in emergency drill exercises.

Graphical displays of keyboard parameters are now displayed as functions of time such that the time axis spans a selected interval (for example: five minutes) and is renewed periodically at the end of every time span. This feature allows the observation of instantaneous plant conditions as well as trends and past histories.

Tabulated results are now available on the IBM PC screen, or a printing terminal, through on-line remote transmission from the host computer of the plant analyzer. The tables contain parameters specifically required for emergency drill exercises. As shown in Table 4.1, the tables contain not only the

Table 4.1 Tabulated Data Display for Simulation of Indefinite Duration

BNL Plant Analyzer

20-JUL-85 16:06

THE CURRENT REACTOR TIME IS		70.0000	MINUTES		
	Time (Hours).....	HRS.	1.167	1.083	1.000
	Time (minutes).....	MIN.	70.00	65.00	60.00
	Time (Seconds).....	SEC.	4200.	3900.	3600.
POWER	Reactor Power.....	MW	24.41	24.41	27.47
PS	Reactor Pressure.....	psia	728.4	790.5	950.0
SWSL	Steam flow.....	Mlb/h	0.2095	0.1914	0.1360
TC13	Inlet Clad Temperature..	F	511.6	521.3	541.4
TC1B	Mid-Core Clad temperature..	F	511.6	522.1	542.7
TC24	Outlet Clad Temperature..	F	507.7	517.8	539.1
T013	Inlet Fuel Temperature..	F	522.1	535.1	555.4
T018	Mid-Core Fuel Temperature..	F	522.2	533.3	553.8
T024	Outlet Fuel Temperature..	F	508.1	518.9	539.7
TLTS12	Core Inlet Fluid sub-cool..	F	0.0000	-13.35	-25.36
TLTS1B	Mid-core Fluid sub-cool..	F	0.3296E-01	-0.3296E-01	-2.291
TLTS24	Core Exit Fluid sub-cool..	F	0.0000	0.3296E-01	0.1648E-01
LEVEL	Reactor Vessel Level.....	ft	-1.854	-2.637	-2.737
MIXLEVE	Reactor Mixture Level.....	ft	-1.854	-2.633	-2.737
SWFW	Feedwater Flow.....	Mlb/h	0.6200E-01	0.6200E-01	0.6200E-01
TPOOL	Suppression Pool Temperatur	F	163.1	164.1	165.1
LPOOL	Suppression Pool Level.....	in	11.31	11.01	10.71
SWLK	MSIV Mass Leakage Rate....	lb/h	732.2	796.5	964.5
MLKTOT	Total MSIV Mass Leakage....	lb	1054.	990.9	917.4
WLF	MSIV Volume Leakage Rate...	ft <sup>3</sup> /h	459.7	458.6	455.1
VLKTOT	Total MSIV Volume Leakage..	ft <sup>3</sup>	514.9	476.8	438.6
VOID	Core Average Void.....	%	10.93	5.707	3.430
VOIDBY	Bypass Channel Void.....	%	1.028	1.370	0.2197
SWHC1	HPCI Flow.....	Mlb/h	0.0000	0.0000	0.0000
SWRIC	RCIC Flow.....	Mlb/h	0.6201E-01	0.6201E-01	0.6201E-01
PCNT	Containment Pressure.....	psia	15.69	15.69	15.69
TCNT	Containment Temperature....	F	145.0	145.0	145.0
CBORON	Boron Concentration.....	ppm	25.09	25.09	25.09
SWLC11	Liquid Core Inlet Flow..	Mlb/h	13.72	4.495	3.689
SWC11	Mixture Core Inlet Flow..	Mlb/h	13.73	4.495	3.689
SWC13	Bypass Mixture Inlet Flow..	Mlb/h	-1.333	-0.9921	-1.566
SWL54	Riser Exit Liquid Flow.....	Mlb/h	11.30	3.767	2.697
SWG18	Mid-core Vapor Mass Flow..	Mlb/h	0.1068	0.1611E-01	0.0000
SWG24	Core Exit Vapor Mass Flow..	Mlb/h	0.1581	0.8057E-01	0.6446E-01
SWG37	Byclass Inlet Vapor Flow....	Mlb/h	0.0000	0.0000	0.0000
SWG42	Bypass Middle Vapor Flow...	Mlb/h	0.0000	0.0000	0.0000
SWG48	Bypass Exit Vapor Flow...	Mlb/h	0.2014E-02	0.5035E-02	0.1007E-02
SWG54	Riser Exit Vapor Flow...	Mlb/h	0.1642	0.1138	0.8863E-01

\*\*\*\*\*

Do you want another ? (N=n=no)  
Y  
Enter (RET) For Print At All Times  
Enter S# To Start Print At Minutes= #  
Enter T# To Print Only At Minutes= #  
Enter E# To End Print At Minutes= #  
T85

current data at the time of request, but also the data from five and ten minutes earlier, thereby presenting trends during slow, long-term transients.

A drill exercise has been planned for the end of July.

#### 4.7 Transatlantic Remote Access (A.N. Mallen)

The plant analyzer at BNL has been accessed successfully for the first time from Europe via commercial telephone lines. One remote access demonstration was performed in Pisa, Italy, as part of the Specialists Meeting on Small Break LOCA Analyses in LWRs. A second demonstration was given for the Consejo Seguridad Nuclear in Madrid, Spain.

The data transmission has been facilitated with a Hayes Smartmodem, having US standard carrier frequency and being powered by a step-down transformer from a 220V, 60 Hz power source. The modem had to be reprogrammed for proper timing because transatlantic connections take longer than domestic ones to be completed.

Difficulties arose from transmission line noise. The plant analyzer operation could be demonstrated fairly reliably at the 300 baud transmission rate and only once for about an hour at the 1200 baud rate from Pisa, Italy. It is strongly recommended that routine simulations be carried out with ground cable connections rather than via satellite, or with special data transmission links.

#### 4.8 Future Plans

Assessment and model improvement will continue. Methods will be developed to improve the display of data trends indefinitely in graphical and tabular forms. Work will be continued to develop new simulation models for the containment.

The plant analyzer will be presented and demonstrated to domestic industries and foreign institutions interested in nuclear power simulation for the purpose of promoting cooperative programs directed toward PWR simulations.

#### REFERENCES

- CHENG, H. S. and WULFF, W., (1981), "A PWR Training Simulator Comparison with RETRAN for a Reactor Trip from Full Power," Informal Report, BNL-NUREG-30602, Brookhaven National Laboratory, September 1981.
- CHEXAL, B., et al., (1984), "Reducing BWR Power by Water Level Control During an ATWS - A Quasi-Static Analysis," Nuclear Safety Analysis Center, Electric Power Research Institute, NSAC-69, May 1984.
- ISHII, M. (1977), "One-Dimensional Drift-Flux Model and Constitutive Equations for Relative Motion Between Phases in Various Two-Phase Flow Regimes," Argonne National Laboratory, Argonne, IL., ANL-77-47.



- KREITH, F. (1973), Principles of Heat Transfer, Intext Educational Publishers, New York & London, 3rd Ed. Chapter 12, Section 12.4.
- WULFF, W., (1980), "PWR Training Simulator, An Evaluation of the Thermohydraulic Models for its Main Steam Supply System," Informal Report, BNL-NUREG-28955, September 1980.
- WULFF, W., (1981a), "BWR Training Simulator, An Evaluation of the Thermohydraulic Models for its Main Steam Supply System," Informal Report, BNL-NUREG-29815, Brookhaven National Laboratory, July 1981.
- WULFF, W., (1981b), "LWR Plant Analyzer Development Program," Ch. 6 in Safety Research Programs Sponsored by the Office of Nuclear Regulatory Research, Quarterly Progress Report, April 1-June 30, 1981; A. J. Romano, Editor, NUREG/CR-2231, BNL-NUREG-51454, Vol. 1, No. 1-2, 1980.
- WULFF, W., CHENG, H. S., DIAMOND, D. J. and KHATIB-RAHBAR, M., (1981c), "A Description and Assessment of RAMONA-3B MOD.0 CYCLE4: A Computer Code with Three-Dimensional Neutron Kinetics for BWR Systems Transients," NUREG/CR-3664, BNL-NUREG-51746, Manuscript completed 1981, published 1984.
- WULFF, W., CHENG, H. S., LEKACH, S. V. and MALLEN, A. N., (1984), "The BWR Plant Analyzer," Final Report, BNL-NUREG-51812, NUREG/CR-3943.
- WULFF, W., (1982a), "LWR Plant Analyzer Development Program," Ch. 5 in Safety Research Programs Sponsored by the Office of Nuclear Regulatory Research, Quarterly Progress Report, January 1-March 31, 1982; A. J. Romano, Editor, NUREG/CR-2331, BNL-NUREG-51454, Vol. 2, No. 1, 1982.
- WULFF, W., (1982b), "LWR Plant Analyzer Development Program," Ch. 5 in Safety Research Programs Sponsored by the Office of Nuclear Regulatory Research, Quarterly Progress Report, July 1-September 30, 1982; compiled by Allen J. Weiss, NUREG/CR-2331, BNL-NUREG-51454, Vol. 2, No. 3, 1982.
- WULFF, W., (1982c), "LWR Plant Analyzer Development Program," Ch. 5 in Safety Research Programs Sponsored by the Office of Nuclear Regulatory Research, Quarterly Progress Report, October 1-December 31, 1982; compiled by Allen J. Weiss, NUREG/CR-2331, BNL-NUREG-51454, Vol. 2, No. 4, 1982.
- WULFF, W., (1983a), "LWR Plant Analyzer Development Program," Ch. 5 in Safety Research Programs Sponsored by the Office of Nuclear Regulatory Research, Quarterly Progress Report, January 1-March 31, 1983; compiled by Allen J. Weiss, NUREG/CR-2331, BNL-NUREG-51454, Vol. 3, No. 1, 1983.
- WULFF, W., (1983b), "LWR Plant Analyzer Development Program," Ch. 5 in Safety Research Programs Sponsored by the Office of Nuclear Regulatory Research, Quarterly Progress Report, July 1-September 30, 1983; compiled by Allen J. Weiss, NUREG/CR-2331, BNL-NUREG-51454, Vol. 3, No. 3, 1983.

WULFF, W., (1983c), "NRC Plant Analyzer Development," Proc. Eleventh Water Reactor Safety Research Information Meeting, held at National Bureau of Standards, Gaithersburg, MD, Oct. 24-28, 1983, U.S. Nuclear Regulatory Commission. To be published.

WULFF, W., (1983d), "LWR Plant Analyzer Development Program," Ch. 5 in Safety Research Programs Sponsored by the Office of Nuclear Regulatory Research, Quarterly Progress Report, October 1-December 31, 1983; compiled by Allen J. Weiss, NUREG/CR-2331, BNL-NUREG-51454, Vol. 3, No. 4, 1983.

WULFF, W., (1984a), "LWR Plant Analyzer Development Program," Ch. 5 in Safety Research Programs Sponsored by the Office of Nuclear Regulatory Research, Quarterly Progress Report, January 1-March 31, 1984; compiled by Allen J. Weiss, NUREG/CR-2331, BNL-NUREG-51454, Vol. 4, No. 1, 1984.

WULFF, W., (1984b), "LWR Plant Analyzer Development Program," Ch. 5 in Safety Research Programs Sponsored by the Office of Nuclear Regulatory Research, Quarterly Progress Report, April 1-June 30, 1984; compiled by Allen J. Weiss, NUREG/CR-2331, BNL-NUREG-51454, Vol. 4, No. 2, 1984.

WULFF, W., (1984c), "LWR Plant Analyzer Development Program," Ch. 5 in Safety Research Programs Sponsored by the Office of Nuclear Regulatory Research, Quarterly Progress Report, July 1-September 30, 1984; compiled by Allen J. Weiss, NUREG/CR-2331, BNL-NUREG-51454, Vol. 4, No. 3, 1984.

WULFF, W., (1984d), "LWR Plant Analyzer Development Program," Ch. 4 in Safety Research Programs Sponsored by the Office of Nuclear Regulatory Research, Quarterly Progress Report, October-December 31, 1984; compiled by Allen J. Weiss, NUREG/CR-2331, BNL-NUREG-51454, Vol. 4, No. 4, 1984.

## 5. Code Assessment and Application

(P. Saha, J. H. Jo, H. R. Connell, C. Yuelys-Miksis, and L. Neymotin)

This project includes the independent assessment of the latest released versions of LWR safety codes such as TRAC, RELAP5, and RAMONA-3B, and their application to the full-scale plant accident and/or transient simulation. In the past, the TRAC-PIA, TRAC-PD2, TRAC-PF1, RELAP5/MOD1 and TRAC-BD1 codes were assessed at BNL primarily through various separate-effects experiments. Also, the code application task at BNL included (i) determination of Appendix K conservatism for a Westinghouse RESAR-3S 4-loop PWR using the TRAC-PD2/MOD1 code, and (ii) comparative analysis of TRAC-BD1 and RAMONA-3B calculations for a typical BWR/4 MSIV closure ATWS. At present, emphasis is placed on the assessment of the TRAC-BD1/MOD1 and RAMONA-3B codes.

The major activities performed during the reporting period of April to June 1985 are described below.

### 5.1 Code Assessment

#### 5.1.1 Simulation of FIST Experiments with TRAC-BD1/MOD1 (J. H. Jo and H. R. Connell)

The following five FIST Phase 1 tests are being simulated using the TRAC-BD1/MOD1 code:

1. BWR/4 MSIV closure ATWS (4PMCI),
2. BWR/6 small break with HPCS failure (6SB2C),
3. BWR/6 large break (6DBA/B),
4. BWR/6 small break with HPCS failure and stuck-open 3/RV (6SB1),
5. BWR/6 main steam line break (6MSB1).

Test 4PMCI is a power transient simulation test for a BWR/4 with MSIV closure and without power scram. The TRAC-BD1/MOD1 transient calculation for this test has progressed up to 400 seconds and some of the results were reported in the last quarterly report (Jo, 1985). The code prediction was generally in good agreement with the test data. However, in the calculation the HPCI/RCIC injection was initiated at 49 seconds, as reported in the test documentation, (Hwang, 1983) with a 20 second delay after the level reached "Level 2." Since it was not clear how this timing was obtained in the test report, the transient calculation has been repeated with different safety injection times to study the sensitivity of the code prediction to the timing of the HPCI/RCIC injection. In the first calculation, the "Level 2" based on the collapsed liquid level was reached at 39 seconds which is about 10 seconds later than in the test; therefore, in the second (or sensitivity) calculation, the HPCI/RCIC injection was initiated at 59 seconds (20 second delay). However, we have been experiencing some difficulty with the code calculation apparently caused by some coding deficiency, particularly division by zero. We are in communication with the INEL staff to resolve this problem and the calculations will resume as soon as this difficulty is resolved.

Test 6SB2C is a small break test, simulating a BWR/6 recirculation line break of  $0.05 \text{ ft}^2$  with HPCS assumed to be unavailable. The MSIVs were closed when the downcomer water level reached "Level 1" and the ADS (automatic depressurization system) was activated with a 120 second delay after the "Level 1" was reached. The calculation has so far progressed to 380 seconds. The preliminary comparisons between the data and the calculation indicates generally good agreement. However, the predicted downcomer water level reached "Level 1" approximately 10 seconds later than in the test (75 seconds in the test vs 85 seconds). Also, the code predicted a slightly slower depressurization after the ADS was activated which resulted in some delays in the LPCS (310 seconds in the test vs 345 seconds) and LPCI (335 seconds in the test vs 365 seconds) initiations. This calculation will be continued out to 500 seconds.

Test 6DBA1B simulates a 200% large break in a recirculation loop of a BWR/6. All the ECCS were assumed to be available. The calculation has been run out to 120 seconds; a preliminary review indicates that the predicted pressure matches the test data very well up to this point. The calculation will be continued up to 200 seconds.

Two more transient calculations, one for Test 6SB1 and the other for Test 6MSB1, have been initiated during the reporting period. These two tests started from the same initial condition. An acceptable steady state has been achieved and the transient calculations have begun.

#### 5.1.2 Simulation of FRIGG Tests with TRAC-BD1/MOD1 (C. Yuelys-Miksis, L. Neymotin, and J. H. Jo)

A series of forced circulation steady-state experiments were performed in the FRIGG loop with an electrically heated rod bundle (Nylund, 1968). Several of these tests have been simulated with the RAMONA-3B/MOD0/Cycle 8 and TRAC-BD1/MOD1 codes to assess the subcooled boiling, vapor generation and slip or interfacial shear models used in these codes. The results of the RAMONA-3B simulations were reported in the previous quarterly report (Yuelys-Miksis, 1985). For comparison, the same tests were simulated with the TRAC-BD1/MOD1 code. Each of these tests had different bundle power, bundle inlet subcooling and flow rates, but all tests were performed at a pressure of approximately 50 bars. The operating conditions of these tests are shown in Table 5.1.

The axial void fraction profiles along with the code predictions for each test are shown in Figure 5.1 through 5.12. Each figure shows a comparison between the experimental data and the RAMONA-3B and TRAC-BD1/MOD1 code results. The RAMONA-3B results were calculated using the Bankoff-Malnes correlation to compute the slip parameter in the core and riser regions. The Bankoff-Malnes correlation is the recommended slip parameter for the RAMONA-3B code.

Table 5.1 Operating Conditions for FRIGG Runs

RUN NO	PRESSURE (bars)	MASS FLUX (kg/m <sup>2</sup> -s)	POWER (MW)	INLET SUBCOOLING (°C)
313006	50.0	729	1.50	3.7
313010	50.0	687	2.98	4.6
313005	49.8	1110	1.50	3.7
313009	50.0	1107	2.98	4.4
313019	49.5	1177	4.39	8.6
313001	49.6	1492	1.50	5.0
313008	50.0	1471	3.00	4.3
313017	49.6	1464	4.40	2.4
313007	50.0	1110	1.50	11.7
313014	49.7	1163	2.93	11.0
313016	49.6	1208	2.91	19.3
313020	49.7	1159	4.415	22.4

For the low inlet subcooling (3.7 and 4.6°C) and low mass flux (~700 kg/m<sup>2</sup>-s) tests, i.e., Run Nos. 313006 and 313010, there was good agreement between the experimental data and the results of both the RAMONA-3B and TRAC-BDI/MODI codes, as shown in Figures 5.1 and 5.2. The RAMONA-3B and TRAC-BDI/MODI predictions are similar at low inlet subcooling, although the TRAC-BDI/MODI code is slightly better at predicting the experimental data.

In the next three tests, i.e., Run Nos. 313005, 313009, and 313019, the mass flux was higher (~1100 kg/m<sup>2</sup>-s), but the inlet subcooling was still low (3.7 to 8.6°C). In these tests the code results were again in good agreement with the experimental data and the RAMONA-3B and TRAC-BDI/MODI predictions were nearly identical. Both codes slightly underpredicted the void fraction for Run No. 313005, which had low power, as shown in Figure 5.3. The results of Run Nos. 313009 and 313019 are shown in Figures 5.4 and 5.5, respectively. As can be seen, the code results for these runs were in good agreement with the experimental data. The results of the highest mass flux (~1475 kg/m<sup>2</sup>-s) tests with low inlet subcooling (2.5 to 5.0°C), i.e.,



Run Nos. 313001, 313008, and 313017, are shown in Figures 5.6 through 5.8. Again, the RAMONA-3B and TRAC-BD1/MOD1 code predictions were nearly identical. The codes slightly underpredicted the void fraction for Run No. 313001 and slightly overpredicted the void fraction for Run No. 313017. However, the results are well within acceptable limits.

Although the TRAC-BD1/MOD1 and RAMONA-3B predictions were very similar at low inlet subcooling, the results for high inlet subcoolings showed large variations. For Run No. 313007 (Figure 5.9) which had higher inlet subcooling (11.7°C) and medium mass flux (~1100 kg/m<sup>2</sup>-s), but low power, the two code predictions were significantly different. For this test, RAMONA-3B significantly overpredicted the axial void fraction while TRAC-BD1/MOD1 significantly underpredicted the same. However, when the power was increased while the inlet subcooling and mass flux were maintained at a similar level, there was better agreement between the code results and the experimental data. This is shown for Run No. 313014 in Figure 5.10, where both codes produced similar results with excellent agreement with the data.

In the last two tests, i.e., Run Nos. 313016 and 313020 (Figures 5.11 and 5.12), the inlet subcooling was very high (19.3 and 22.4°C, respectively). For Run No. 313016, which had medium power (2.91 MW), RAMONA-3B and TRAC-BD1/MOD1 produced very different results. For this test RAMONA-3B significantly overpredicted the void fraction whereas TRAC-BD1/MOD1 significantly underpredicted the void fraction. In contrast, for Run No. 313020, which had higher power (4.415 MW), both codes slightly underpredicted the void fraction.

In summary, for low inlet subcoolings (2 to 9°C), where the subcooled boiling effect is minimal, both the RAMONA-3B and TRAC-BD1/MOD1 codes showed good agreement with the FRIGG data over a wide range of mass fluxes and bundle power. Thus the slip (Bankoff-Maines) model used in RAMONA-3B and the interfacial shear model used in TRAC-BD1/MOD1 seem to be adequate. However, for higher inlet subcoolings (>10°C) the code results significantly differed from each other and the experimental data. The onset of net vapor generation (NVG) in the TRAC-BD1/MOD1 code is determined by the Saha-Zuber correlation (1974) which appears to be adequate. However, the Lahey (1974) subcooled boiling model as used in TRAC-BD1/MOD1 appears to underpredict the vapor generation rate.

It is recommended that the TRAC-BWR code developers at INEL include a different model (Saha, 1981 for example) for vapor generation in the subcooled boiling region. For RAMONA-3B, BNL has developed a plan to implement a new model for subcooled boiling. The new model will consist of the Saha-Zuber correlation (1974) for the onset of net vapor generation (NVG) as used in TRAC-BD1/MOD1, and the Saha (1981) model for net vapor generation. This model has already been proven to produce good results for subcooled boiling (Saha, 1981) and was developed for possible inclusion in the NRC advanced codes, i.e., TRAC and RELAP5.

## REFERENCES

- HWANG, W.S. et al. (1983), "BWR Full Integral Simulation Test (FIST) Phase 1 Test Results," NUREG/CR-3711, EPRI NP-3602, GEAP-30426, November 1983.
- JO, J.H. and CONNELL, H.R. (1985), "Simulation of FIST Experiments with TRAC-B11/MOD1," in "Safety Research Programs Sponsored by Office of Nuclear Regulatory Research, Quarterly Progress Report January 1- March 31, 1985," Section 5.1.1, NUREG/CR-2331, BNL-NUREG-51454, Vol. 5, No. 1.
- LAHEY, R.T. (1978), "A Mechanistic Subcooled Boiling Model," Proceedings of the 6th Int. Heat Transfer Conference, Vol. 1, Toronto, Canada, pp. 293-295.
- NYLUND, O. et al. (1968), "Hydrodynamic and Heat Transfer Measurements on a Full-Scale Simulated 36-Rod Marviken Element with Uniform Heat Flux Distribution," FRIGG-2, R4-447/RTL-1007.
- SAHA, P. and ZUBER, N. (1974), "Point of Net Vapor Generation and Vapor Void Fraction in Subcooled Boiling," Proceedings of the 5th Int. Heat Transfer Conference, Vol. IV, Tokyo, Japan, pp. 175-179.
- SAHA, P. (1981), "A Simple Subcooled Boiling Model," ANS Transactions, Vol. 39, pp. 1058-1060. Also, BNL Memorandum "Improved Subcooled Boiling Model for TRAC," dated June 2, 1981.
- YUELYS-MIKSIS, C and NEYMOTIN, L. (1985), "Simulation of FRIGG Tests with RAMONA-3B," in "Safety Research Programs Sponsored by Office of Nuclear Regulatory Research, Quarterly Progress Report January 1 - March 31, 1985," Section 5.1.2, NUREG/CR-2331, BNL-NUREG-51454, Vol. 5, No. 1.

FRIGG RUN NO. 313006  
SUB=3.7, G=729 KG/M<sup>2</sup>-S, Q=1.5 MW, P=50.0

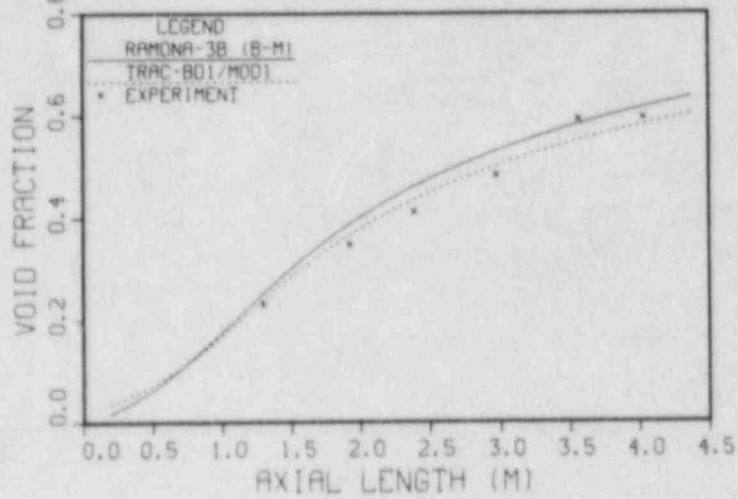


Figure 5.1 Comparison Between the Experimental Data and the Code Predictions of Axial Void Fraction for FRIGG Test 313006.

FRIGG RUN NO. 313010  
SUB=4.6, G=687 KG/M<sup>2</sup>-S, Q=2.98 MW, P=50.0

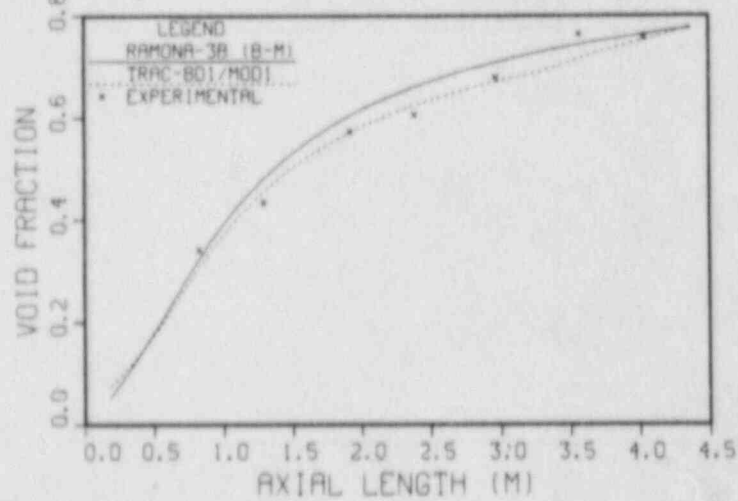


Figure 5.2 Comparison Between the Experimental Data and the Code Predictions of Axial Void Fraction for FRIGG Test 313010.

FRIGG RUN NO. 313005  
SUB-3.7, G=1110 KG/M2-S, Q=1.5 MW, P=49.8

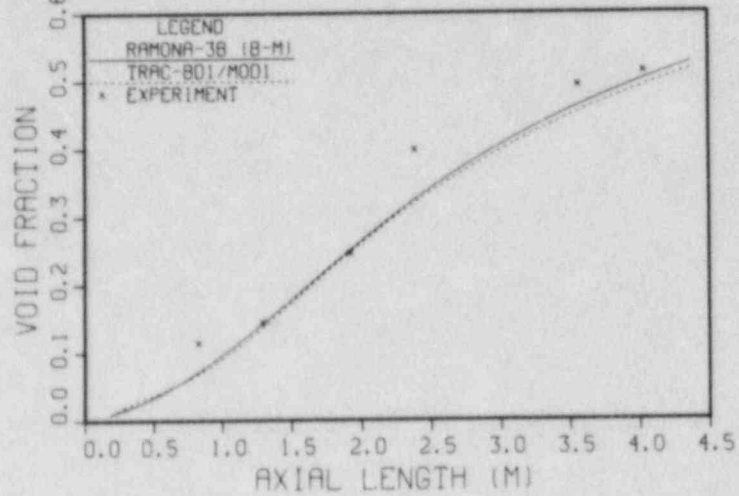


Figure 5.3 Comparison Between the Experimental Data and the Code Predictions of Axial Void Fraction for FRIGG Test 313005.

FRIGG RUN NO. 313009  
SUB-4.4, G=1107 KG/M2-S, Q=2.98 MW, P=50.0

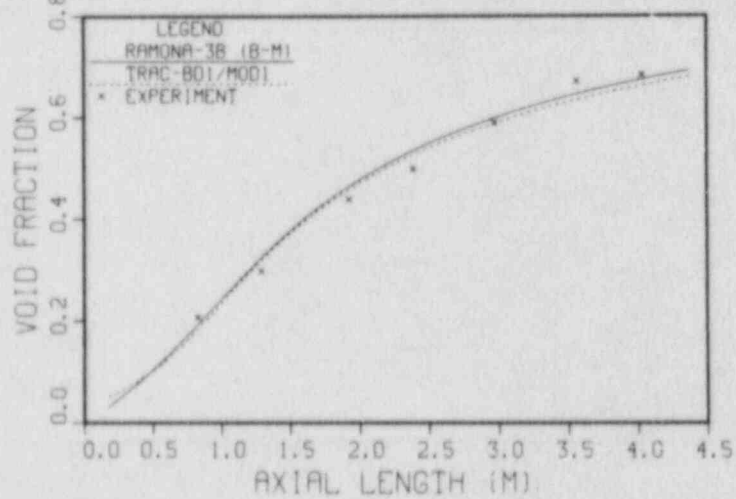


Figure 5.4 Comparison Between the Experimental Data and the Code Predictions of Axial Void Fraction for FRIGG Test 313009.

FRIGG RUN NO. 313019  
 SUB=8.6, G=1177 KG/M<sup>2</sup>-S, Q=4.39 MW, P=49.5

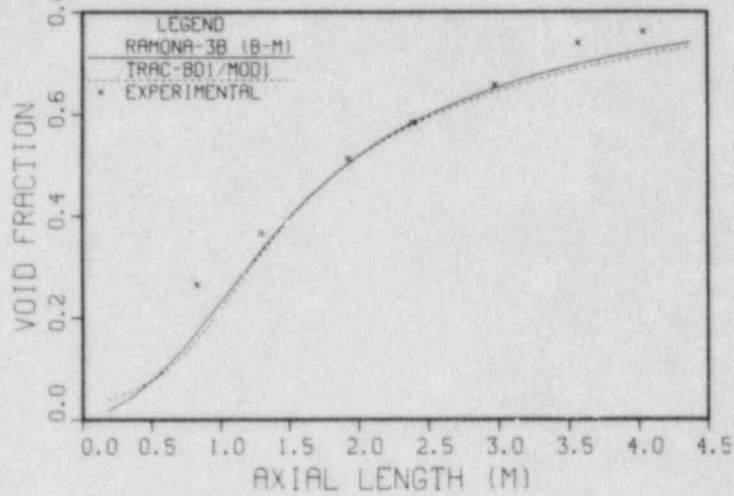


Figure 5.5 Comparison Between the Experimental Data and the Code Predictions of Axial Void Fraction for FRIGG Test 313019.

FRIGG RUN NO. 313001  
 SUB=5.0, G=1492 KG/M<sup>2</sup>-S, Q=1.5 MW, P=49.6

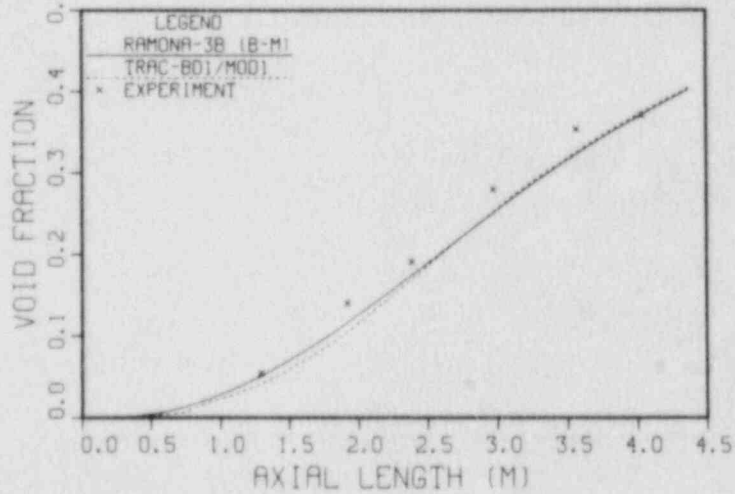


Figure 5.6 Comparison Between the Experimental Data and the Code Predictions of Axial Void Fraction for FRIGG Test 313001.



FRIGG RUN NO. 313008  
SUB=4.3, G=1471 KG/M2-S, Q=3.0 MW, P=50.0

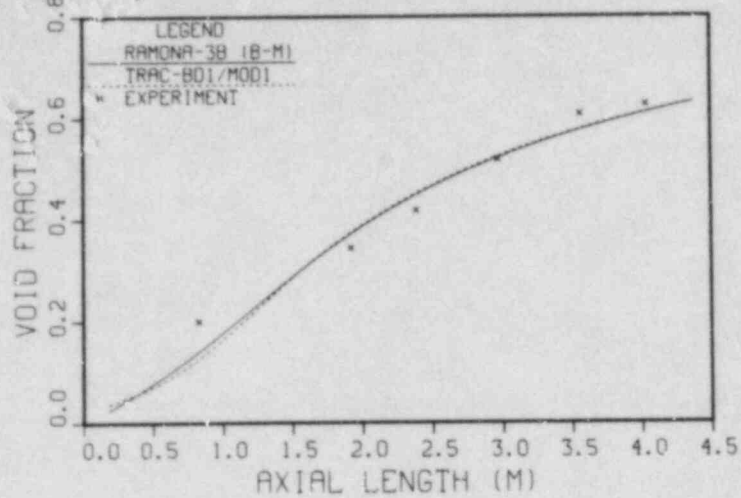


Figure 5.7 Comparison Between the Experimental Data and the Code Predictions of Axial Void Fraction for FRIGG Test 313008.

FRIGG RUN NO. 313017  
SUB=2.4, G=1464 KG/M2-S, Q=4.40 MW, P=49.6

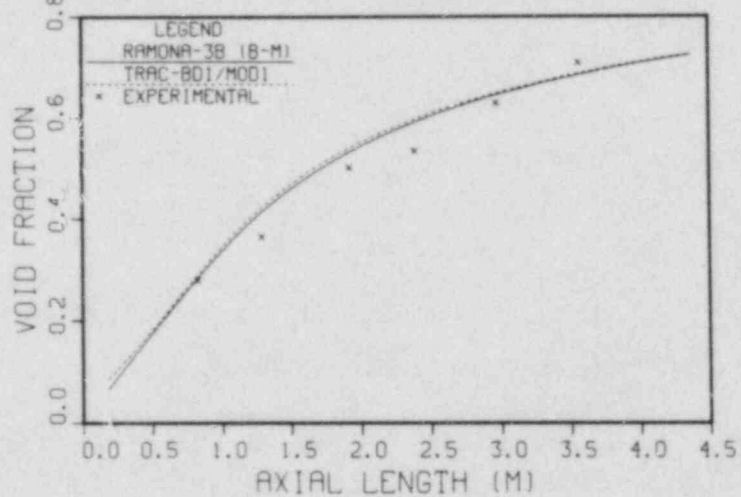


Figure 5.8 Comparison Between the Experimental Data and the Code Predictions of Axial Void Fraction for FRIGG Test 313017.

FRIGG RUN NO. 313007  
SUB=11.7, G=1110 KG/M2-S, Q=1.5 MW, P=50.0

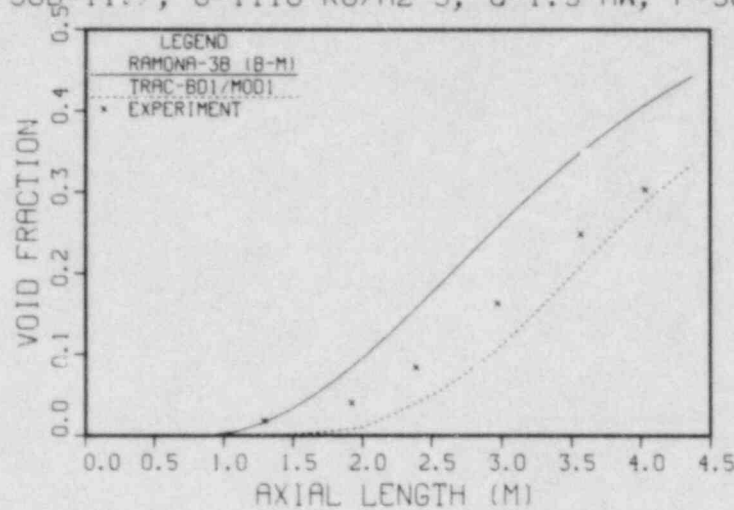


Figure 5.9 Comparison Between the Experimental Data and the Code Predictions of Axial Void Fraction for FRIGG Test 313007.

FRIGG RUN NO. 313014  
SUB=11, G=1163 KG/M2-S, Q=2.93 MW, P=49.7

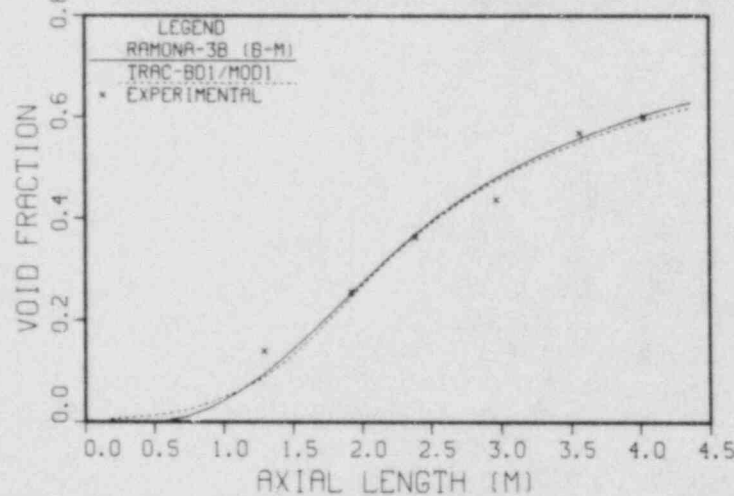


Figure 5.10 Comparison Between the Experimental Data and the Code Predictions of Axial Void Fraction for FRIGG Test 313014.

FRIGG RUN NO. 313016  
SUB=19.3, G=1208 KG/M2-S, Q=2.91 MW, P=49.6

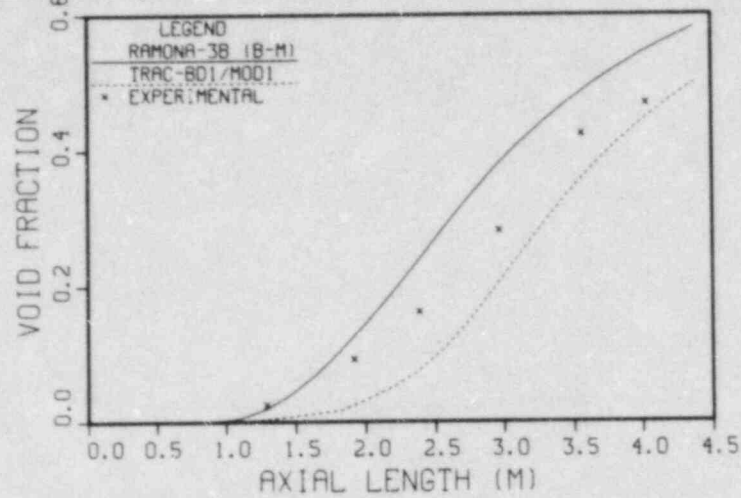


Figure 5.11 Comparison Between the Experimental Data and the Code Predictions of Axial Void Fraction for FRIGG Test 313016.

FRIGG RUN NO. 313020  
SUB=22.4, G=1159 KG/M2-S, Q=4.415 MW, P=49.

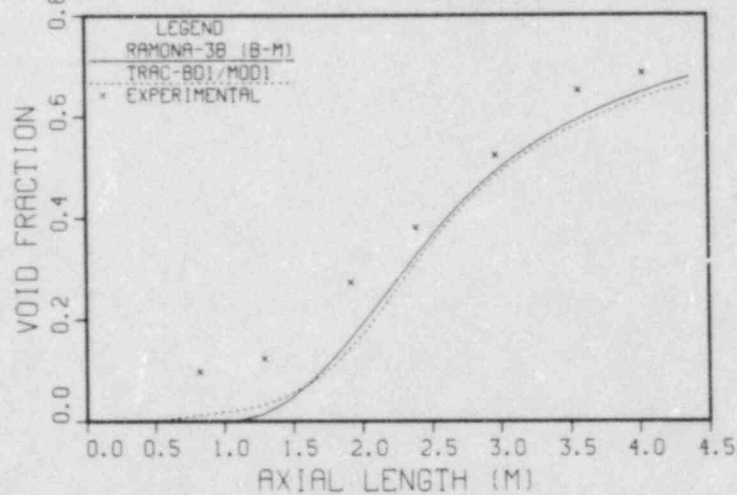


Figure 5.12 Comparison Between the Experimental Data and the Code Predictions of Axial Void Fraction for FRIGG Test 313020.

## 6. Code Maintenance (FAMONA-3B)

(P. Saha, L. Y. Neymotin, G. C. Slovik, and H. R. Connell)

This project consists of improvement and maintenance of the BWR plant transient code RAMONA-3B. The code employs three-dimensional neutron kinetics coupled with parallel hydraulic core channels and is complete with jet pump, recirculation pump, steam separator, steam line with all necessary valves, safety injection system and limited plant control and protection system. Under user option, the code can also be used with one-dimensional (axial) neutron kinetics. The code is most suitable for analyzing the BWR core and systems transients where the coupling between neutron kinetics and thermal hydraulics is important (e.g., ATWS, CRDA, etc.). The code is available to any U.S. organization, on a royalty-free basis, for the analysis of U.S. reactors.

The details of the progress achieved during the reporting period of April to June 1985 are described below.

### 6.1 Pressure Suppression Pool (PSP) Model (L.Y. Neymotin and H.R. Connell)

A simple model for calculation of the pressure suppression pool water temperature and level has been implemented in RAMONA-3B. The model is based on a lumped parameter approach. It is assumed that the steam entering the pressure suppression pool will be completely condensed in the water. The governing differential equations based on mass and energy balances are the following:

$$\frac{dM_{PSP}}{dt} = W_{steam} \quad (6.1)$$

$$\frac{dh_{PSP}}{dt} = \frac{(h_g - h_{PSP}) W_{steam} - \dot{Q}_{RHR}}{M_{PSP}} \quad (6.2)$$

where:  $M_{PSP}$  = PSP water mass  
 $W_{steam}$  = SRV steam mass flow rate,  
 $h_g$  = steam enthalpy at S/RV,  
 $h_{PSP}$  = PSP liquid enthalpy,  
 $\dot{Q}_{RHR}$  = Residual Heat Removal (RHR) cooling rate.

The above equations are solved by the first-order Euler method at each hydraulic time step. The check-out calculations are being performed at this time.



6.2 New Cycle of RAMONA-3B/MODO  
(L.Y. Neymotin, G.C. Slovik, and H. R. Connell)

A new cycle of RAMONA-3B, namely, RAMONA-3B/MODO/Cycle 10, has been created during this reporting period. This cycle includes a number of modifications, improvements and corrections. Major among them are:

1. Steam condensation on safety injection water and return water exiting the steam separators.
2. Improvements to reverse flow modeling in core and bypass channels,
3. Complete 1-D neutronics capability including 3-D to 1-D collapsing procedure,
4. Improvements to the feedwater controller,
5. Corrections to restart and backstepping procedures,
6. Plotting enhancements and output corrections,
7. Streamlining certain areas of neutronics part of the code.

The new cycle was checked by running the sample problems.

The source coding and the input for the redimensioning code, AUTODIM, have been revised to operate on the above Cycle 10 version of RAMONA-3B/MODO. A "small" version of the code had been created and checked out. This small version, when put in production use, greatly decreases both the computer running cost (by 15-30%) and the computer "turn around" time.

6.3 Distribution of RAMONA-3B/MODO/Cycle 10

The source deck of RAMONA-3B/MODO/Cycle 10 has been distributed to the Idaho National Engineering Laboratory. Distribution of this code version to several other U.S. organizations, namely, GPU Nuclear, Fauske & Associates, Westinghouse, and Oregon State University, is in progress.



## 7. Benchmarking and Verification of LWR Severe Accident Codes

(W. T. Pratt)

### 7.1 MELCOR Benchmarking and Verification (K. R. Perkins)

#### 7.1.1 Background

The MELCOR code is being developed for NRC by SNL to be used in probabilistic risk assessment (PRA) studies. It is intended to be fast running, user friendly and portable. In addition, the code models primary system and containment thermal/hydraulic behavior and fission product release and transport. Therefore, MELCOR has the potential to be a unified source term/PRA code if its development incorporates up-to-date information from both technical areas. The objective of this project is to evaluate MELCOR's potential as a source term code and make specific modeling recommendations. In addition, the project will also benchmark MELCOR against more mechanistic codes.

#### 7.1.2 Technical Approach and Project Status

This project consists of a Development Phase and a Benchmark Phase as discussed below.

##### 7.1.2.1 Development Phase (M. Khatib-Rahbar, K. R. Perkins)

Subsequent to the MARCH review meeting each of the source term experts submitted written comments to BNL on the status of MELCOR as a source term code. These comments were transmitted to SNL and formed the basis for a second review meeting held at Sandia on June 4th. The meeting resulted in ten preliminary recommendations and identified a need for additional information on the core degradation models.

##### 7.1.2.2 Benchmark Phase (R. Jaung, W. Bornstein)

A BNL staff member (Dr. Perkins) attended the Severe Fuel Damage and Source Term Research Program Review Meeting held in Idaho Falls, April 16-20. The meeting was a forum for the mechanistic severe fuel damage codes SCDAP (EG&G), MELPROG (SNL) and CORMELT (EPRI). A new version of SCDAP was acquired by BNL for the benchmarking program.

#### 7.1.3 Future Plans

##### 7.1.3.1 Development Phase (M. Khatib-Rahbar, K. R. Perkins)

A final meeting is planned at BNL to discuss the review team's assessment of MELCOR's potential as a source term code and to make recommendations for any necessary modeling improvements. The expert's assessment and recommendations will be incorporated into a letter report to the NRC Project Manager R. O. Meyer. In addition, a BNL staff member (Dr. Perkins) will make a second visit to SNL and work with the MELCOR team for several weeks in order to familiarize himself with the various features of the code and to facilitate installation of MELCOR on the BNL computer system.

### 7.1.3.2 Benchmark Phase (K. R. Perkins)

BNL staff will acquire the MELPROG code from SNL to use as a benchmarking tool for MELCOR.

## 7.2 Source Term Code Package Benchmarking and Verification (H. Ludewig)

### 7.2.1 Background

Significant research activity has been undertaken in the area of fission product source terms since the publication of the RSS in 1975. An updated basis for estimating fission product behavior was published in NUREG-0772 by NRC/RES. In addition, updated fission product source term methods were developed under the direction of the Accident Source Term Program Office (ASTPO) and published in BMI-2104. Several computer codes (refer to BMI-2104) were developed to calculate source terms. Consequently, calculating individual source terms is now a highly complex process involving significant data transfer between all of the ASTPO codes. In addition, as these codes are not coupled, a number of coupled phenomena cannot be readily addressed, e.g., local heating effects due to primary system retention of fission products. It was therefore decided by the NRC staff to fund Battelle Columbus Laboratories (BCL) to integrate these codes into one self-consistent source term code package (STCP). This package would eliminate the need for assuring correct data transfer and compatibility between codes and also allow the user to assess the influence of the coupled phenomena. The objective of this project is to provide quality assurance of the STCP. BNL staff will obtain the code package from BCL and install it on the BNL computing system. The code package will be reviewed specifically to ensure that models and options have been correctly implemented. In addition, the coupling of the various codes in the package will be carefully checked. Finally, the portability of the code package and its ease of use will be assessed.

### 7.2.2 Technical Approach and Project Status

Work on this project was initiated during May 1985 and discussions were held with the NRC Project Manager related to the scope of work. A meeting was held at BCL to discuss plans for packaging STCP and to develop a schedule for transfer of the package to BNL. Assistance was provided to BCL staff by G. Greene (Experimental Modeling Group, BNL) on the CORCON/VANESA code coupling that he developed at BNL.

### 7.2.3 Future Plans

Further meetings are planned at BCL to discuss the status of the STCP. A working version of the STCP is expected to be installed on the BNL computer system during the next quarter.

## II. DIVISION OF ENGINEERING TECHNOLOGY

### SUMMARY

#### Stress Corrosion Cracking of PWR Steam Generator Tubing

The experimental program on stress corrosion cracking (SCC) at Brookhaven National Laboratory is aimed at the development of a quantitative model for predicting the behavior of Inconel 600 tubing in high temperature aqueous media, with special reference to its use in nuclear plant steam generators. Empirical relationships are being established between SCC failure time, crack growth rate and factors influencing cracking.

The experimental work has reached the point where some of the longer term tests are continuing to complete the data needed for the final equations. In several instances, the final experiments are being completed.

In this quarter, additional U-bends have been exposed to improve the statistical base for our model. No data are yet available.

#### Probability-Based Load Combinations for Design of Category I Structures

A probability-based reliability analysis method for shear wall structures has been developed. The method can be used to evaluate the reliability level of existing shear walls subjected to dead load, live load and in-plane earthquake forces. In addition, utilizing the reliability analysis method, the load and resistance factors are also determined to establish the load combination criteria for the design of shear walls structures. Two technical reports have been prepared to present the details.

#### Soil-Structure Interaction Evaluations

Three separate tasks are under study in the SSI area. First, lift-off capability has been incorporated into SIM, and numerical results generated to assess the effect of lift-off on structural response. Second, interaction compliance functions have been generated for a wide range of layering conditions. The effect of these coefficients a floor response spectra is being studied. Third, the influence of pore fluid on SSI is being studied by generating more numerical data on interaction coefficients as well as improving and extending the capability of the finite element program.

### Identification of Age Related Failure Modes

During this period, NUREG/CR-4156 describing the aging and seismic assessments of electric motors was sent for publication after the incorporation of comments received from NPAR participants. The second phase of this study is in progress, focusing on identifying methods of inspection, surveillance, and monitoring to detect significant aging and service wear effects.

The failure data was compiled for battery chargers and inverters, the second component assigned to BNL. Further studies were made on the review of the data base to identify the most significant failure modes and mechanisms and their effect on plant safety. A summary of findings will be reported in the first-phase report.

The relay and circuit breaker aging assessment effort was continued by Franklin Research Center (FRC). The operating experiences of these components continue to be reviewed and analyzed to determine failure/aging correlation. A systems interaction study to determine failure effects on safety system operation has also been initiated.



## 8. Stress Corrosion Cracking of PWR Steam Generator Tubing

(D. van Rooyen)

The objective of this program is to develop quantitative data to serve as a basis for determining the useful life of Alloy 600 tubing in service from accelerated test data.

The present experimental program addresses two specific conditions, i.e., 1) residual stress conditions where deformation occurs but is no longer active, such as when denting is stopped and 2) where plastic deformation of the metal continues.

### 8.1 Constant Load

During this quarter our work has provided no new data, and, as before failure remains proportional to the  $-4.3$  power of stress; this value relates to pure water, and it is yet to be established whether simulated primary water will provide the same value.

### 8.2 U-bends

Tests with split tube type U-bends in pure water are practically complete at 315°C, and many cracks have now occurred at .01, .02 and .03% carbon. Activation energy still increases with increasing carbon content but less strongly in the .02-.03% range of carbon. No cracks have been seen yet at any carbon level at 290°C. Activation energy values fall between about 40 Kcal/mole and >60 Kcal/mole for the various carbon levels in our tests. More work has been started to improve the certainty of the above trends, and these new points should be ready for inclusion in the report for the 13th Water Reactor Safety Research meeting in October.

### 8.3 Future Work

Future work will be the continuation of long-term tests. Arrangements will be made to obtain Surry and/or other "known" steam generator tubes for model verification.



## 9. Probability-Based Load Combination for Design of Category I Structures

(H. Hwang, M. Reich, J. Pires, P. C. Wang,  
M. Shinozuka, B. Ellingwood and S. Pepper)

### 9.1 Reliability Analysis Method for Shear Wall Structures

For the safety evaluation of shear wall structures, a probability-based reliability analysis method has been developed. In the method, shear walls are modeled by stick models with beam elements, and may be subjected to dead load, live load and earthquake during their lifetimes. In addition to the appropriate probabilistic models for dead load and live loads, the earthquake load is assumed to be a segment of a stationary Gaussian process with a zero-mean and a Kanai-Tajimi power spectral density function. The seismic hazard at a site, represented by a hazard curve, is also included in the reliability analysis. Both shear and flexure limit states are analytically defined. The flexure limit state is defined according to the ACI strength design formula, while the shear limit state is established from test data. The limit state probabilities, on the basis of these limit states, are then computed. The details of the methodology and its application are described in a draft report entitled "Reliability Analysis of Shear Wall Structures", NUREG/CR-4293.

### 9.2 Probability-Based Load Combinations for Design of Shear Walls

Utilizing the reliability analysis method described above, the load combination criteria for the design of shear wall structures has also been established. The proposed design criteria are in the load and resistance factor design (LRFD) format. In order to test whether the proposed criteria meet the reliability-based performance objectives, four representative structures are selected using a Latin hypercube sampling technique. These representative structures are designed using trial load and resistance factors. Then, a reliability analysis method is employed to assess their reliabilities. An objective function is defined and a minimization technique is developed to find the optimum load factors. In this study, the resistance factors for shear and flexure, and load factors for dead and live loads are preassigned to simplify the minimization work. The load factor for SSE is determined for the target limit state probabilities of  $1.0 \times 10^{-6}$  or  $1.0 \times 10^{-5}$  with a lifetime of 40 years.

If the target limit state probability is selected as  $1.0 \times 10^{-6}$  per 40 years, the proposed load combinations for design of the shear walls subjected to dead load, live load and earthquake during the service life are as follows:

$$\left. \begin{array}{l} 1.2D + 1.0L + 1.4 E_{SS} \\ 0.9D \quad - 1.4 E_{SS} \end{array} \right\} \leq \phi_1 R_1 \quad (9.1)$$

where

- D = load effect due to design dead load
- L = load effect due to design live load
- ESS = load effect due to safe shutdown earthquake (SSE)
- $\phi_i$  = resistance factor for the i-th limit state under consideration
- $R_i$  = nominal structural resistance for the i-th limit state under consideration

The resistance factor for shear,  $\phi_v$ , is 0.85 and the resistance factor for compression or compression with flexure,  $\phi_m$ , is 0.65. The determination of the nominal design values for loads and nominal resistance follows current practice. The details of the development of the load combination criteria are described in a draft report (NUREG/CR-4238) entitled "Probability-Based Load Combination Criteria for Design of Shear Wall Structures".

The proposed load combinations are similar to those specified in ANSI Standard A58.1-1982. The proposed load factor for earthquake in this study is 1.4 instead of 1.5 in the A58 standard. However, the definition of earthquake is quite different from the design earthquake in the A58 standard. In general, the safe shutdown earthquake specified for nuclear structures is much stronger than that specified for conventional structures. Another difference appears in the resistance factor for shear. In this study, the resistance factor for shear is recommended to be 0.85, while 0.70 was recommended for use with the A58 load criteria. In this connection, however, it should be noted that the mean shear capacity of low-rise walls is much higher with respect to the nominal shear capacity specified by ACI than is the mean shear capacity of slender walls and beams.

## 10. Soil-Structure Interaction Evaluations

(A. J. Philippacopoulos, C. A. Miller,  
C. J. Costantino, Q. Liu and M. Reich)

### 10.1 Lift-Off Effects

The SIM Code, which was modified to include liftoff effects, has been used in a variation-of-parameter numerical study. The code modifications were centered in two areas. First, nonlinear distributed base springs and dampers are included in the model to account for separation between the basemat and the soil foundation. Second, the interaction model was improved to account for the effect of impact of the foundation as it comes back into contact with the ground after separation occurs. This impact leads to increased effective damping in the interaction process. This model was used to improve the correlation of the numerical calculations with the measured SIMQUAKE data.

The equations of motion describing liftoff were placed in nondimensional form to facilitate compilation of computed data. These nondimensional parameters were used to generate curves predicting the onset of liftoff, including parameters valid for typical nuclear power plants. Numerical work is continuing to generate data indicating the impact of liftoff on floor response spectra.

### 10.2 Water Table Effects

Work has continued on the numerical studies of ground water effects on soil/structure interaction. The finite element program that was developed to treat the linear two-phased soil/water system is continuing to be exercised to generate more interaction data. The data generated to date indicates that pore fluid primarily changes the effective interaction coefficients for the vertical and rocking modes of structural response. Impact on horizontal interaction coefficients for surface structures is not as great.

The numerical phase of the study is continuing by extending the range of parameters for which interaction parameters are being determined. This activity is centered primarily in the study of the effect of depth of ground water on these parameters. At the same time, effort is being expended to expand the program capability by increasing the problem description that can be treated and by improving the transmitting boundary formulation.

### 10.3 Layering Effects

During this period an investigation of layering effects for the vertical component of the earthquake input was carried out. Vertical impedance functions for a set of representative layered foundations were generated using the CLASSI code. These impedances were then used to evaluate the transfer functions of a simplified structural model.

A parametric study was undertaken in order to access the influence of structural and foundation parameters on the frequency and amplifications of the SSI system in vertical direction. The basic parameters varied in the foundation model were the layer thickness and the contrast in shear wave velocity between layers. This parametric study has been completed.

Furthermore, a simplified procedure was developed with the aim to approximate the layering parameters of the foundation. This procedure avoids the long computational requirements of the exact solution. The bounds of the approximation involved in the response of the SSI system using this simplified procedure are currently under investigation. Some comparisons between the exact and simplified methods were made. From the results obtained it was found that the approximation is within engineering limits. Further studies will be carried out during the next quarter period in order to establish some guidelines for the use of the method.



## 11. Identification of Age Related Failure Modes (J. H. Taylor)

Under the auspices of the NRC Nuclear Plant Aging Research (NPAR) Program, BNL is currently performing aging assessments of nuclear components such as electric motors, battery chargers and inverters, and relays and circuit breakers. The goals of this program are to resolve issues related to the aging and service wear of equipment and systems at operating reactor facilities and to assess their possible impact on plant safety.

### 11.1 Electric Motors (M. Subudhi and W. Gunther)

#### 11.1.1 Operating Data Review

The aging and seismic assessments of electric motors based on the operating experience data base are reported in NUREG/CR-4156. Comments from other NPAR participant labs were incorporated into the report and the report, was sent for printing.

#### 11.1.2 Preventive Maintenance Program

The second phase of the study on electric motors focused on identifying methods of inspection, surveillance, and condition monitoring to detect significant aging service wear effects and recommendations of acceptable maintenance practices which can be undertaken to mitigate these effects.

Following is the status of the studies identified in the last quarterly report:

- Motors in a typical PWR power plant were identified. Identification of BWR plant motors is being processed. Both safety and non-safety motors are considered.
- General techniques for surveillance, in-service testing, and condition monitoring are identified. These include noise/vibration analysis, bearing and winding temperature monitoring, and stroke time for MOVs.
- General techniques for maintenance testing of motors include insulation resistance, AC/DC insulation leakage, dissipation factor, motor running current, surge testing, and inspection of bearing lubrication. Each of these is studied in context to present industry practices (data from 4 operating plants), measurement errors, and recommendations for improved diagnosis.
- Functional indicators for dielectric, rotational, and mechanical integrities of motors are being studied to prioritize their measurements to indicate any age-related degradation in motor components.
- Recommendations for a preventive maintenance program will be provided in optimizing the maintenance data and frequency interval and in trending the functional indicators.
- Cost-benefit considerations for key recommendations will be provided for an intermittent duty motor (i.e., MOV) and a continuous duty motor.



- After completing the above studies, recommendations will be provided for upgrading current regulatory and industrial guidelines.

#### 11.1.3 Aging Seismic Correlation Study

- BNL is in the process of developing a pilot program to study some selected equipment which has experienced actual earthquake conditions in a west coast power plant. The program will investigate the age-related degradation of components during and after the earthquake.
- FRC, as a contractor to BNL, has received some relays from the Shippingport Nuclear Station. A test program is being considered to examine these naturally aged relays for aging-seismic correlation study.

#### 11.2 Battery Chargers and Inverters (W. Gunther and M. Subudhi)

A detailed review was made of battery charger and inverter applications at nuclear power plants including the advantages of various configurations employed. Failure events with significant plant and safety system effects were summarized and compared to the bus arrangement design noting the existence of automatic or manual throwover capability. Preliminary conclusions indicated that configuration differences are directly related to plant safety impact. Further investigation into the effects of other variables such as component manufacturer, size, and type for each of the plants studied must also be completed before a final conclusion can be developed. Ebasco Services has assisted BNL in obtaining specific plant design and technical specification information to support this effort.

Writing of the phase I Battery Charger and Inverter report was initiated during the past quarter with several sections completed and distributed for internal comment. The report outline is very similar to BNL's recently completed report on motor aging, NUREG/CR-4156. The report will include a plant systems interaction discussion based on the significant plant safety effects experienced due to component failures.

The first components to be extracted from the Shippingport Nuclear Station were received by Franklin Research Center (relays) and BNL (inverter and motor-generator set) during this quarter. Testing of these components is not scheduled until FY86; however, work plans and procedures for testing the inverter will be initiated during the next quarter. Additional components from Shippingport, such as a second inverter and a battery charger, are scheduled to be received during the next quarter.

#### 11.3 Relays and Circuit Breakers (Franklin Research Center)

Franklin Research Center, as a subcontractor to BNL, has surveyed the industry to determine the types and sizes of circuit breakers used in nuclear safety-related applications. In addition, a comprehensive review of Licensee Event Reports (LERs) was completed, and a review of NPPDS data obtained from INPO has been initiated. The NPRDS and IPRDS data review will be completed during the next quarter.

Considerable effort has been expended in performing a systems interaction study to determine the circuit breaker and relay impact on safety injection system operation. This aspect of the NPAR study has required a detailed review of system logic drawings to determine the system effect of various relay and circuit breaker failures.

### III. DIVISION OF RISK ANALYSIS AND OPERATIONS

#### SUMMARY

#### Application of HRA/PRA Results to Resolve Human Reliability and Human Factors Safety Issues

Brookhaven National Laboratory has been tasked in the program to identify approaches for using anticipated Human Reliability Analysis (HRA)/Probabilistic Risk Assessment (PRA) data to resolve human reliability/human factors issues of interest, and development of techniques for implementing those approaches.

The initial research in this project involved a comparison of the data needed to address human performance regulatory issues and the data currently available from PRA. To accomplish this, two separate efforts were undertaken: (1) identifying, collecting, and storing all quantitative human performance data contained in all PRAs done to date and (2) listing all human performance regulatory issues and systematically deriving from the issues the data needed to address them.

As a result of these efforts, BNL is developing the following document which reports on the findings in the above program.

- Uses of Human Reliability Analysis Probabilistic Risk Assessment Results to Resolve Human Performance Issues That Could Affect Safety (NUREG/CR-4103).

#### PRA Technology Transfer Program (PRATTP)

TTP has been an ongoing NRC program since 1982, but is new to BNL with efforts initiated this fiscal year. The program is designed to provide research support to transfer the technology of Probabilistic Risk Assessment (PRA) to the NRC staff. This will be accomplished through conducting pre-established courses, formulating curriculum changes and additions based on the needs of the NRC staff, and publishing textbooks on the subject for future NRC usage.

The purpose of this program is, therefore, to provide the NRC with an adequate PRA resource capability with which independent validations of the effectiveness of regulatory, risk-related programs can be performed and from which risk and reliability methods can be applied to inspection and enforcement decisions.

During this quarter substantial progress has been made. Courses developed previously by the PRATTP have all been given. The structure, content,

purpose, and scope of two new courses, namely, PRA Basics for Inspection Application and PRA Applications have been finalized with cognizant NRC staff concurrence, and actual course development is currently under way. Program scope has been increased during this quarter to not only develop the PRA Basics for Inspection Application course, but to also present the course this fiscal year. Primarily designed to instruct inspectors within the Regions, close coordination with the IE staff is planned.

Documentation which will essentially provide a synthesis of existing PRATTP course material is currently being prepared. Purpose, scope, and content of the three-volume set was reviewed by the staff, and the go-ahead was given this quarter for detailed preparation.

#### Protective Action Decisionmaking

In this program, BNL staff are developing a technical basis for NRC guidance on protective action decisionmaking based on an evaluation of the consequences of nuclear power plant accidents. Potential actions under consideration include sheltering, evacuation, and relocation. In the past, specific recommendations have proven to be difficult to justify because of uncertainties in potential accident sequences. Consequently, BNL will establish strategies appropriate to those sequences for which emergency planning is necessary, emphasizing credible failure modes, links to emergency action levels based on in-plant observables and containment status, and other factors such as weather.

#### Operational Safety Reliability Research

The Operational Safety Reliability Research Project is structured to develop and recommend a program of coordinated reliability engineering and management approaches with demonstrated potential for beneficial application in the nuclear industry environment. The end product of this project is intended to be a guidance document that will indicate the required elements of a technically acceptable reliability program and how these elements would be applied to individual components and systems involved in nuclear plant operations.

This project has been ongoing for some time in NRC; however, it is a new, recently funded program for BNL. During this quarter, efforts have primarily included initial technical planning, internal staffing and manpower allocations, and the development of a detailed program planning document which was submitted to the NRC for review and comment. A presentation was also made to the NRC to further describe and discuss the purpose, scope, content, and organizational structure of the project, especially how the current effort will utilize and implement past products generated by this program.



12. Application of HRA/PRA Results to Resolve  
Human Reliability and Human Factors Safety Issues

(J. N. O'Brien, C. M. Spettell and R. K. Perline)

Brookhaven National Laboratory has been tasked in this program to identify approaches for using Human Reliability Analysis (HRA)/Probabilistic Risk Assessment (PRA) data to resolve human reliability/human factors issues of interest and development of techniques for implementing these approaches.

The initial research in this project involved a comparison of the data needed to address human performance regulatory issues and the data currently available from PRAs. To accomplish this, two separate efforts were undertaken: (1) identifying, collecting, and storing all quantitative human performance data contained in all PRAs done to date and (2) listing all human performance regulatory issues and systematically deriving from the issues the data needed to address them. Each of these efforts is described below.

12.1 Identifying, Collecting, and Storing all HRA/PRA Data

Every volume of all 19 currently available PRAs were collected and placed in a dedicated library. Technical readers closely examined every page of every PRA volume in order to identify the presence of any a set of approximately 20 key words relating to human reliability or performance. After these key words were identified, experienced human reliability analysts examined each key word to determine if any HRA/PRA data were present. If so, the particular datum was entered into a computer data base as a single data record along with any information pertinent to it including the type of datum (i.e., human error or system unavailability due to testing and maintenance), confidence or uncertainty bounds, factors affecting human performance (e.g., stress, time available, training), the situation involved (e.g., LOCA, transient, external event), the plant system involved, the type of error (i.e., omission or commission), the particular human action involved, and the particular personnel involved (e.g., operator, maintenance, I&C). In most cases all of this information was not available from the PRA so that most data records are not complete. Each PRA is a separate file in the data base so that comparisons between PRAs, as well as among the data generally, are possible.

12.2 Listing of Human Performance Regulatory Issues and Data Needs

It was recognized that the issues facing NRC are somewhat different at any given time. As a result, an effort was made to systematically generate a representative list of human performance regulatory issues. First, each Generic Safety Issue (i.e., TMI Action items, Risk Action items, and New Generic Issues) was examined and the human performance issues attendant upon it listed. Second, to refine and clarify these issues, NRC planning documents were reviewed and over 25 NRC personnel with cognizance over the issues were interviewed. This resulted in a refined list of human performance regulatory



issues. Each issue was broken down into a set of data records which would address the issue in question. Each data record includes the personnel involved, the actions involved, the presence of factors affecting performance, the situation involved, and the plant system involved.

### 12.3 Comparison of HRA/PRA Data Records and Issues Data Records

In order to assess the usefulness of current HRA/PRA data with regard to human performance regulatory issues a comparison of HRA/PRA data records and issue data records was made. The cases where HRA/PRA data records existed to address issues, data records were noted. This project is documented in a NUREG/CR-4103 entitled "Uses of Human Reliability Analysis Probabilistic Risk Assessment Results to Resolve Personnel Performance Issues That Could Affect Safety." This document is currently in press.

It was found during this analysis that only a small number of issue data records are addressed by current HRA/PRA data. Each working level issue previously identified is being classified according to (1) what type, amount, and format of data are needed to address the issue, (2) what types of analysis the data needed will be subject to, and (3) what type of criteria will be used to draw conclusions from the analysis. Clusters of issue types, analysis, techniques, and conclusion criteria are being developed so that general HRA/PRA data use methods can ultimately be developed.

### 12.4 Grouping of Approaches and Data Types

During the third quarter of FY 1985, the following was accomplished:

- Five classes of HRA/PRA data were developed to classify data needs appropriately. These are: (1) static probability/human performance measure data, (2) trend data, (3) deviation data, (4) personnel subsystem analysis data and (5) actuarial data. A selected set of Generic Safety Issues were analyzed according to this taxonomy of needed data. Means of acquiring these data, either from PRAs or other sources, are currently under investigation.

13. PRA Technology Transfer Program  
(J.L. Boccio and R.E. Hall)

During this quarter, NRC management of the Probabilistic Risk Assessment Technology Transfer Program (PRATTP) was transferred from the Division of Risk Analysis and Operations (DRAO) within the Office of Research to the Management Development and Training Staff (MDTS) within the Office of Administration. Since this program is now not directly sponsored by the Office of Research, subsequent descriptions of PRATTP activities and progress will no longer be included within this document.

13.1 Objectives

The objectives of this program have not changed as a result of this transfer within the NRC. It is still structured to formulate a curriculum for training selected NRC staff members in the use of PRA techniques, to develop training aids, to conduct training courses, and to document these courses for future reference and use.

The curriculum is designed to enhance the capability within NRC to perform independent validations of the effectiveness of its regulatory program and to apply the results of PRAs. Since the first presentation in August 1982, the courses have been continually updated to incorporate the latest information available on PRA methodologies and applications. Courses have been added and combined as needs have changed.

BNL has been tasked to provide research and administrative support to transfer the technology of PRA and PRA techniques to the NRC staff. This transfer is to be accomplished by conducting courses given in the past, formulating curriculum changes and additions based upon the current needs of the NRC, developing training aids, and publishing a series of textbooks to supplant present course notes.

13.2 Work Performed During Period

Under Task 1, Program Management, work performed entailed the continuing task of administering the PRATTP including planning, scheduling, budgeting, staffing, coordinating, monitoring, and reporting the various activities related to presenting existing courses, developing and presenting new courses consistent with the changing PRA needs of the staff, and producing technically-edited, peer-reviewed documentation. During this reporting period briefings with the MDTS were made to apprise them on the background of the program, its current progress, and future direction. Also the Office of Inspection and Enforcement (IE) staff were briefed on a new course developed during FY 1985 entitled "PRA Basics for Inspection Application." The scope of the PRATTP has increased to include conducting this course within this fiscal year.

Under Task 2, Course Presentation, the System Reliability and Analysis Techniques course which includes Sessions B/C (Event Trees/Fault Trees) and Sessions A/D (Reliability/Quantification) were presented at the NRC Training Center during this quarter. The formal presentation of past PRATTP-developed courses was completed during this quarter.

Under Task 3, External Peer Review, the process has been formulated whereby new documentation will be reviewed for technical accuracy, completeness, audience suitability, and material relevance. Peer reviewers have been identified for NRC concurrence; those which have been mutually agreed upon have been notified. A three-phase process has been suggested with the first two peer-review phases scheduled to be completed by the end of the next quarter. These two phases include reviews by the principal authors, by staff of the major subcontractors, and by staff within the NRC. The final phase suggests reviews by representatives of industry.

Work under Task 4, Text Preparation for Publication, entailed finalization of actual documentation content of the three-volume set, viz.,

- Volume I - PRA Fundamentals
- Volume II - Systems Analysis for PRA
- Volume III - PRA Applications

The assigned principal authors have initiated writing their respective documents. The purpose of Volume I is to provide an overview of the PRA process from a regulatory/industry perspective. Details of the analytical tools employed in evaluating plant risk will essentially comprise Volume II with Volume III stressing past, current, and potential uses of risk/reliability methods within the regulatory fabric.

Under Task 5, New Curriculum Development, final agreement has been achieved with the NRC staff on the structure, content, purpose, and scope of the two new courses, viz., PRA Applications and PRA Basics for Inspection Applications. Work is now under way for presenting these two courses during the next quarter. Instructors have been assigned and daily schedules for each course have been prepared and reviewed by the cognizant NRC staff, with preparation of actual course documentation and training aids currently under way.

## 14. Protective Action Decisionmaking

(W. T. Pratt, A. G. Tingle, H. Ludewig,  
W. R. Casey\*, and A. P. Hull\*)

### 14.1 Background

NRC regulations require that, in the case of a major nuclear power plant accident, licensees recommend protective actions to reduce radiation dose to the public. When certain emergency action levels are exceeded, the licensee recommends protective actions to State and local officials. The nature of the protective actions recommended is determined by which emergency action levels are exceeded.

In practice drills, decisions on protective action recommendations have proven to be difficult. NUREG-0654 states that if containment failure is imminent, sheltering is recommended for areas that cannot be evacuated before the plume arrives, but evacuation is recommended for other areas. The assumption in NUREG-0654 is that there would be a greater dose savings if the population were sheltered during plume passage rather than evacuated, but this assumption has not been proven. Furthermore, the recommended protective actions must be based on estimated containment failure times, which are difficult to determine.

Alternatively, other NRC publications suggest that the appropriate response would be early evacuation of everyone within a distance of about 2 or 3 miles for all events that could lead to a major release even if containment failure is imminent or a release is underway. Those at greater distances should take shelter. Further, if a release occurs, the appropriate action would be for monitoring teams to find "hot spots" (radiation dose rate exceeding about 1 R/hr) and for people to evacuate these "hot spots."

### 14.2 Project Objectives

The objectives of the activities to be performed in this project are to:

- (1) characterize the family of potential accident sequence for which emergency planning is necessary,
- (2) establish strategies appropriate to these sequences, emphasizing credible failure modes,
- (3) identify those factors which would influence the implementation of these strategies,
- (4) determine how these factors should be incorporated into the decisionmaking process, and

---

\*BNL Safety and Environmental Protection Division



- (5) develop a guidance report on the protective actions to be recommended for combinations of these factors.

#### 14.3 Technical Approach

The technical approach is based on an evaluation of the consequences of nuclear power plant accidents as they relate to protective action decision-making. The evaluation includes a careful review of previous work (e.g. NUREG/CR-2339, NUREG-0654, NUREG/CR-2025, NUREG-0396, and reports and memoranda by the NRC staff) and its applicability to protective action decision-making. The approach is also based on a consideration of a wide range of potential accident sequences and on up-to-date assessments of containment performance. Thus the technical basis will reflect the new fission product source term information under development (BMI-2104) by the NRC/RES Accident Source Term Program Office (ASTPO). BNL staff are closely following the activities of ASTPO and, in addition, are participating in the SARP Containment Loads Working Group (NUREG-1079) and in the Containment Performance Working Group (NUREG-1037). The results of these various activities will be described in NUREG-0956, which will be published in draft form (for comment) during July 1985. This information will be integrated into our development of protective action strategies. In addition, the American Physical Society is currently reviewing the new source term methodology and the results of this review will be factored into our evaluation.

The evaluation will also be based in large part on results obtained from the CRAC2 computer code (Consequence of Reactor Accident Code, version 2). The output is being analyzed for a variety of release characterizations, weather sequences, and protective action strategies.

In accordance with the above, we have selected the following six facilities to represent the range of U.S. reactor and containment designs:

Zion: PWR with a large dry containment  
Surry: PWR with a subatmospheric containment  
Sequoyah: PWR with an ice condenser containment  
Brown's Ferry: BWR with a Mark I containment  
Limerick: BWR with a Mark II containment  
Grand Gulf: BWR with a Mark III containment

#### 14.4 Project Status

Work continued during this quarter on the development of an appropriate set of representative source terms for each of the six nuclear reactors identified in Section 14.3. These source terms are derived from ongoing NRC/RES research programs (refer to Section 14.3). A second draft report, which assesses the impact of the new source terms on potential off-site protective action strategies, was completed and sent to the NRC for review.



15. Operational Safety Reliability Research  
(J.L. Boccio and M.A. Azarm)

15.1 Background

The general purpose of a reliability program is to help minimize the frequency of transients, to control faults that challenge LWR safety systems, and to provide assurances that safety systems function reliably when called upon to mitigate abnormal occurrences. The overall objectives of a reliability program are therefore to design and build systems with acceptable reliability consistent with specified requirements and to ensure that the designed reliability does not degrade to an unacceptable level during plant operations. Under a previous project, Argonne National Laboratory (ANL) identified elements of existing reliability programs that have been implemented by defense and air carrier industries that appear applicable for LWR operation safety.

15.2 Objectives

Brookhaven National Laboratory (BNL) has been requested by the Division of Risk Analysis and Operations (DRAO) to build upon this past work by evaluating the effectiveness of these reliability elements and identifying the attributes of successful programs. Products generated will provide the NRC with the technical basis for evaluating the effectiveness of reliability elements as well as the degree of reasonableness of explicit tradeoffs in achieving needed functional reliability. An underlying theme is that it could provide the NRC with the ways and means to establish a performance-based regulatory process.

15.3 Major Tasks

To conduct this program, which has been initiated during this quarter, nine major tasks have been identified. These are:

- Task 1 - Development of project plan.
- Task 2 - Evaluation of reliability program effectiveness vs. outstanding generic issues, abnormal occurrences, and accident precursors.
- Task 3 - Identification of successful attributes of a reliability program and its potential effectiveness through case studies of utility practices.
- Task 4 - Adaptation of reliability techniques for trial application.
- Task 5 - Evaluation of reliability program effectiveness, practicality, and attributes through initial trial application on an example system at one plant.
- Task 6 - Reliability program description update based on case studies and initial trial use.
- Task 7 - Further evaluation of reliability program elements/attributes through broader trial application involving several systems at one plant.
- Task 8 - Peer review.
- Task 9 - NUREG publication reflecting peer review comments.

#### 15.4 Work Performed During Period

This project was initiated during this reporting period. As such, efforts primarily include initial technical planning, internal staffing and manpower allocation, development of project and budget proposal, technical evaluation of subcontractor proposals, the development of a detailed planning document and presentation of the program plan to the cognizant NRC staff. Specific work by tasks entails the following:

Task 1 - A detailed project plan was completed and submitted to the NRC for review and comment. A presentation was made to the NRC to further describe and discuss the purpose, scope, content, and organizational structure of the project.

Task 2 - A review of generic safety issues was initiated in order to determine areas in which a reliability program could be beneficial. Here emphasis has been placed upon current outstanding safety issues and attempting to categorize these issues with elements of a reliability program identified from the previous ANL study.

Task 3 - A process has been developed for selecting utilities considered as likely candidates for identifying attributes of a successful reliability program. Using this developed process and criteria, several utilities for subsequent case study of their reliability practices have been selected and submitted to the NRC for concurrence. In addition, a draft questionnaire was developed to act as a guide in subsequent meetings with the selected utilities.

Task 4 - Effort during this reporting period concentrated on developing reliability monitoring techniques for identifying sub-standard performance. Methods for rapid detection of "band aid" fixes are also being studied by means of statistical data analysis.

Task 5 - With NRC concurrence, the candidate plant-specific system for evaluating the effectiveness of elements of a reliability program through trial application has been the Emergency AC Power System, specifically the diesel generator. During this reporting period, work primarily entailed information gathering, notably information within the plant's FSAR and from the technical specifications for the diesel generator system.

NRC FORM 325 (2-84) NRCM 1102 3201, 3202		U.S. NUCLEAR REGULATORY COMMISSION		1 REPORT NUMBER (Assigned by TIDC add Vol. No., if any)	
<b>BIBLIOGRAPHIC DATA SHEET</b>			NUREG/CR-2371 BNL-NUREG-51454, Vol. 5, No. 2		
SEE INSTRUCTIONS ON THE REVERSE					
2 TITLE AND SUBTITLE			3 LEAVE BLANK		
Safety Research Programs Sponsored by Office of Nuclear Regulatory Research, Quarterly Progress Report April 1 - June 30, 1985			DATE REPORT COMPLETED		
5 AUTHOR(S)			MONTH YEAR		
Compiled by Allen J. Weiss			October 1985		
7 PERFORMING ORGANIZATION NAME AND MAILING ADDRESS (Include Zip Code)			6 DATE REPORT ISSUED		
Brookhaven National Laboratory Department of Nuclear Energy Upton, New York 11972			MONTH YEAR		
10 SPONSORING ORGANIZATION NAME AND MAILING ADDRESS (Include Zip Code)			8 PROJECT/TASK/WORK UNIT NUMBER		
U. S. Nuclear Regulatory Commission Office of Nuclear Regulatory Research Washington, D. C. 20555			9 FUND OR GRANT NUMBER		
12 SUPPLEMENTARY NOTES			A-3014, 15, 16, 24, A-3208, 15, 26 27, 42, 68, 70, 72, 74, 77, 81, 82, 84		
13 ABSTRACT (200 words or less)			14 TYPE OF REPORT		
<p>This progress report will describe current activities and technical progress in the programs at Brookhaven National Laboratory sponsored by the Division of Accident Evaluation, Division of Engineering Technology, and Division of Risk Analysis &amp; Operations of the U.S. Nuclear Regulatory Commission, Office of Nuclear Regulatory Research.</p> <p>The projects reported are the following: High Temperature Reactor Research, SSC/MINET Development, Validation and Application, Thermal-Hydraulic Reactor Safety Experiments, Plant Analyzer, Code Assessment and Application, Code Maintenance (RAMONA-3B), Benchmarking and Verification of LWR Severe Accident Codes; Stress Corrosion Cracking of PWR Steam Generator Tubing, Probability Based Load Combinations for Design of Category I Structures, Soil-Structure Interaction Evaluations, Identification of Age-Related Failure Modes; Application of HRA/PRA Results to Resolve Human Reliability and Human Factors Safety Issues, PRA Technology Transfer Program, Protective Action Decisionmaking, and Operational Safety Reliability Research.</p>			Quarterly		
14 DOCUMENT ANALYSIS - KEYWORDS/DESCRIPTORS			15 AVAILABILITY STATEMENT		
High Temperature Graphite Reactor Super System Code MINET Code Thermal-Hydraulic Reactor Safety Severe Accident <small>IDENTIFIERS OPEN ENDED TERMS</small>			Plant Analyzer RAMONA-3B Stress Corr. Crack. Protective Action Prob. Risk Assess Load Combinations Nuc. Plant Aging Human Error Human Factors		
			16 SECURITY CLASSIFICATION		
			(This page)		
			(This report)		
			17 NUMBER OF PAGES		
			18 PRICE		



120555078877 1 1A1R11R41R51  
US NRC  
ADM-DIV OF TIDC  
POLICY & PUB MET ER-PDR NUREG  
W-501  
WASHINGTON DC 20555